UNIVERSITY OF CRETE
MEDICAL SCHOOL
LABORATORY OF CLINICAL VIROLOGY

Study of the cellular signaling pathways during latent infection and reactivation by HSV-1 (Herpes Simplex Virus type 1).

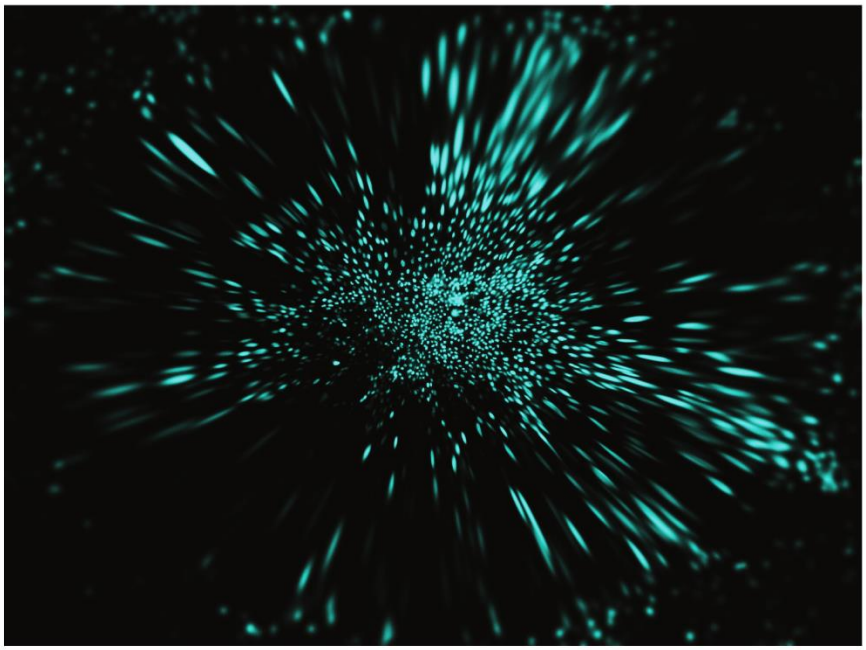

DOCTORAL THESIS

VIRGINIA-MARIA VLAHAVA

HERAKLION 2015

ΠΑΝΕΠΙΣΤΗΜΙΟ ΚΡΗΤΗΣ
ΣΧΟΛΗ ΕΠΙΣΤΗΜΩΝ ΥΓΕΙΑΣ
ΤΜΗΜΑ ΙΑΤΡΙΚΗΣ
ΕΡΓΑΣΤΗΡΙΟ ΚΛΙΝΙΚΗΣ ΙΟΛΟΓΙΑΣ

Μελέτη των κυτταρικών, σηματοδοτικών μονοπατιών κατά τη διάρκεια λανθάνουσας μόλυνσης κ επανενεργοποίησης από τον ιό του απλού έρπητα τύπου 1 (Herpes Simplex Virus type I, HSV-1).

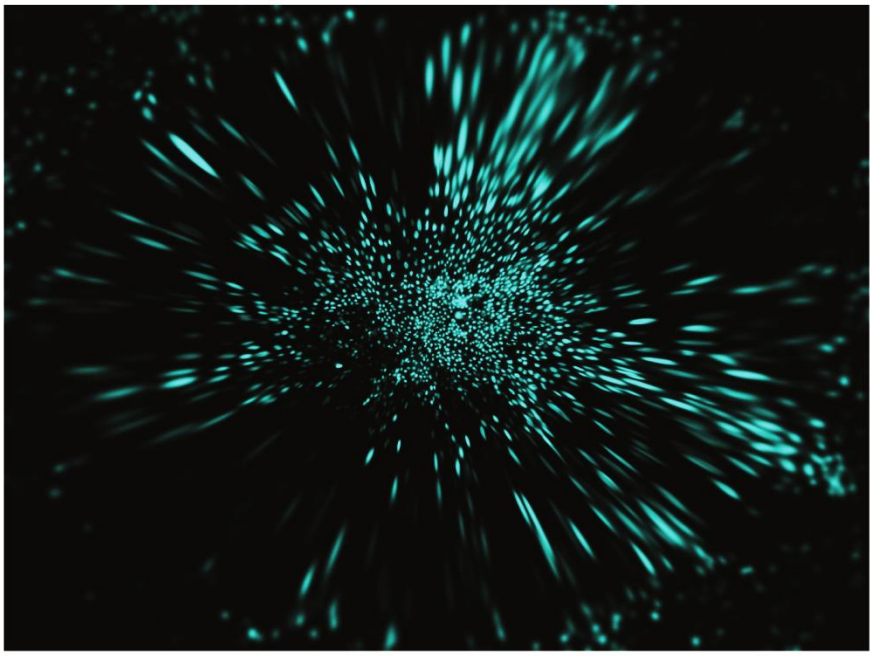

ΔΙΔΑΚΤΟΡΙΚΗ ΔΙΑΤΡΙΒΗ

ΒΙΡΓΙΝΙΑ-ΜΑΡΙΑ ΒΛΑΧΑΒΑ

ΗΡΑΚΛΕΙΟ 2015

This work has been co-financed by the European Union (European Social Fund - ESF) and Greek National funds through the Operational Program “Education and Lifelong Learning” of the National Strategic Reference Framework (NSRF) – Research Funding Program: Heracleitous II. Investing in knowledge society through the European Social Fund.

Thesis supervisor:

G. Sourvinos, Associate Professor of Clinical Virology, University of Crete, Medical School

Members of advisory committee:

G. Sourvinos, Associate Professor of Clinical Virology, University of Crete, Medical School

A. G. Eliopoulos, Professor of Molecular & Cellular Biology, University of Crete, Medical School

V. Panoutsakopoulou, PhD, Investigator - Associate Professor Level, Biomedical Research Foundation of the Academy of Athens (BRFAA)

Members of examination committee:

G. Sourvinos, Associate Professor of Clinical Virology, University of Crete, Medical School

A. G. Eliopoulos, Professor of Molecular & Cellular Biology, University of Crete, Medical School

V. Panoutsakopoulou, PhD, Investigator - Associate Professor Level, Biomedical Research Foundation of the Academy of Athens (BRFAA)

S. Kampranis, Assistant Professor of Biochemistry, University of Crete, Medical School

D. Kardassis, Professor of Biochemistry, University of Crete, Medical School

E. Papadaki, Professor of Hematology, University of Crete, Medical School

C. Tsatsanis, Associate Professor of Clinical Biochemistry, University of Crete, Medical School

Virginia-Maria Vlahava CV

Mobile phone: +306977696277
Email: Vlachava.Evi@gmail.com
Nationality: Greek

RESEARCH

Research experience

1. 6/2008-today: I performed my Master's thesis and PhD at the Laboratory of **Clinical Virology, University of Crete**, Medical School, under the supervision of the assistant professor of Clinical Virology George **Sourvinos.**

   Projects:

   a. Study of the antiviral activity of **CD40L** during lytic infection by HSV-1 (Herpes Simplex Virus type I).
   b. Study of the methylation profile of genes related to **epigenetic regulation** of the cell during HSV-1 infection.
   c. Detection of HSV-1 in patients with **fibrotic lung diseases**.
   d. Study of the **antiviral activity of various plant extracts** during lytic infection by HSV-1 or HCMV. Plant extracts tested: dandelion root and leaf extract and a herbal extract of a blind trial.

2. 02/2006 - 06/2007 : **Undergraduate thesis**: **"Study Of The Apoptotic Characteristics Of Human Bone Marrow (BM) Mesenchymal Stem Cells (MSC) In Primary Cultures"** University of Crete, Medical School, Hematology Laboratory, supervisor: professor of Hematology **Papadaki** Helen.

3. 07/05- 08/05: **undergraduate training** at the Institute of Molecular Biology and Biotechnology (IMBB) of the Foundation for Research and Technology of Heraklion Crete (FORTH), Laboratory of Immune Gene Regulation, supervisor: professor J. **Papamatheakis**

Laboratory skills

Cell culture, virus propagation and titration, adenoviral/retroviral vectors, silencing techniques, immunofluorescence, microscopy (live-imaging, fluorescence, confocal), western blots, cytoplasmic-nuclear extract fractionation, flow cytometry, RT-PCR, qPCR, transfection,etc

Publications

1. **V.M. Vlahava**, A.G. Eliopoulos, G. Sourvinos (2015) **CD40 ligand exhibits a direct antiviral effect on Herpes Simplex Virus type-1 infection via a PI3K-dependent, autophagy-independent mechanism**. Submitted.

2. Lasithiotaki I, Antoniou KM, **Vlahava V-M**, Karagiannis K, Spandidos DA, Nikolaos M. Siafakas, George Sourvinos (2011) **Detection of Herpes Simplex Virus Type-1 in Patients with Fibrotic Lung Diseases.** PLoS ONE 6(12): e27800. doi:10.1371/journal.pone.0027800

3. M-C Kastrinaki, P Sidiropoulos, S Roche, J Ringe, S Lehmann, H Kritikos, **V-M Vlahava**, B Delorme, G D Eliopoulos, C Jorgensen, P Charbord, T Häupl, D T Boumpas, H A Papadaki. **"Functional, Molecular and Proteomic Characterization of Bone Marrow Mesenchymal Stem Cells in Rheumatoid Arthritis"** Annals of the Rheumatic Diseases, 2008;67;741-749

Conferences

1. **Vlahava V.M.**, Stavrakaki E., Eliopoulos A., Sourvinos G. Study of the effect of CD40L on the lytic cycle of Herpes Simplex Virus type-1 (HSV-1), 5th European Congress of Virology, Lyon, France, 11-14/9/2013, poster.

2. **Vlachava V.M.**, Eliopoulos A., Sourvinos G. Study of the effect of CD40L on the lytic cycle of Herpes Simplex Virus type-1 (HSV-1), 63o Panhellenic Conference of the Hellenic Society for Biochemistry and Molecular Biology (HSBMB), FORTH, Heraklion, Crete, Greece, 9-11/11/2012, poster.

3. Antoniou KM, Lasithiotaki, **Vlahava VM**, Karagiannis K, Spandidos DA, Siafakas, Sourvinos G. Detection of herpes simplex virus type-1 in patients with fibrotic lung diseases. 20th Hellenic Congress of Thoracic Diseases, Athens 24-27/11/2011, oral presentation.

4. H. Papadaki, **V.M. Vlahava**, M.C. Kastrinaki, A. Damianaki, C. Gemetzi, G.D. Eliopoulos, Study of apoptosis and expression pattern of tnf receptor family members in human bone marrow mesenchymal stem cells. HAEMATOLOGICA-THE HEMATOLOGY JOURNAL Volume: 92 Pages: 358-358 Supplement: Suppl. 1 Meeting Abstract: 0962, 2007, poster.

5. H. Papadaki, M.C. Kastrinaki, A. Damianaki, **V.M. Vlahava**, P. Fragioudaki, E. Stavroulaki, G.D. Eliopoulos, Study of functional and molecular characteristics of three different bone marrow cell populations for expansion of mesenchymal stem cells. HAEMATOLOGICA-THE HEMATOLOGY JOURNAL Volume: 92 Pages: 118-118 Supplement: Suppl. 1 Meeting Abstract: 0327, 2007, poster.

6. Maria-Christina Kastrinaki, Athina Damianaki, **Virginia-Maria Vlahava**, Helen A. Papadaki. Isolation of Human Bone Marrow MSCs Using Different Membrane Markers: Comparison Of Colony/Cloning Efficiency And Molecular Profile Of Three Different Cell Populations. Genostem General Assembly, Barcelona, Spain, 7-9/2/2007, poster.

7. Maria-Christina Kastrinaki, Prodromos Sidiropoulos, **Virginia-Maria Vlahava**, Athina Damianaki, George D. Eliopoulos, Dimitrios Boumpas, Helen A. Papadaki. Premature Telomere Loss of Bone Marrow MSCs In Patients With Rheumatoid Arthritis. Genostem General Assembly, Barcelona, Spain, 7-9/2/2007, poster.

8. **Virginia-Maria Vlachava,** M.C. Kastrinaki, E. Stavroulaki, M. Ximeri, G.D. Eliopoulos, H. Papadaki. Study of apoptosis and expression pattern of tnf receptor family members in human bone marrow mesenchymal stem cells, 17th Congress of the Hellenic Society of Haematology, Athens, 22-26/11/2006, oral presentation.

9. **Virginia-Maria Vlahava**, Maria-Christina Kastrinaki, Athina Damianaki, George D. Eliopoulos, Helen A. Papadaki. Study of the Apoptotic Characteristics of Human Bone Marrow Mesenchymal Stem Cells in Primary Cultures. European Hematology Association (EHA) Scientific Workshop, Biology and Clinical Applications of Mesenchymal Stem Cells. Cannes, France, 6-8/10/2006, poster.

Grants / Awards

1. **"Maria Michail Manassaki" scholarship** for excellence in graduate studies for the academic year **2013-2014**, Medical School, **University of Crete**.

2. **Scholarship "IRAKLITOS II - University of Crete"** of the Operational Program for Education and Lifelong Learning 2007 - 2013 (E.P.E.D.V.M.) of the NSRF (2007 - 2013), which is co-funded by the **European Union (European Social Fund) and National Resources** for the PhD thesis: "Study of the cellular signaling pathways during latent infection and reactivation by HSV-1 (Herpes Simplex Virus type I)" **09/2010-8/2013**.

3. **Travel grant** for attendance of the Eurovirology meeting in Lyon, September 2013 from the **European Society of Clinical Virology (ESCV).**

4. **3rd place award** for the paper "Detection of herpes simplex virus type-1 in patients with fibrotic lung diseases." presented on the 20th **Hellenic Congress of Thoracic Diseases**, Athens 24-27/11/2011

5. **"Maria Michail Manassaki"** scholarship for excellence in graduate studies for the academic year **2008-2009**, Medical School, **University of Crete**.

Teaching

I have trained both undergraduate and postgraduate students during their thesis in various molecular biology and virology techniques.

Memberships

1. European Society for Clinical Virology
2. Hellenic Society for Biochemistry and Molecular Biology

Work experience

1. **Translation from English to Greek** of the virology chapters (ch. 31-45) of the **textbook "Schaechter's Mechanisms of Microbial Disease"** , Redaction of the Greek edition, Antoniou M., Skoulika E., Sourvinos G., Psaroulaki A.

2. Detection of **deletions on Y chromosome** by PCR for diagnostic reasons.

3. Preparation of bronchoalveolar lavage **(BAL)** fluid for analysis by both FACS and May Grunwald – Giemsa staining for diagnostic reasons and storage of samples for a biobank.

4. **Museum educator** at the **Natural History museum** of the University of Crete at Heraklion, Crete, Greece.

5. **Private tutor of biology** preparing high school students for the Greek national examinations that grant access to universities.

Education

1. 9-2009- today: **PhD** student, **University of Crete, Medical school**, PhD thesis: **"Study of the cellular signaling pathways during latent infection and reactivation by HSV-1 (Herpes Simplex Virus type I)."** Laboratory of Clinical Virology, supervisor: assistant professor of Clinical Virology George **Sourvinos**.

2. 9/2008 – 6/2010: **Graduate studies**, University of Crete, Medical school, graduate program **"Molecular Basis of Human Disease".** Graduate thesis: "Antiviral activity of CD40L during lytic infection by HSV-1 (Herpes Simplex Virus type I)".

3. 25/9/2002- 7/4/2008: **Undergraduate studies**, University of Crete, Biology Department, **Biology Degree specialized on "Molecular Biology and Biotechnology**", Grade (6,86/10).

4. 1999-2002 : **Student**, 2nd **Senior high school** of Nea Ionia, Volos, Greece (orientation: exact sciences) (Grade 18/20)

5. 1996-1999: **Student**, 3rd **high school** of of Nea Ionia, Volos, Greece (Grade 19 $^{9/13}$ / 20)

Languages

1. **Greek**, native speaker
2. **English** : fluent
   a. University of **Cambridge**, **Certificate of Proficiency in English**, Grade B, December 1999.
   b. University of **Michigan**, **Certificate of Proficiency in English**, March 2000

IT skills

Competent user of Microsoft office, GraphPad and Photoshop

Seminars

1. 11-15 /7/ 2011: **The 2011 Lectures in Biology: Basic and Applied Virology**, The Onassis Foundation Science Lecture Series 2011 in Biology, Heraklion, Crete

2. 5/11/04-18/12/03: **"From theory to practice"** which included the sections: A. Introduction to the substantiation/ application of original ideas, B. Financing of new enterprises, C. Legalities for the substantiation of ideas and copyright. D. Development of a business plan. New Ideas Project, UNISTEP (80 hours).

Ευχαριστίες

Η παρούσα διδακτορική διατριβή εκπονήθηκε στο εργαστήριο Κλινικής Ιολογίας του Πανεπιστημίου Κρήτης. Για ‘μένα αποτέλεσε μια πραγματική περιπέτεια, με έντονες στιγμές, με απογοητεύσεις και χαρές, γεμάτη ενδιαφέροντες ανθρώπους κα με βοήθησε να ωριμάσω σε επιστημονικό και προσωπικό επίπεδο. Τελειώνοντας λοιπόν τη διδακτορική μου διατριβή θα ήθελα να ευχαριστήσω όλους τους ανθρώπους που συνέβαλαν σε αυτή άμεσα ή έμμεσα.

Αρχικά, θα ήθελα να ευχαριστήσω τον επιβλέποντα της διατριβής μου, Αναπλ. Καθηγητή Κλινικής Ιολογίας Γεώργιο Σουρβίνο, για την καθοδήγηση, τις συμβουλές του κ την πίστη του σε εμένα. Με βοήθησε να κάνω τα πρώτα βήματα στην ιολογία, να πατήσω σε σταθερές βάσεις κ έπειτα με άφησε να εξερευνήσω μόνη μου και να ανακαλύψω, όντας πάντα δίπλα μου να με επαναφέρει στη σωστή πορεία όποτε παρασυρόμουν. Πραγματικά ευχαριστώ πολύ.

Θα ήθελα επίσης να ευχαριστήσω την ερευνήτρια της Ακαδημίας Αθηνών Βίλυ Πανουτσακοπούλου και τον καθηγητή Άρη Ηλιόπουλο για τη συμμετοχή τους στη τριμελή συμβουλευτική επιτροπή και για το ενδιαφέρον τους. Η συμβολή του κ. Άρη Ηλιόπουλου ήταν καθοριστική και τον ευχαριστώ ιδιαιτέρως για την ενδελεχή αξιολόγηση των αποτελεσμάτων και την εποικοδομητική κριτική του. Επίσης ευχαριστώ θερμά και τους υπόλοιπους καθηγητές της επταμελούς επιτροπής μου, Δημήτρη Καρδάση, Σωτήρη Καμπράνη, Ελένη Παπαδάκη και Χρήστο Τσατσάνη για την εξέταση της διατριβής μου. Θα ήθελα να ευχαριστήσω ιδιαιτέρως τον κ. Χρήστο Τσατσάνη και για τη συμβολή του σε τεχνικό επίπεδο όπως επίσης και τον κ. Γεώργιο Χαμηλό που απλόχερα προσέφερε τη βοήθειά του και τις συμβουλές του.

Φυσικά δε θα μπορούσα να μην ευχαριστήσω όλα τα μέλη του εργαστηρίου Κλινικής Ιολογίας, νέα και παλιά για την ανεκτίμητη βοήθειά τους και το ωραίο κλίμα συνεργασίας στο εργαστήριο.

Πολλά ευχαριστώ οφείλω και στους φίλους μου Εύα, Νίκο, Παναγιώτη, Κατερίνα, Χάρη, Αντιγόνη, Μελίνα, Ελίζα, Σοφία, Δημήτρη, Έλενα και Αλέξη. Ο υπέρτατος όμως φίλος και συνοδοιπόρος σε αυτό το ταξίδι ήταν ο Ανδρέας. Ντρου, σ’ευχαριστώ τόσο πολύ!

Τέλος, το μεγαλύτερο ευχαριστώ το οφείλω στην οικογένειά μου. Στον μπαμπά μου Κώστα, στη μαμά μου Ελένη και στην μικρή μου αδερφούλα Βίκυ που πάντα με στήριζαν και πίστευαν σε εμένα. Χωρίς αυτούς τίποτα δεν θα ήταν εφικτό!

Στους γονείς κ την αδερφή μου…

Abstract

HSV-1 is a DNA virus of the herpesviruses family (*Herpesviridae*) and specifically belongs to the Alpha subfamily (*Alphaherpesvirinae*). It is a neurotropic virus that alternates from a lytic cycle in epithelial cells to a latent cycle in neurons. Its lytic cycle takes place in three phases, the immediate early (IE), the early (E) and the late (L).
In the present thesis, we studied the mechanisms that govern infection by Herpes Simplex virus type-1 investigating two directions; the effect of CD40L on the outcome of infection and the methylation profile of host genes during the course of infection.

In the first part, the effect of CD40L on HSV-1 infection was studied and it was found that CD40L directly inhibits infection by HSV-1 following entry of the virus in the host cell. Different stages of viral infection were analyzed as well as antiviral mechanisms with a particular emphasis on autophagy. Collectively, it was demonstrated that HSV-1 is directly inhibited by the activation of the CD40L pathway by a mechanism that is PI3K-dependent and autophagy-independent.

At the second part of the study, the methylation profile of the host cell genome was analyzed during lytic and latent infection by HSV-1 with particular interest on the enzymes associated to epigenetic phenomena. PCR-array analysis showed that there is a great variation in the methylation profile during the immediate early (IE) and early (E) phase of infection while in the late (L) phase of infection and in latently infected cells the methylation profile remains stable, however, different from the steady state methylation of the host. Several histone deacetylase genes were identified as targets for alterations in DNA methylation and an effort was made to correlate the changes in DNA methylation to gene expression and their impact on the progeny virus.

Περίληψη

Ο HSV-1 είναι ένας DNA ιός που ανήκει στην οικογένεια των ερπητοϊών (*Herpesviridae*) και συγκεκριμένα στην οικογένεια των α-ερπητοϊών (*Alphaherpesvirinae*). Είναι νευροτρόπος ιός ο οποίος πραγματοποιεί λυτικό κύκλο στα επιθηλιακά κύτταρα ενώ στα νευρικά κύτταρα βρίσκεται σε λανθάνουσα φάση. Ο λυτικός κύκλος του HSV-1 λαμβάνει χώρα σε τρεις φάσεις, την άμεσα πρώιμη (α), την πρώιμη (β) και την όψιμη(γ) και αποτελεί χαρακτηριστικό τρόπο έκφρασης των γονιδίων των ερπητοϊών.

Στα πλαίσια της παρούσας διδακτορικής διατριβής διερευνήθηκαν μηχανισμοί που διέπουν την μόλυνση από τον ιό του απλού έρπητα τύπου Ι (HSV-1). Συγκεκριμένα, διερευνήθηκε η δράση του CD40L και ο ρόλος του στην έκβαση της μόλυνσης από τον HSV-1. Επιπλέον, διερευνήθηκε το πρότυπο μεθυλίωσης κυτταρικών γονιδίων σε διάφορα στάδια της μόλυνσης από τον ιό.

Ως προς το πρώτο σκέλος της εργασίας, κατά την οποία διερευνήθηκε η δράση του CD40L στην μόλυνση από τον HSV-1, βρέθηκε ότι ο CD40L παρεμποδίζει την εξέλιξη της μόλυνσης άμεσα, μετά την είσοδο του ιού στο κύτταρο. Μελετήθηκαν διάφορα στάδια της μόλυνσης καθώς κ αντιϊκοί μηχανισμοί ενώ έμφαση δόθηκε στον μηχανισμό της αυτοφαγίας. Συνολικά, ο ιός παρεμποδίζεται από την ενεργοποίηση του μονοπατιού του CD40L μέσω ενός μηχανισμού που σχετίζεται με την κινάση PI3K και είναι ανεξάρτητος της αυτοφαγίας.

Ως προς το δεύτερο σκέλος της διατριβής, μελετήθηκε το πρότυπο μεθυλίωσης του κυτταρικού γονιδιώματος σε λυτική κ λανθάνουσα μόλυνση με τον ιό HSV-1 δίνοντας ιδιαίτερη έμφαση στο πρότυπο μεθυλίωσης γονιδίων που κωδικοποιούν για ένζυμα που σχετίζονται με επιγενετικά φαινόμενα. Βρέθηκε ότι στην άμεσα πρώιμη κ πρώιμη φάση του λυτικού κύκλου υπάρχει έντονη διακύμανση των επιπέδων μεθυλίωσης των κυτταρικών γονιδίων ενώ στην όψιμη φάση της μόλυνσης και κατά τη λανθάνουσα κατάσταση το πρότυπο μεθυλίωσης είναι διαφορετικό από την κατάσταση ηρεμίας αλλά σταθερό.

Contents

1.Introduction

Herpes Simplex Virus type 1 (HSV-1 or HHV-1) is a dsDNA virus that belongs to the alpha subfamily of the family *Herpesviridae*[1]. It is a neurotropic virus characterized by a relatively short life cycle, a rapid cytopathic effect (CPE) and an ability to establish latent infections in sensory ganglia. Sensory neuron infection is the result of a primary infection of a mucosal epithelial surface usually during childhood or adolescence. The virus follows a lytic replicative cycle in the epithelia before entering neuronal cell bodies surrounding the infected area via retrograde transport[2].

HSV-1 worldwide seroprevalence rates have been found to fluctuate between 50-90%[3,4]. Its clinical manifestation varies from asymptomatic which is the most common, to severe neurological conditions such as encephalitis. Generally, HSV-1 infections display combinations of symptoms such as fever, sore throat, ulcerative and vesicular lesions, gingivostomatitis, edema, localized lymphadenopathy, anorexia and malaise while infection of the eye can cause keratoconjunctivitis[5]. Recent data have demonstrated that there is also a strong association between HSV-1 and Alzheimer's disease[6,7].

Pathology and Epidemiology of HSV-1.

HSV-1 clinical manifestations, though characterized by cold sores, vary from asymptomatic, to severe neurological conditions such as encephalitis. Generally, HSV-1 infections display combinations of symptoms such as fever, sore throat, ulcerative and vesicular lesions, gingivostomatitis, edema, localized lymphadenopathy, anorexia and malaise while infection of the eye can cause keratoconjunctivitis. Recent data have demonstrated that there is also a strong association between HSV-1 and Alzheimer's disease[8,9].

HSV is a human virus and is transmitted only from infected humans to other humans during episodes of productive infection and by close personal contact. There is no seasonal variation of HSV infection frequency. The infection is rarely fatal and since this virus becomes latent and persists for the lifetime of the host, more than 50% of the world population has been infected[9].

Reactivation of the virus can be triggered by a variety of factors such as stress, ultraviolet light, fever, fatigue, sideropenia and impaired cell mediated immunity in the host (reviewed in [10]). However, in immunocompetent individuals, HSV infection is usually self-limiting. On the contrary, it causes significant morbidity and mortality in immunocompromised individuals who are in danger of acute herpetic disease. For neonates infected in utero or during delivery HSV infection can be lethal. In USA approximately 1500 newborns are infected each year and despite the availability of antiviral therapies, the mortality rate is still high. AIDS patients are also at high risk of severe herpetic disease and most drug resistant HSV strains derive from those patients. There are also some immunocompetent hosts that suffer from serious herpetic disease. Ocular infection is another serious condition. Recurrent herpes

keratitis can cause corneal scarring and blindness. Moreover, central nervous system HSV infections or encephalitis can lead to death despite the antiviral therapies and even in those patients that manage to overcome encephalitis severe neurological conditions persist.

As mentioned above, it is estimated that more than 50% of the world population has been infected. Studies in more specific groups have shown some variability between populations yet the general tendency is that HSV-1 prevalence in non-high risk populations increases with age or plateaus after about 30 years of age with most acquisition taking place in childhood and adolescence. It has also been estimated that HSV-1 seroprevalence is lower at higher socioeconomic groups[10]. A USA based population study showed that HSV-1 seropositivity increased from 44% in young adults aged 12-19 years to 90% in adults over 70 years old. In contrast, HSV-1 seroprevalence decreased in women over 40 years old in Uganda, New Mexico and Turkey[11]. In European countries, namely Germany and Spain, 40-50% of adolescents aged 14-17 years have HSV-1 antibodies and the percentage reaches 90% by the fifth decade of life[10].

Concerning high risk populations, such as South Africa populations that practice higher risk sexual behaviors, HSV-1 seroprevalence is over 97% in all age groups. Among young, female, commercial sex workers aged 16-22 years in Mexico City HSV-1 seroprevalence was over 93% (reviewed in [11]).

Nevertheless, worldwide epidemiology of HSV-1 is not static. There has been a decline in the age specific HSV-1 prevalence rates in industrialized middle class populations over the past years. For instance, pre-adolescent populations in the UK in 1953 exhibited a 63% HSV-1 seroprevalence which decreased to 23% in 1995 probably due to improved socioeconomic conditions[10].

To sum up, global HSV-1 prevalence is high regardless of the fluctuations in percentages while aggravating factors which are latency and recurrent infections prevent eradication of the disease. Those data point to the direction of discovering new more efficient drugs that target the central regulation machinery of HSV-1.

Classification of Herpesviruses

The first attempt to classify herpesviruses was undertaken in 1971 by the International Committee on Taxonomy of Viruses (ICTV) mainly on the basis of structure. In general, the classification of herpesviruses incorporates morphological, serological, biological and genomic criteria. Though morphological criteria have a prominent role in the classification of herpesviruses, recent advances in sequencing methods have dominated herpesvirus taxonomy[12].

In order for a virus to be classified as a member of the *Herpesviridae* family it needs to satisfy some fundamental morphological criteria. The virion should be spherical, consist of an icosahedral capsid, a tegument and an envelope and the genome inside the capsid should be linear double stranded DNA [13,14].

Serological criteria are also useful, but only on the basis of characterizing closely related viruses, while biological criteria mainly refer to the host. Herpesviruses are particularly adapted to their host and can cause severe disease mainly to immunocompromised individuals. Individual herpesvirus species usually infect a specific host though cross-species transmission can occasionally occur. They are transmitted via aerosols or via contact with infected mucosal surfaces and they have evolved intricate mechanisms to cause lifelong latent infections.

As for genomic criteria, they used to refer mainly to the genome structure but this criterion is not particularly useful since similar structures are common among the family. However, sequencing data, both from nucleotide and amino acid sequences, are of great significance to herpesvirus taxonomy[12].

The order *Herpesvirales* is so far divided in three families, the *Alloherpesviridae*, the *Herpesviridae* and the *Malacoherpesviridae* family (Table 1). The *Alloherpesviridae* family integrates the fish and frog viruses, the *Herpesviridae* family is the one containing viruses of mammals, birds and reptiles and the *Malacoherpesviridae* family contains two viruses of mollusks[1,15]. The *Herpesviridae* family is further divided in three subfamilies, the *Alphaherpesvirinae,* the *Betaherpesvirinae* and the *Gammaherpesvirinae* (Fig. 1.1).

Alphaherpesvirinae are characterized by a variable host range, a short life cycle, a rapid spread in culture conditions, an intense cytopathic effect and an ability to establish latent infections mainly in sensory ganglia. Among others the Alphaherpesvirinae contain the human affecting genera *Simplexvirus* (HSV-1 or HHV1 and HSV-1 or HHV2) and *Varicellovirus* (VZV or HHV3).

Betaherpesvirinae, in contrast to alphaherpesviruses are more restricted in their host range, they progress slowly in culture conditions and they have a long life cycle. They also cause a distinctive enlargement of their host cells called cytomegalia. Betaherpesviruses establish latent infections as well, but in contrast to alphaherpesviruses they do so in secretory glands, lymphoreticular cells, kidneys and other tissues. *Betaherpesvirinae* genera that contain human herpesviruses are the *Cytomegalovirus* genus (HCMV or HHV5) and the *Roseolovirus* genus (HHV6 and HHV7).

Order	*Herpesvirales*
Family	*Herpesviridae*
Subfamily	*Alphaherpesvirinae*
Genus	Iltovirus
Genus	Mardivirus
Genus	Scutavirus
Genus	Simplexvirus
Genus	Varicellovirus
Subfamily	*Betaherpesvirinae*
Genus	Cytomegalovirus
Genus	Muromegalovirus
Genus	Roseolovirus
Genus	Proboscivirus
Subfamily	*Gammaherpesvirinae*
Genus	Lymphocryptovirus
Genus	Rhadinovirus
Genus	Macavirus
Genus	Percavirus
Family	*Alloherpesviridae*
Genus	Batrachovirus
Genus	Cyprinivirus
Genus	Ictalurivirus
Genus	Salmonivirus
Family	*Malacoherpesviridae*
Genus	Aurivirus
Genus	Ostreavirus

Table 1.1. Taxonomic structure of the order *Herpesvirales*[15]

Last, *Gammaherpesvirinae* limit their host range to a family or order of organisms. They are lymphotropic viruses and they can all replicate in lymphoblastoid cells in vitro. Some can additionally cause lytic infection to epithelial cells and fibroblasts. However, gammaherpesviruses are usually specific for B or T lymphocytes. There are two genera containing human herpesviruses in this subfamily, the *Lymphocryptovirus* genus (EBV or HHV4) and the *Rhadinovirus* genus (Kaposi's sarcoma-associated herpesvirus or HHV8)[14].

In respect of evolution, the herpesviruses precise origins have not yet been deciphered. There is evidence though of an evolutionary relationship between herpesviruses and bacteriophages. Similarity has been detected between a terminase gene encoded by HSV-1 and a bacteriophage gene of related function. In addition, conserved unique protein folds consisting of three α-helices and two β-sheets have been found in the capsids of both herpesviruses and bacteriophages[16].

Within the Herpesviridae family, the alpha-, beta- and gammaherpesviruses have arisen from a common ancestor. Although there is apparently little genetic similarity between the three subfamilies, the capsid structures are highly conserved. There is some controversy over the evolutionary succession of alpha-, beta- and gammaherpesviruses but it is well accepted that herpesviruses evolved in parallel with their hosts[16,17].

As for Herpes simplex virus type 1 (HSV-1) or Human herpesvirus 1 (HHV-1), genus *Simplexvirus*, it belongs to the subfamily of *Alphaherpesviruses* of the family *Herpesviridae* in the order of *Herpesvirales*.

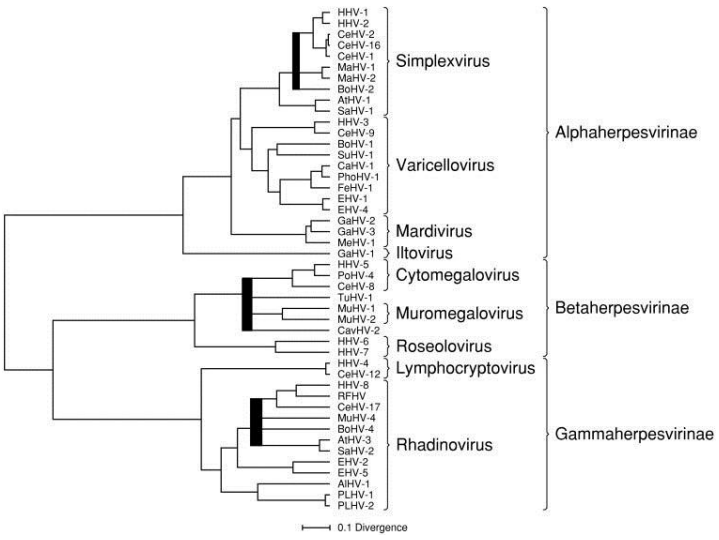

Figure 1.1: Phylogenetic relationships within the family Herpesviridae. The unrooted Bayesian tree is based on amino acid sequence alignments for the orthologs of HHV-1 genes UL15, UL19, UL27, UL28, UL29 and UL30. The scale indicates the number of amino acid substitutions per site. (Adapted from McGeoch, D.J., Davison, A.J., Dolan, A., Gatherer, D. and Sevilla-Reyes, E.E. (2008). Molecular evolution of the Herpesvirales. In: Origin and Evolution of Viruses, 2nd edn (E. Domingo, C.R. Parrish and J.J. Holland, Eds.), Elsevier, London, pp. 447–475; [12]

HSV-1 Structure

HSV-1, bears the characteristic morphology of all herpesviruses, more specifically a dsDNA core surrounded by an icosahedral capsid, an amorphous tegument and an envelope[14] (Fig.1.4).

The DNA core consists of a linear double stranded DNA molecule wrapped as a toroid[18] or a spool[19] in a liquid crystalline state[20] which occupies most of the capsid space. The DNA of the virus is 152kb and it is not chromatinized inside the capsid, i.e. it does not contain any histones. Given the negative charge of the DNA backbone, the presence of the polyamines spermine and spermidine[21] are indispensable to packaging. Moreover, packaging of DNA in the capsid is a process that requires ATP. The internal capsid pressure has been measured to tens of atmospheres and constitutes a propelling mechanism for entrance of the viral DNA in the host nucleus, another feature that HSV-1 shares with bacteriophages[22].

The capsid is a T=16 icosahedron that occupies one third of the volume of the virus[23]. It consists of 162 capsomeres, more specifically 150 hexons and 12 pentons[14]. One of the pentons is called the portal and exhibits a very specific structure that enables the entry of the viral DNA to the capsid[24] (Fig. 1.2). The location of the capsid inside the envelope is such, that there is a distal pole and a proximal pole to the envelope[23].

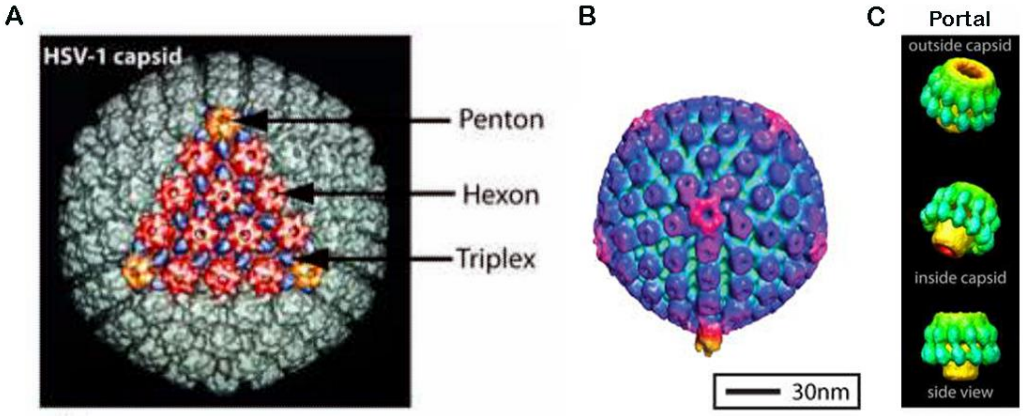

Figure 1.2: (A) Structure of the capsid highlighting one of the capsid faces illustrated in color with the hexons, pentons and triplexes shown in red, orange and blue, respectively[25]. **(B)** Portal complex located beneath a unique vertex of the capsid shell[26]. **(C)** Structure of HSV-1 portal. The portal is cylindrical in shape with 12- fold rotational symmetry and an axial channel through which virus DNA enters and exits the capsid [25].

There are three kinds of capsids that can be detected inside a host cell infected with HSV-1, the A, B and C capsids. The A capsids have no core structure –they are empty- while the B capsids contain an assembly scaffold but not the viral genome. Only C capsids carry the herpesviral genome and therefore A and B capsids are considered developmental dead ends[25]. The assembly of the capsid takes place inside inclusion bodies in the host nucleus and is orchestrated is three stages: assembly of partial procapsids, assembly of a spherical procapsid and lastly formation of the icosahedral

capsid[27]. Formation of the capsid starts by assembly of the major capsid protein VP5 and the scaffolding protein pre-VP22a that form angular parts of the spherical procapsid. The proteins VP19C and VP23, called the triplex proteins, act as glue to hold the capsomers together as the capsid assembles. The portal is incorporated in the structure at the initiation of the procapsid formation by a unique mechanism ensuring that there is only one portal per capsid[28]. Gradually the spherical procapsid is formed. It has the same icosahedral symmetry as the mature capsid and the same diameter, i.e. 125nm but it is not polyhedral. DNA enters the capsid at the spherical procapsid phase while the scaffolding protein is cleaved by a viral protease and exits the procapsid. At that point the capsid becomes angular and takes its mature form[25] (Fig. 3).

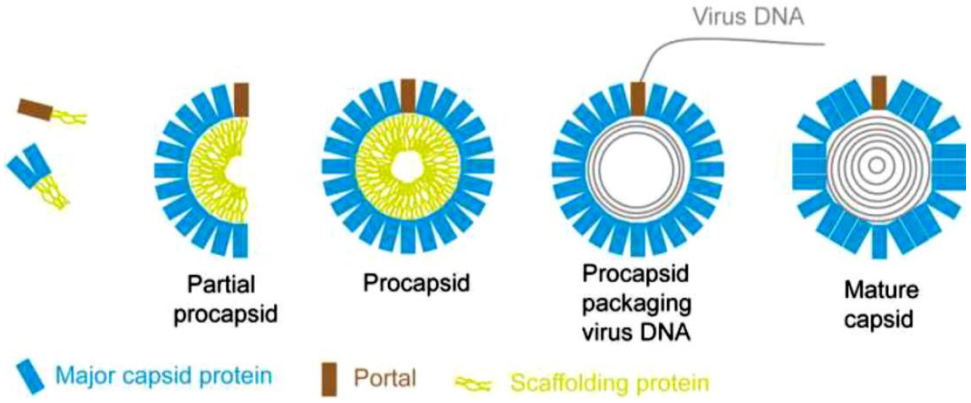

Figure 1.3: Illustration of the capsid formation. Adapted from Brown JC et al, (2011)[25]

The tegument is an "amorphous" proteinaceous layer located between the capsid and the envelope[14] that occupies two thirds of the space defined by the latter[23]. The structure of the tegument has not been fully characterized but it has been shown lately that there are capsid-associated and envelope associated layers[19,23,29] and that there is a characteristic distribution of tegument proteins near the capsid[30]. In addition, there is accumulation of tegument material over the capsid pentons[19] while at sites where there are spikes on the surface of the envelope the tegument is connected to the envelope by linkers[23]. Furthermore, there have been detected some filamentous structures up to 40nm long suggesting that either there is a polymer in the tegument or that actin filaments are packaged from the host cell[31]. Lastly, it has been found that upon binding to the host cell the structure of the tegument is altered[32]. So the tegument is not exactly amorphous as was originally believed. Moreover, it carries proteins that are critical to the initiation of infection, among which is the protein pUL36 that is essential for capsid transport[30,33] and release of the viral DNA and VP16 which is a fundamental transcription factor for initiation of the viral gene transcription[34].

Lastly, the envelope is the exterior of the virus, the part that interacts directly with its environment. It consists of a lipid bilayer in which they are embedded about 13

distinct glycoproteins of the virus. The copy numbers of each protein vary from just a few to thousands. The viral glycoproteins form 600-750 functional clusters that emerge from the membrane as spikes. The envelope originates from the cytoplasmic membrane of the host cell and is different from the nuclear membrane though the virus initially buds from the nucleus[14,23].

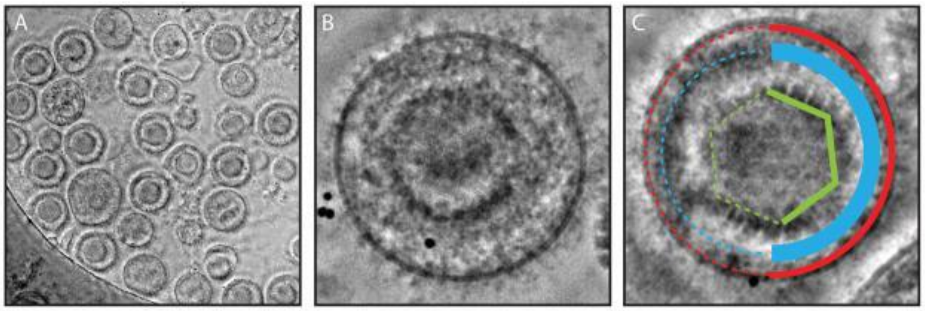

Figure 1.4: Virions and their components (Red: Envelope, Blue: Tegument, Green: Capsid)[26]

HSV-1 Genome Organization

HSV-1 genome is a double stranded linear molecule. However, its ends are either held together or they are in close proximity since HSV-1 DNA rapidly circularizes in the absence of protein synthesis after it enters the nucleus. The genome is 152kb long, its G+C content is 68.3% and it does not contain any histones inside the capsid.

The genome comprises of two main unique sequences flanked by repeats. The two main sequences are not equal in length and therefore they are termed the long sequence (**L**) and the short sequence (**S**). The L and S sequences are flanked by inverted repeats. The inverted repeats flanking L are the **ab** and **b'a'** (or TR_L and IR_L) sequences and they are different in average base composition from the sequences flanking S. The S sequence is flanked by the **a'c'** and **ca** (or IR_S and TR_S) sequences (Fig. 1.5). The L and S components can invert relative to each other and that leads to the production of four populations of molecules bearing the four orientations of the L and S sequences of the HSV-1 genome. These are the prototype (P), the I_S (Inverted Short) molecule that has the S sequence inverted, the I_L molecule that has the L sequence inverted and the I_{LS} molecule that has both sequences inverted[14,35].

HSV-1 genes are classified in 3 kinetic classes, the α or immediate early genes that are transcribed first, the β or early genes that are transcribed after and with the help of α gene products and the γ genes that are transcribed last. The viral genome contains at least 90 transcriptional units of which 84 encode for proteins. Each transcript encodes for one protein apart from three exceptions: 1) two proteins, ORF-O and ORF-P, are produced by two distinct transcripts but share the same start codon, 2) the gene UL26 produces two proteins from the same transcript by cleavage

of the polypeptide and 3) the mRNA of UL3 contains the ORFs of UL1 and UL2 though UL1 and UL2 are coded from distinct mRNAs.

Some other characteristics of HSV-1 genome are that most HSV-1 genes do not have introns and that there are several transcripts that do not code for protein. Moreover some expressed ORFs are antisense to each other[14].

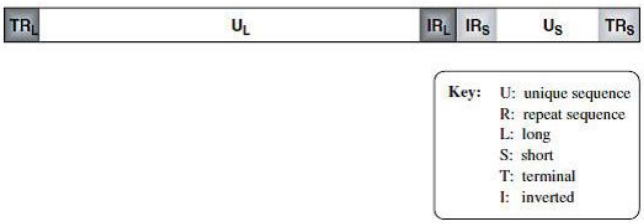

Figure 1.5: HSV-1 genome organization.

Replication

Briefly, in order to initiate infection HSV-1 has to attach to the cell surface of the host cell. Following attachment, it enters the cell either by fusion or endocytosis. The viral capsid utilizes the microtubule network to reach the nucleus. Upon docking on the nuclear pores, the DNA of the virus is released inside the host nucleus and viral transcription and replication events start. As mentioned earlier, HSV-1 genome is classified in three kinetic classes, the α, β and γ genes. Following entrance of the viral DNA in the nucleus, the tegument proteins carried by the virus initiate transcription of the α or immediate early genes. The α gene products act as transcription factors for β genes. The β products are involved in the replication of the viral DNA. The viral DNA replicates with a rolling circle mechanism that produces concatamers of viral DNA that are cleaved in monomers and packaged into capsids. After the replication of the viral DNA the γ genes are transcribed and their products are responsible for the assembly and packaging of the viral DNA. The DNA-containing capsid or nucleocapsid buds through the nuclear membrane or exits through the nuclear pores. Its course towards the cell surface is not fully defined but it's believed that the virion passes through the Golgi where it de-envelopes and re-envelopes gradually acquiring its final structure[14] (Fig. 1.6).

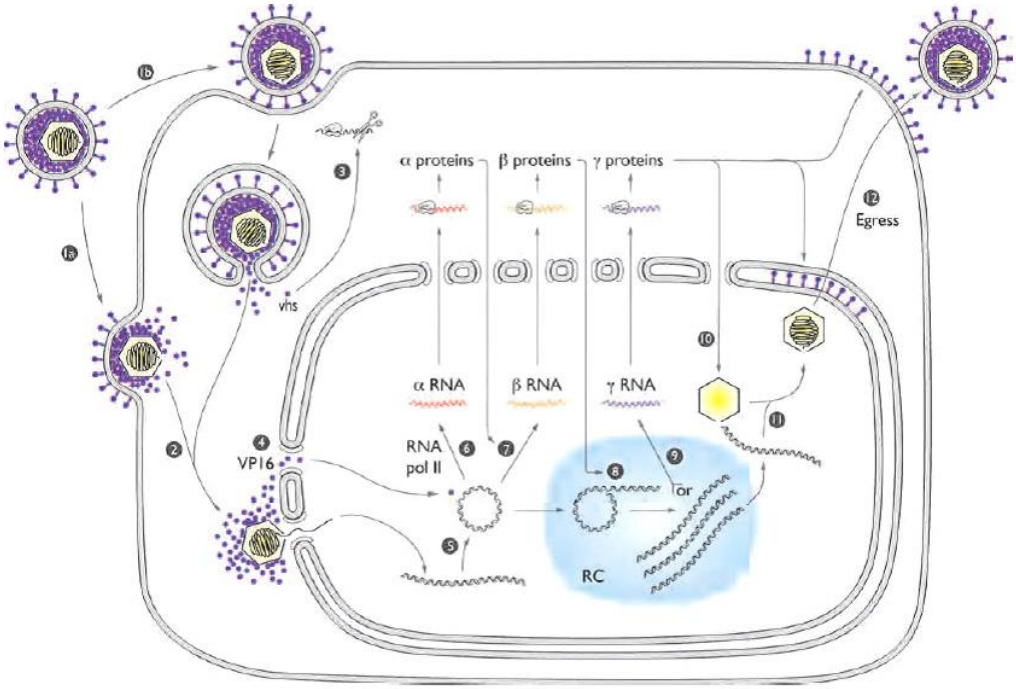

Figure 1.6: Diagram of the replication cycle of HSV. 1: The virus binds to the cell plasma membrane, and the virion envelope fuses with the plasma membrane **(1a)** or the virus enters by endocytosis **(1b**), releasing the capsid and tegument proteins into the cytoplasm. **2:** The capsid is transported to the nuclear pore, where the viral DNA is released into the nucleus. **3:** The *vhs* protein acts to cause degradation of host mRNAs. **4:** VP16 localizes into the nucleus. **5:** The viral DNA circularizes **6:** It is then transcribed by host RNA polymerase II to give first the IE or a mRNAs. IE gene transcription is stimulated by the VP16 tegument protein. Five of the six IE proteins act to regulate viral gene expression in the nucleus. **7:** IE proteins transactivate E or b gene transcription. **8:** The E proteins are involved in replicating the viral DNA molecule. **9:** Viral DNA synthesis stimulates L or g gene expression. **10:** The L proteins are involved in assembling the capsid in the nucleus and modifying the membranes for virion formation. **11:** DNA is encapsidated in the capsid. **12:** The filled capsid buds through the inner membrane to form an enveloped virion, and the virion exits from the cell.[9]

Binding of HSV-1 on the Host Cell

The initial event in HSV-1 infection is binding of the virus on the host cell membrane. Subsequent to binding there is fusion of the viral envelope with the cell membrane or endocytosis, and release of the capsid in the cytoplasm. The process of the viral entry depends on the cell type. Thus, HSV-1 can either enter cells via fusion at the plasma membrane or following endocytosis it can fuse with the membrane of an acidic or neutral endosome and escape to the cytoplasm (Fig. 1.7). In some cells, HSV-1 can also enter by macropinocytosis (reviewed in [36]).

Binding of HSV-1 is achieved with the help of the viral glycoproteins gC and gB that bind heparan sulfate proteoglycans (HSPGs) on the cell surface. Entry of the virus requires the glycoproteins gB, gH/gL and gD. The glycoproteins gB and gH/gL form the core of the viral fusion machinery which promotes viral entry and they are conserved across the *Herpesviridae* family[36,37]. The cellular proteins involved in the process are nectin-1[38,39], herpesvirus entry mediator (HVEM)[40], 3-O-sulfated heparan sulfate[41,42],

integrin αvβ3[43] and paired immunoglobulin-like type 2 receptor alpha (PILRa)[36,44]. Some strains with mutations in gD can also enter via nectin-2[45]. While HSV-1 can enter fibroblasts through various receptors, it requires nectin-1 in order to enter neurons[46–48].

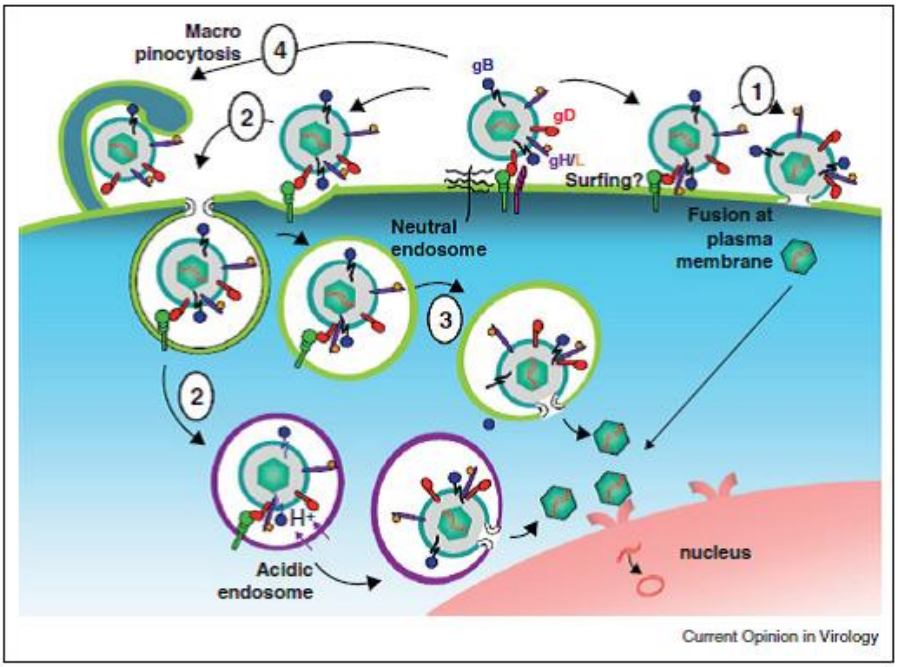

Figure 1.7: HSV entry pathways: (1) fusion at plasma membrane, (2) endocytosis into acidic or (3) neutral endosomes, (4) macropinocytosis[36].

Lytic Infection

Upon entry in the cell, the capsid is transferred to the nucleus either inside an endosome or as it is, in both cases utilizing the microtubule network[33,49]. The inner tegument proteins of HSV-1 recruit dynein or kinesin-1 in order to transport the capsid along microtubules[33,50]. In addition, the tegument protein VP1-2 carries an NLS signal that is indispensable for targeting of the capsid to the nuclear pores[51]. Proteasomal activity is also important at a postpenetration level for transport of the capsid to the nucleus whether it enters via endocytosis or through a non-endocytic pathway[52]. Docking of the capsid on the nuclear pores requires importin-β[53] while viral DNA release in the nucleus involves a mechanism that employs the nuclear pore complex (NPC) and tegument proteins[54] , and is dependent on hydrophobicity[55]. Moreover, VP1-2 has to be proteolytically cleaved in order for the viral DNA to be released from the capsid[56].

When the capsid docks on the nuclear pores the viral DNA enters the nucleus independently of the viral protein 16 (VP16), a tegument protein that acts as the transcriptional activator of the immediate early (IE) genes. However, VP16 not only colocalizes with, but also targets the HSV-1 genome to the nuclear lamina, where it

keeps it in a euchromatin state and assembles the transcactivator complex[57–59]. In the nuclear periphery the viral DNA circularizes in the first hour following entry of the virus in the cell[60]. Cellular components are also recruited towards the area; more specifically, components of the promyelocytic leukemia protein (PML) nuclear bodies or ND10 such as PML, Sp100 and hDaxx are recruited to the nuclear periphery and form de novo ND10 structures that are associated with viral genomes and develop into viral replication compartments[61–63].

As mentioned earlier, the viral gene products are divided in three main categories, the α gene products or immediate early (IE), the β gene products or early (E) and the γ gene products or late (L). The β genes products are further divided in the β1 (early-early) and β2 (early-late), and the γ gene products are divided in the γ1 (leaky-late) and γ2 (true late). After circularization of the genome, the immediate early genes are transcribed with the help of the VP16 transactivator complex that comprises of VP16, the transcription factor Oct-1 and the cellular factor HCF-1 (host cell factor) which carries the nuclear localization signal (NLS) that targets the complex to the nucleus[14,64]. Transcription of the IE mRNAs is facilitated by the host RNA polymerase II and the six products produced are ICP0, ICP4, ICP22, ICP27, Us1.5 and ICP47. Their role is to activate early genes and interfere with the hosts' innate immunity. The early products are required for the replication of the viral genome and act as transcription factors for the late products. Lastly, the late genes code for structural proteins of the virus while translation of at least some of the γ2 genes also requires viral DNA synthesis[14].

Viral DNA synthesis starts from an origin site (oriL or ori S) where the viral origin-binding protein UL9 initiates unwinding of the DNA. Then UL9 recruits the single stranded DNA-binding protein ICP8 to the replication fork. Finally, the helicase-primase complex consisting of the three viral proteins UL5, UL8, and UL52 and the viral DNA polymerase catalytic subunit UL30 with its processivity factor UL42 are also recruited at the site. Assembly of the complexes on the replication fork leads to initiation of viral DNA replication through a theta form intermediate which generates several circular molecules. Eventually, the replication continues by an origin-independent rolling circle mechanism[9,65].

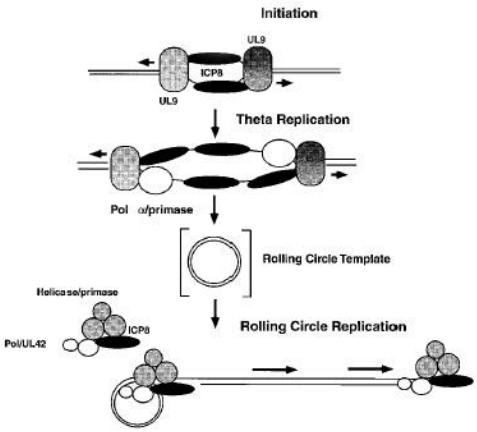

Figure 1.8: Model for the replication of the HSV-1 genome. The initial transient phase of theta replication is followed by a rolling circle model[65].

The nucleocapsid is assembled inside the nucleus and it initially contains the scaffolding protein pre-VP22a[25]. The viral DNA, replicating through a rolling circle mechanism, produces concatamers of herpes DNA that are encapsidated via an

energy-dependent mechanism. Insertion of the viral DNA occurs in parallel with removal of the scaffolding proteins. The L region enters the capsid first and the concatamer is cleaved near the packaging signals pac1 and pac2[66,67].

Once the mature nucleocapsid is formed, it exits the nucleus and traverses the cell towards the surface where it is released to the extracellular space. The way this process is performed is not entirely clear. There are three models on HSV-1 egress, ie the dual pathway, the lumenal pathway, and the nuclear pore egress pathway (Fig. 1.8). There are data for all of them but the first model is considered the most prominent one. According to the dual pathway or envelopment–de-envelopment–re-envelopment model, the virus undergoes envelopment at the inner nuclear membrane, de-envelopes at the outer nuclear membrane and acquires a new envelope through budding into cytoplasmic membranes such as the Golgi apparatus, the trans-Golgi network (TGN) or the endosomes producing virus-containing vesicles that are exocytosed. The lumenal model supports that after acquiring an envelope at the inner nuclear membrane the virion buds into the outer nuclear membrane, is transported to the plasma membrane and is released. Lastly, according to the nuclear pore egress model the nucleocapsid exits the nucleus from enlarged nuclear pores, buds into cytoplasmic membranes where it acquires its envelope and is transported to the plasma membrane to be released[14]. Studies on the membrane origin of the virion have shown that the envelope derives from the plasma membrane which contradicts the lumenal pathway. The data on the nuclear pore egress model on the other hand are contradictory [68,69] and at least it does not seem to be the primary route for HSV-1 egress. Further research on HSV-1 egress has shown that the viral proteins UL31 and UL34 form the nuclear envelopment complex (NEC) that accumulates in the inner nuclear membrane and is central to nucleocapsid envelopment[70]. However this complex is not detected on extracellular virions[71]. Moreover, the extracellular virion membrane is of TGN/endocytic origin[72,73]. In addition, experiments with gD carrying a mutation that retains it to the ER have shown that while the perinuclear virions contained gD the extracellular virions did not, suggesting that there was a de-envelopment stage[74]. Overall, following nucleocapsid assembly, HSV-1 seems to follow the double envelopment model in order to assemble its virion and exit the cell [9,14,75,76].

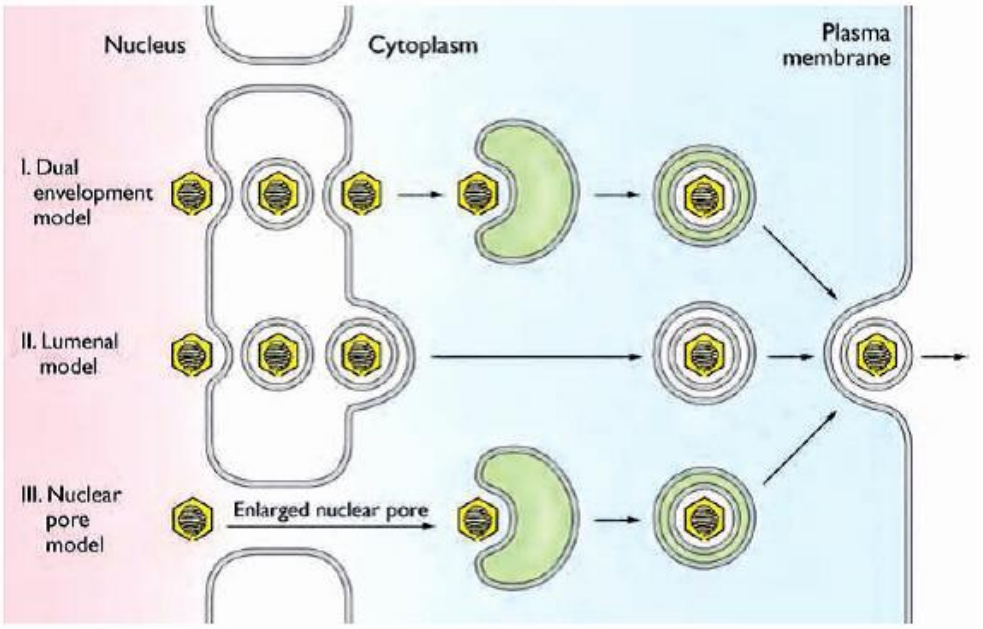

Figure 1.9: Models for egress of HSV-1 from the host cell. I: the dual envelopment model **II:** the lumenal model **III:** the nuclear pore complex model[9]

Latent Infection and Reactivation

HSV-1 is a neurotropic virus characterized by its ability to establish lifelong latent infections in sensory neurons. Latency is a state during which the virus remains dormant and there is no production of infectious virions until it reactivates. In the case of HSV-1, the virus enters sensory neurons that innervate the infected dermatome during a lytic infection, it is translocated to the neuronal nucleus via anterograde transport and it initially replicates. The replication is terminated soon after infection but the viral DNA persists in the neuron as a circular episome and reactivates upon stress stimuli[2].

During latency the viral genome is silenced and is associated with nucleosomes[77]. Only the region that codes for LATs, the Latency Associated Transcripts, remains active. There have been identified insulator elements that prevent silencing of LAT, keeping it in an active state, while outside the boundaries of these elements it remains in a heterochromatic state[78]. LATs are transcripts that are not translated into proteins and they are abundant during latent infection. The primary transcript is 8.3kb and maps to the inverted repeats flanking the U_L region. There are two major species processed from the 8.3 kb transcript, two introns 2 kb and 1.5kb, that accumulate in the nuclei of latently infected neurons. Accumulation of LATs is associated with increased heterochromatin on lytic genes[9,79]. Interestingly, the LAT promoter exhibits enhanced activity in neurons and there are neuron-specific transcription factors that bind to it[80].

Another key molecule thought to be involved in the regulation of HSV-1 state is the IE protein ICP0. ICP0 forms a complex with an HDAC repressor complex, namely the

RE1 silencing transcription factor corepressor to REST, (REST/CoREST)-HDAC repressor complex, dissociating HDAC1 from the latter[81,82] and possibly preventing the complex from regaining its repression activity[83] .

However, silencing of the viral genome does not happen instantly. The naked nucleocapsid is transported to the nucleus along microtubules and the α, β, γ and LAT transcripts are detected in neuronal cells over the first 24 to 72 hours [9]. One of the factors crucial to the establishment of latency is likely the decrease in the expression of α genes in combination with the accumulation of LATs. There are several reasons for the decrease of α proteins. For instance, neuronal repressors of α gene expression such as REST, repression of viral expression by NGF (neuronal growth factor), low availability of Oct-1 in neurons and retention of HCF-1 in the cytoplasm, all contribute to the reduction of IE gene products. Since ICP0, an α protein antagonizes histone-mediated gene silencing by interfering with the activity of HDACs, blocking of its expression promotes the accumulation of heterochromatin on HSV-1 genome which is characteristic of latency[2,9].

The model that has been proposed by D.M. Knipe and A. Cliffe in 2008 is that the balance between lytic and latent infection is epigenetically regulated. Specifically, the proposed model is that in epithelial and other non-neuronal cells, viral proteins function towards reducing histone association with viral lytic gene promoters and promoting euchromatin histone modifications on those histones associated with viral DNA. Yet, in neuronal cells, to which LAT shows specificity as mentioned above, HSV-1 activity causes the acquisition of heterochromatin marks on viral lytic gene promoters so that lytic genes are silenced and a latent state can be established[83].

Reactivation in neurons occurs upon stress stimuli such as exposure to UV, hyperthermia, physical or emotional stress, menstruation and hormonal imbalance. The exact series of molecular events that lead to reactivation are not yet delineated and many aspects of the process are still debated, such as the fate of neurons following reactivation. Moreover, it is still not clear if the virus follows the α, β, γ activation cascade that is customary of the lytic cycle. Concerning virion egress, it has been shown that there are two mechanisms of anterograde transport. Either intact virions undergo anterograde transport, or viral capsids and vesicles containing viral glycoproteins are transported independently. Lastly, HSV-1 can be released either from the axonal shaft or terminus[9].

Virus-Host Interactions

HSV-1 has been coevolving with humans since their speciation[84] and has adapted to the cell's immune response alternating from a lytic to a latent state depending on the dynamics of the cellular environment. From the moment HSV-1 attaches to the cell surface, it has to circumvent several immune defense mechanisms in order to establish lytic infection.

One of the first interactions of HSV-1 with the host cell is binding of the glycoprotein D (gD) on HVEM. Apart from mediating fusion with the plasma membrane, gD also exhibits antiapoptotic properties[85]. Inhibition of apoptosis is also mediated by glycoprotein J which also facilitates the production of reactive oxygen species (ROS) upon infection[86–88]. Another glycoprotein, gC protects the virus from cytolysis by complement either on the virion or on the surface of the infected cell[89–91].

Following entry, the viral endoribonuclease UL41 or vhs (virus host shutoff)[92,93] that resides in the tegument, cleaves all cellular mRNAs. Moreover, it has been shown that in cerebellar granule neurons (CGNs) vhs protects cells from apoptosis in the onset of infection[94]. In systems of dendritic cell infection, it has been shown that vhs can block the activation of cDCs through a TLR-independent pathway[95] and that deletion of vhs enables the activation of DCs[96]. Lastly, vhs prevents the production of the IFN-inducible, antiviral protein viperin by reducing the accumulation of its mRNA[97].

Another key molecule for the outcome of HSV-1 infection is the viral protein ICP0. ICP0 is an immediate early protein that is also packaged in the tegument[98] and has E3 ubiquitin ligase activity. After the virus enters the cell, ICP0 is targeted to ND10 bodies and prevents their antiviral effect via degradation of PML and SP100. Moreover it targets the nuclear DNA sensor IFI16 inhibiting that way IRF3 signaling[99] while it also abrogates IRF3 activity at later stages of infection by retaining it to the cytoplasm[100]. ICP0 also interferes with a negative feedback loop that regulates TLRs, ie deubiquitination of TRAF6 and IKKγ by USP7 that leads to termination of the NFkB and JNK signaling activated after the TLRs are engaged. Specifically, ICP0 causes the translocation of USP7 to the cytoplasm that exerts its role in abrogating the TLR response[101].

Apart from a role in dampening the immune response, ICP0 also has an active role in preventing repression of the viral genome. Thus, ICP0 dissociates HDAC1 or HDAC2 from the HDAC-RCOR1-REST-KDM1A repressor complex, also localized at ND10 structures[81]. In addition, ICP0 interacts with, and degrades proteins of the DNA repair pathway, more specifically RNF8 and RNF168[102]. RNF8 and RNF168 are histone ubiquitin ligases that anchor repair factors at sites of DNA damage. This way, ICP0 prevents the deposition of repressive ubiquitin marks on the viral genome[103]. A recently identified target that is degraded by the viral protein is the transcriptional repressor TRIM27. Paradoxically, depletion of TRIM27 prevents replication of HSV-1 suggesting that there is a more complex regulation for this molecule [104].

The immediate early protein ICP27 regulates alternative splicing of the host mRNA and promotes the transport of viral, intronless mRNAs[105,106] via the export receptor TAP[107]. One of the targets of ICP27 is again PML. ICP27 disturbs normal splicing of PML mRNA by inhibiting removal of the intron 7a[108]. Furthermore, in conjuction with vhs, ICP27 blocks the cell cycle at the G1 phase by inhibiting host gene transcription[109]. Finally, ICP27 also has an effect on immune suppression of the host

cell and it has been found to suppress phosphorylation of STAT-1 as well as phosphorylation and ubiquitination of IkBα[110,111].

An additional immediate early protein, ICP22, exerts its effect on the host by interfering with the phosphorylation of RNA polymerase II [112]. In conjunction with US1.5, a viral product coded from a domain inside the ICP22 ORF, ICP22 regulates cell-cycle associated proteins of the S-phase to support virus replication[113]. Finally, the immediate early product ICP47 binds to TAP (transporter for antigen processing) with a higher affinity than other peptides and prevents antigen presentation by MHC class I molecules[114].

Of the early products of HSV-1, UL12.5, is of particular interest since it has been shown to recruit the mitochondrial nucleases ENDOG and EXOG in order to degrade mitochondrial DNA (mtDNA)[115].

ICP34.5 is a leaky late (γ1) product of HSV-1 and is characterized as a neurovirulence factor. Via ICP34.5, HSV-1 can block autophagy in neurons through binding to Beclin-1, a major autophagosome component essential for neuron survival[116], and inhibiting its autophagy function[117]. Furthermore, ICP34.5 is regulated by viral microRNAs encoded by the latency-associated transcript (LAT) of both HSV-1 and HSV-2[118,119]. ICP34.5 also has a role in the inhibition of host immune response. By forming a complex with TBK1 it disrupts its interaction with IRF3 preventing the latter from activating the interferon stimulated promoters[120]. Moreover it affects EIF2a activity. EIF2a is phosphorylated by PKR upon viral infection and this leads to translational shutoff. ICP34.5 bridges EIF2a with the protein phosphatase PP1 which causes dephosphorylation of EIF2A and override of the translation shutoff posed by the cell as an antiviral mechanism[121,122].

UL24 is also a leaky late protein of HSV-1. Its role is to cause a cell cycle arrest from the G2 to the M phase by inactivating the mitotic cyclinB/cdc2 complex, allowing HSV-1 to replicate its genome before the cell enters mitosis [123].

Glycoprotein B in cooperation with US3, prevent antigen presentation and NKT cell function by inhibiting the recycling of CD1d to the cell membrane. gB binds to CD1d and retains it to the trans Golgi network (TGN) while US3 is required for the enrichment of TGN in gB[124]. US3 also interferes with the apoptotic pathway of the cell and blocks apoptosis[86,125,126].

Glycoproteins gE and gI act in concert to neutralize anti-HSV antibodies by creating an Fc receptor. Specifically, antibodies bind through their Fc domain to the gE/gI complex leaving the infected cell surface clear of antiviral IgG[127,128].

Finally, the true late protein US11 has a role both in inhibiting apoptosis[129] and also in blocking autophagy and autophagosome formation[130].

This short review of viral host interactions makes it clear that most of them belong in the following categories: inhibition of apoptosis, immune evasion, prevention of silencing, cell cycle modulation as well as autophagy modulation. Co-evolution of HSV-

1 with its human host has led to this intricate web of interactions which can lead to a lytic or latent infection depending on the dynamics of the cellular environment.

Epigenetics of Infection

Epigenetics refers to chromatin modifications that alter gene expression without altering the DNA sequence[131,132]. Two major mechanisms that have been identified are histone modifications and DNA methylation. They both respond to developmental and environmental stimuli and they control genomic imprinting, X-chromosome inactivation, heterochromatin formation, transcriptional regulation and DNA damage repair. However, the definition of epigenetics remains a matter of debate with scientists arguing on which parameters can be included as well as on the causality of the modifications[133]. It has also been proposed that epigenetic modifications comprise an ON-OFF switch and the ON or OFF state is heritable even if the original stimulus disappears[134].

Regarding histone modifications and DNA methylation, they regulate repression and derepression of the genome. In more detail, DNA is condensed into chromatin. Chromatin comprises of nucleosomes and DNA is wrapped around them. Nucleosomes are tetramers of the core histone proteins H2A, H2B, H3 and H4 and there is also a linker histone (H1) that links DNA to the nucleosome. Core histone modifications result in a more relaxed or more condensed chromatin, euchromatin or heterochromatin respectively, and cause DNA expression or silencing. Acetylation of histone tails (parts of the histone molecules that stick out of the nucleosomes) by acetyltransferases leads to relaxation of DNA packaging and is associated with active gene expression. Histone methylation can lead either to silencing or decondensation of the genome depending on the specific modification. For instance H3K9me2,3, H3K27me3, H4K20me3 are associated with heterochromatin while H3K4me2,3 is associated with euchromatin (reviewed in[83]). As for DNA methylation it has been traditionally considered a repressive mark especially when it is observed on CpG islands on promoters. Recent advances in methylation sequencing have shown that this might not be the case and that extensive methylation might not correlate with silencing (reviewed in [133]).

Considering HSV-1, the transition from a lytic to a latent infection and vice versa constitutes an epigenetic event which results from the interplay between the cell's silencing mechanisms of viral genes and the virus's own activating mechanisms. HSV-1 genome is not associated with histones inside the capsid. Once it enters the host cell nucleus there is a rapid accumulation of histones on the viral genome. However, during lytic infection HSV-1 viral proteins induce the reduction of heterochromatin and maintain the viral genome in an active state. On the contrary during latent infection heterochromatin on the viral genome is increased and the only sequence transcribed is LAT (Fig.10).

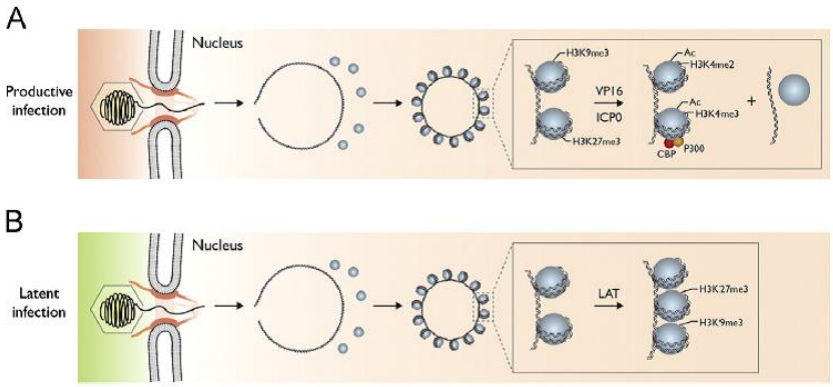

Figure 1.10: Model for epigenetic regulation of the lytic versus latent infection by HSV. (A) Productive infection **(B)** Latent infection[135]

The immediate early viral protein ICP0 possesses a central role in the regulation of viral genome expression[136]. During lytic infection, it causes the increase of euchromatin on the genes related to the lytic cycle and in parallel it reduces the interaction of histones with promoters of the immediate early and early genes[137]. Recovery of ICP0 in cells infected with mutant viruses, leads to acetylation of histone H3 engaged on viral promoters[138]. Relative to this observation is the ICP0 ability to dissociate HDAC1 and HDAC2 from the HDAC-RCOR1-REST-KDM1A repressor complex[81].

Another gene actively involved in the epigenetic regulation of HSV-1 is LAT. As mentioned earlier, LAT shows specificity in neuronal cells and accumulation of LAT mRNAs is associated with increased heterochromatin on lytic genes[9,79].

Autophagy

Autophagy is a highly conserved cellular mechanism with multiple functions. Apart from recycling nutrients for the cell, it is also involved in pathogen removal and antigen presentation[139–141]. Autophagy is triggered by nutrient deprivation hypoxia, high temperature, overcrowding, reactive oxygen species, and endoplasmic reticulum (ER) stress[142]. There are at least three types of autophagy, microautophagy, chaperone-mediated autophagy and macroautophagy. Usually autophagy refers to macroautophagy. Microautophagy involves budding of small vesicles that contain cytosolic material into the lysosomal lumen. Chaperone mediated autophagy proteins bind to the lysosomal transporter LAMP-2a for transfer to the lysosome. Finally, during macroautophagy a cup-shaped membrane called the isolation membrane starts to form, probably originating from the ER that encloses cytoplasmic material. However, apart from the ER, autophagosome formation can also initiate from mitochondrial membranes and the Golgi apparatus. Subsequently, the fully formed autophagosome fuses with lysosomes and the enclosed material is degraded (reviewed in[140]).

Initiation of autophagy requires the ULK complex that comprises of the ULK1 and ULK2 kinases, ATG13, FIP200 and ATG101. The ULK complex is negatively regulated by the mammalian target of rapamycin complex 1 (mTORC1) and positively regulated by AMP-activated protein kinase (AMPK). Normally, mTORC1 binds to the ULK complex and prevents the initiation of autophagy. Upon nutrient deprivation, mTORC1 dissociates from ULK allowing its association with the isolation membrane. Another complex that is involved in the expansion of the isolation membrane is the autophagy-specific class III PI3K complex (or Beclin complex) that comprises of the class III PI3K VSP34, as well as p150, ATG14 and Beclin 1. Once the ULK and Beclin complexes are activated they produce a pool of (PtdIns(3)P) that leads to the nucleation of the isolation membrane. Next, the ATG16L1 complex comprising of ATG5-ATG12 and ATG16L1 is recruited, lipidates LC3 and other ATG8 family members and targets them to the autophagosomal membrane. LC3 is a ubiquitin-like protein and its lipidated form (LC3-PE or LC3-II) is considered a specific autophagosome marker. Moreover LC3 functions as an adaptor molecule that enables selective autophagy. Following formation, the autophagosome can fuse with endocytic compartments such as early and late endosomes and multivesicular bodies (MVB) before fusing with the lysosome (reviewed in[143]).

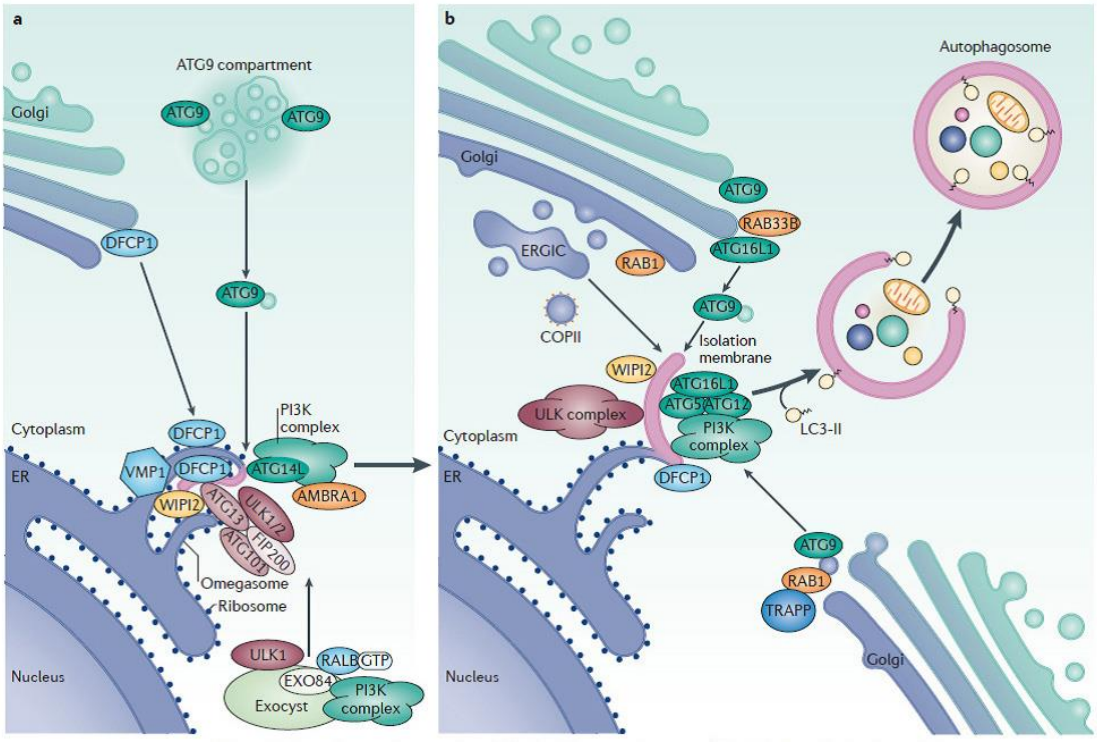

Figure 1.11: Formation and expansion of the isolation membrane[143].

The importance of autophagy to the immune system has started become apparent. Autophagy has been shown to be an important regulator of viral, bacterial and parasitic infections since it does not only restrict their replication but it also delivers

antigens for MHC II presentation, highlighting its role for both innate and adaptive immunity. Despite the fact that both bacteria, parasites and viruses are targeted by macroautophagy, viruses have developed intricate interactions with the autophagic machinery in order to manipulate and/or escape it in order to avoid restriction of their replication or recognition by the TLRs. For instance, some single-stranded RNA viruses interfere with autophagosome maturation in order to replicate on the surface of autophagosomes while HIV-1 induces autophagy-dependent apoptosis on CD4+ Tcells by engaging the CXCR4 receptor on their surface. The single-stranded RNA virus, bovine viral diarrhea virus (BVDV) on the other hand has incorporated part of the LC3 sequence in order to process its polyprotein in an autophagy-dependent manner. As for DNA viruses and specifically members of the herpesvirus family (KSHV and HSV-1) they express inhibitors of the macroautophagy pathway (reviewed in[140].

Concerning HSV-1, blocking autophagy is an essential step in the progression of infection in neurons. Via the neurovirulence factor ICP34.5, HSV-1 can block autophagy in neurons by binding to Beclin-1, a major autophagosome component essential for neuron survival [116], and inhibiting its autophagy function[117]. HSV-1 carrying a mutation in the ICP34.5 gene exhibited impaired ability to cause encephalitis in mice [117]. Moreover, the late HSV-1 protein US11 has also been implicated in the HSV-1-associated autophagy through modulation of RKR which functions upstream of Beclin-1[130].

CD40 Signaling

CD40 or TNFRSF5 is a member of the Tumour Necrosis Factor (TNF) Receptor superfamily. CD40 is a glycoprotein receptor that contains 4 TNFR – Cys repeats but no death domain as opposed to other TNF receptors. It appears in two isoforms, a single pass, type I membrane protein and a secreted one. Upon engagement of its ligand (CD40L) CD40 initiates a signaling cascade through recruitment of adaptor proteins of the TNF receptor-associated factor (TRAF) family, namely TRAF1, TRAF2, TRAF3, TRAF5 and TRAF6[144].

The receptor was first identified as a surface marker of B lymphocytes that causes cell proliferation to activated B cells[145]. However, CD40 is not only expressed on B cells. It is also expressed on monocytes, dendritic cells, endothelial cells, fibroblasts, neuronal cells, smooth muscle cells and thymic epithelial cells. Moreover, CD40 expression is detected at low levels in the basal proliferative compartment of human stratified squamous epithelium and normal ovarian and breast epithelial tissue. Lack of CD40 expression can lead to serious conditions. CD40 mutations are the cause of an autosomal recessive disorder termed hyper-IgM immunodeficiency type 3 (HIGM3)[146]. This disorder is characterized by inability of B cells to undergo isotype switching and mount an antibody-specific immune response, in addition to lack of germinal center formation.

CD40 ligand (CD40L) is also a TNF superfamily member (TNFSF5) and appears in two forms: a single pass, type II membrane protein, and a soluble, secreted form. The soluble form derives from proteolytic cleavage of the membrane bound form. CD40L is expressed on activated but not resting T lymphocytes and is primarily limited to CD4+ T lymphocytes; yet, it is also encountered on the surface of a small portion of CD8+ T cells. However, CD40L is not only detected on T lymphocytes. It has also been detected on B lymphocytes and B cell lines as well as on primary mast cells and their cell lines, on basophils and eosinophils, NK cells, monocytes/macrophages, endothelial and smooth muscle cells, epithelial cells and platelets (reviewed in [147,148]) . Platelets also secret large amounts of CD40L and are the main source of circulating soluble CD40L[149].

Lack of CD40L expression is the cause of an X-linked immunodeficiency syndrome named Hyper IGM type 1 (HIGM1) syndrome or XHIM. Patients with HIGM1 syndrome have defects in the CD40L gene which is located at the X chromosome. As a result isotype switching is impaired and leads to elevated IgM in the serum and absence of all other isotypes. The disorder usually manifests during infancy with recurrent upper and lower respiratory tract bacterial infections. Patients are prone to opportunistic infections such as *Pneumocystis jeroveci* pneumonia and diarrhea due to *Cryptosporidium parvum* infection. In addition, patients are susceptible to encephalitis caused by Toxoplasma gondii[150]. Hematologic disorders are also common. Such conditions include neutropenia, thrombocytopenia, and anemia[151].

CD40 signals as a homotrimer. Trimeric CD40L leads to the trimerization of membrane bound CD40 as part of the signaling cascade of CD40/CD40L interaction[152]. Binding of CD40L on CD40 initiates a signaling cascade mediated through the adapter molecules TRAFs (TNF Receptor Associated Factors). After engagement of the ligand on the receptor, TRAF molecules are sequestered to the cytoplasmic tail of CD40. The outcome of CD40 signaling depends on the specific TRAFs that will engage the receptor.

The TRAF family consists of 6 members named TRAF1 through TRAF6. Concerning CD40, TRAF1, TRAF2 and TRAF3 are drawn to binding sites with a PxQxT motif at the membrane distal domain of CD40's cytoplasmic tail, while TRAF6 is recruited at a membrane proximal binding site with a QxPxE motif[153]. Moreover, TRAF1, 2, 3 and 6 have been shown to interact with different affinities with trimeric CD40, namely TRAF2 > TRAF3 >> TRAF1 and TRAF6[154].

The most characterized signaling pathways activated via CD40 are the canonical and non-canonical or alternative NFκB pathways and TRAFs orchestrate signaling towards those two different directions. The canonical NFkB pathway begins with the formation of the IKK complex (ie Inhibitor of KappaB (IkB) Kinase complex) which contains two catalytic subunits- IKKα and IKKβ, and a regulatory subunit called IKKγ or NEMO. This complex phosphorylates IkB, the inhibitor of NFkB leading to its proteasomal degradation and to the release of the NFkB subunits p50/RelA and p50/c-Rel. The

heterodimers translocate to the nucleus and induce gene transcription. The non-canonical pathway begins with NIK (ie NFkB Inducing Kinase). NIK phosphorylates an "alternative IKK complex", a homodimer of IKKα. Activation of IKKα leads to phosphorylation of p100 on the p100/RelB complex which causes ubiquitin/proteasome-dependent proteolysis of the precursor p100 and generates p52. The p52/RelB complex translocates to the nucleus inducing the expression of a different set of genes comparing to the canonical NFkB signaling[144,153].

The antiviral properties of CD40/CD40L on HSV-1 have been studied before. Several lines of evidence suggest that CD40L exhibits antiviral properties against HSV-1 in vivo [155–157]. Notably, patients with X-linked hyper-IgM syndrome are more susceptible to herpetic infections [158,159]. The ability of CD40L to control HSV-1 is supported by findings in various mouse models. Thus, CD40 deficient mice exhibit impaired survival upon HSV-1 infection[157] and poor clearance of avirulent HSV-1 administered intravaginally[160]. Moreover, in a murine model of posttransplant infection by HSV-1, mice that had undergone bone marrow transplantation and developed graft versus host disease (GVHD) exhibited increased mortality rates from herpetic encephalitis which was attenuated by CD40L administration[156]. Whilst the induction of anti-viral immune responses represents a major route by which CD40L controls HSV-1, a previous study has also indicated direct effects of CD40 activation in susceptibility to HSV-1 infection in L929 cells [155] but the mechanisms involved remain unexplored.

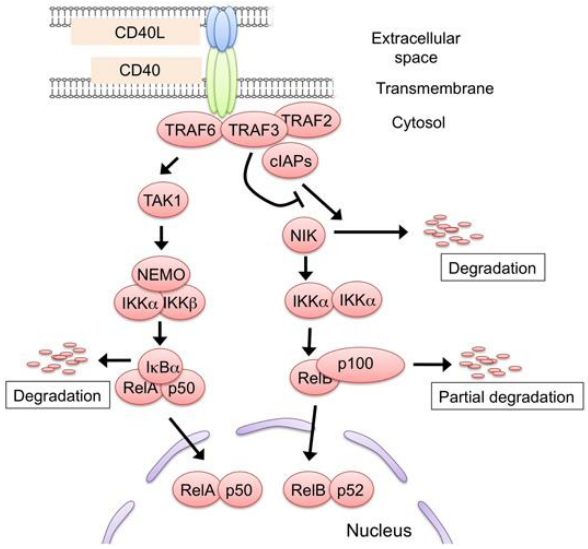

Figure 1.12: The two NFκB activation pathways induced by CD40 signaling.

2.Materials & Methods

Cells

U2OS, Vero and HEK293T were maintained in complete DMEM, ie DMEM (High Glucose w/ L-Glutamine w/ Sodium Pyruvate, Cat.No L0104, Biosera, UK) supplemented with 10% (vol/vol) Fetal Bovine Serum (FBS), penicillin (100 u/ml) and streptomycin (100 μg/ml). BHK cells were maintained in complete Glasgow MEM BHK 21 (GMEM) supplemented with 10% (vol/vol) New Born Calf Serum (NBCS), penicillin (100 u/ml), streptomycin (100 μg/ml) and 10% Tryptose Phosphate Broth (TPB).

CD40-U2OS cells derived after stable transfection of the U2OS cell line with phCD40[161]. Half a microgram of phCD40/cDNA was transfected into 1×10^5 U2OS cells using TurboFect™ in vitro Transfection Reagent (Fermentas) according to the manufacturer's protocol. Transfected cells were selected with 500μg/ml geneticin (GIBCO) and resistant cells were maintained in complete DMEM supplemented with geneticin (500μg/ml). CD40 expression of the CD40-U2OS cells was evaluated by flow cytometry.

CD40-3x-U2OS cells derived after stable transfection of U2OS with the triple substitution plasmid phCD40 P233G/E235A/T254A1 which bears mutations that prevent binding of any of the TRAFs (TRAF1,2,3 and 6) to the cytoplasmic tail of CD40. Resistant cells were also maintained in complete DMEM supplemented with geneticin (500μg/ml). Both phCD40/cDNA and phCD40 P233G/E235A/T254A cDNA3.1 were kindly provided by Dr. S. Pullen, Boehringer Ingelheim Pharmateuticals, Inc.

Vero shHDAC1 B8, Vero shHDAC2 A7, Vero shHDAC2 A9, Vero shHDAC2 A10, Vero shHDAC3 and Vero shscrambled cells derived after lentiviral transduction of the respective plasmid clones for silencing. In a 12-well-plate well containing 1×10^5 Vero cells, there was added 1ml of complete DMEM and 2 ml of lentivirus isolated as described below along with hexadimethrine bromide (Polybrene, Sigma-Aldrich) at a final concentration of 8μg/ml, for 24 hours. Following incubation the medium was removed and the cells were selected with 18μg/ml puromycin (Sigma-Aldrich). Resistant cells were scaled up and maintained in complete DMEM supplemented with 18μg/ml puromycin (Sigma-Aldrich). ShHDAC1 and shHDAC2[162] were kindly provided by Dr. B.L. Ebert, The Dana-Farber Cancer Institute, Boston, MA. ShHDAC3[163] was kindly provided by Dr. L. Zeng, King's College, London.

For Vero shHDAC1 B4/B5/B8 and Vero shHDAC2 A7/A9/A10 cells the same procedure as the one described above was followed differing in that instead of 2 ml of lentivirus, there was added 1 ml of each lentivirus in the same well in order to achieve a triple knock down and maximize the efficiency of silencing. Following a 24 hour incubation period the medium was removed and the cells were selected with 18μg/ml puromycin. Resistant cells were scaled up and maintained in complete DMEM supplemented with 18μg/ml puromycin.

Vero shLSD1 derived after retroviral transduction of the shLSD1 plasmid with 2 ml of retrovirus isolated as described below along with hexadimethrine bromide (Polybrene) at a final concentration of 8μg/ml. Following 24 hour incubation the

medium was removed and the cells were selected with 18μg/ml puromycin. Resistant cells were scaled up and maintained in complete DMEM supplemented with 18μg/ml Puromycin. Vero shLacZ cells derived after stable transfection of Vero with pSuper-shLacZ. Half a microgram of pSuper-shLacZ was transfected into 1×10^5 Vero cells using TurboFect™ in vitro Transfection Reagent (Fermentas) according to the manufacturer's protocol. Transfected cells were selected with 18μg/ml puromycin and resistant cells were maintained in complete DMEM supplemented with 18μg/ml puromycin. ShLSD1 [164] was kindly provided by Dr. S. Kato, Institute of Molecular and Cellular Biosciences, University of Tokyo. Knock down of HDAC1, HDAC2, HDAC3 and LSD1 was evaluated in the respective cell lines by RT-qPCR.

Viruses

The wild type virus used was HSV-1 17syn. The rHSV-RYC[165] virus containing three fluorescent tags (RFP-VP26, YFP-gH and CFP-VP16) was kindly provided by Dr. C. Fraefel. The dl0C4 mutant HSV-1 CFP tagged on ICP4 and lacking ICP0 was a kind gift from Prof. R. Everett. The virus stocks were propagated and titrated on Vero, BHK or U2OS cells according to standard protocols[166].

Virus Propagation

Propagation of HSV-1 was performed either on Vero, BHK or U2OS cells. dl0C4 should be propagated on U2OS to maximize the efficiency of propagation since U2OS complement for ICP0 functionality[167]. According to standard protocols cells were infected approximately at MOI1 and they were harvested when the cytopathic effect was extensive. The cells and the supernatant were separated by centrifugation at 2000rpm for 10min at 4^{o}C. Subsequently the virus was isolated from both fractions. In order to collect the cell released virus the supernatant was centrifuged at 13000 rpm for 2 hours at 4^{o}C. Following the 2hr centrifugation the supernatant was discarded and the viral pellet was incubated in 1ml of DMEM overnight at 4^{o}C to allow for gentle resuspension of the virus. The cell released virus or CRE was stored at -80^{o}C. Concerning the cells kept from the first centrifugation step they were also utilized for collection of the cell associated virus. The cells were mechanically disrupted either by sonication (3 pulses of 1 min at 40% amplitude at 4^{o}C with intermediate cooling steps) or three freeze thaw cycles. Once the cells were disrupted they were centrifuged for 10min at 2000 rpm at 4^{o}C, the supernatant was stored and the pellet was discarded. Before storing the virus at -80^{o}C it was filtered using a 0.45nm filter.

Titration of HSV-1

Vero or BHK cells were plated in 6-well-plates until they were 80-90% confluent. Once the cells reached the desired confluence, serial dilutions of the viral stock were prepared on ice. Dilutions were usually between 10^{-4}-10^{-10}. The medium covering the cells prior to infection was reduced to minimum so that the virus was in close contact with the cells. Usually 100μl of the dilution were used for infection. Calculation of the final titer depends on the volume of the dilution added and the magnitude of dilution. Following infection the cells were transferred at 37^{o}C and shaken every 10 minutes for 2 hours. Subsequently, the medium covering the cells was removed and replaced with new medium containing 1/100 HSV-1 specific human IgG+ antibodies. The cells were incubated at 37^{o}C until plaques were formed in well infected with high dilutions of the virus.

Upon plaque formation, the cells were fixed and stained and the plaques were counted. For fixation, the cells were carefully washed with cold PBS and fixed by addition of methanol for 5min. Methanol was subsequently removed, cells were allowed to air-dry and they were subsequently incubated with Giemsa solution (1/15 Giemsa in tap water) for 10 min. Afterwards, Giemsa solution was removed carefully by submersion of the plates in tap water and cells were allowed to air-dry. Following Giemsa staining the plaques that developed were counted and the viral titer was estimated by this formula: $\boldsymbol{x = (\#\ of\ plaques)/(d * V)}$ where X= the titer, d=dilution factor and V =the volume of diluted virus instilled on the cells.

Lentiviral and Retroviral Propagation and Transduction

HEK293T were plated in a 60mm plate at 50% confluence and transfected with the packaging plasmids pVSV-G (0.5μg) and pDR8.1 (1.0 μg) as well as 1.5μg of a pLKO plasmid to be packaged and transduced. Transfection was performed using TurboFect™ in vitro Transfection Reagent (Fermentas) according to the manufacturer's protocol. For a 60mm plate 450μl Optimem were required along with 8μ Turbofect added in 4,5ml of DMEM in the plate. An optional step of the procedure was removal of the supernatant, which can be also kept since it contains an amount of packaged lentivirus, and repeat of the transfection procedure. 48 hours after the second transfection the supernatant was collected, centrifuged for 5min at 2000rpm at 4^{o}C to remove any cells, filtered with a 0.45 filter and stored at -80^{o}C.

For retroviral propagation the same procedure as the one described above was followed but the packaging plasmid was Amphopack (1μg) and there were used 3μg of the pSuper plasmid to be packaged and transduced.

For lentiviral or retroviral transduction of a cell line, the desired cells were plated in a 12-well-plate and transduced with 1-2 ml of virus in 1ml of medium along with hexadimethrine bromide (Polybrene) at a final concentration of 8μg/ml.

Gene Silencing

CD40-U2OS cells were transfected with either ATG5 siRNA (sc-41445, Santa Cruz) or control siRNA-A (sc-37007, Santa Cruz) at a final concentration of 50nm using TurboFect™ in vitro Transfection Reagent (Fermentas) according to the manufacturer's protocol. At 48 hours post transfection, the cells were used for experimentation.

Inhibitors and recombinant molecules

The inhibitors used for the experiments were the PI3K inhibitor LY294002 (PHZ1144, Invitrogen) at a final concentration of 25μM, the JNK inhibitor SP600125 (420119, CalBiochem) at a final concentration of 7.5μM and the Specific Autophagy Inhibitor (Spautin-1, SML0440 SIGMA) at a final concentration of 10μM. All inhibitors were diluted in dimethyl sulfoxide (DMSO). For the induction of the CD40 pathway, we used recombinant soluble human CD40L (BMS308/2, Bender MedSystems) at a final concentration 0.5μg/ml diluted in PBS.

MTT Assay

The cells to be tested were plated in a 12-well-plate in such a way that they would be in an exponential phase during the MTT assay. The compound that needed to be tested for its effect on the proliferation, or more accurately on the mitochondrial function, was added for a period of time depending on the experiment. Next the medium containing the compound of interest was removed and there was added MTT, diluted in free DMEM at a final concentration of 1mg/ml. The cells were incubated at 37^{o}C for 4 hours. The MTT solution was subsequently removed. At that point an insoluble substance, formazan, a product of the reduction of MTT by mitochondria was visible in the bottom of the well. This was diluted by addition of acidified isopropanol (4% HCl in isopropanol) and pipetting, producing a colored dilution that was measured in a photometer at 570nm.

Treatments and infections

CD40-U2OS cells or CD40-3x-U2OS cells were first treated for 30min with the appropriate inhibitors, then for another 30min with CD40L and HSV-1 was added last, at a multiplicity of infection (MOI) of 1 pfu/cell or at variable multiplicities depending on the experiment. For experiments requiring synchronized entrance of the virus in the cells a binding step was added. Specifically, after incubation with CD40L, cells were incubated on ice for 5 minutes and then the virus was added on the cells and was allowed to bind on the cell surface for 1-1.5 hours. Subsequently, cells were transferred in a humidified incubator at 37oC and 5% CO2 for the required time depending on the experiment.

Immunofluorescence

For immunofluorescence, 1×10^5 cells were plated on glass coverslips placed in 24-well plates. The conditioned medium was aspirated, the cells were washed with PBS, fixed with formaldehyde (4% [vol/vol] in PBS containing 2% sucrose) and permeabilized with Permeabilization Solution (Cat.No 5115, Millipore). The coverslips were incubated for 1h with primary antibodies diluted in PBS containing 1% (vol/vol) fetal bovine serum at room temperature and they were subsequently washed in the same buffer twice before incubation with the secondary antibodies. Incubation with the secondary antibodies was performed likewise. The nuclei were stained with TO-PRO-3 (Cat.No T3605, Invitrogen) at a dilution of 1:1000 in PBS. FM 1-43FX (Cat.No F35355, Invitrogen) dye was also used according to the manufacturer's instructions where there was need for visualization of the plasma membrane. The cells were mounted in Ibidi Mounting Medium (Cat.No 50001, Ibidi) and examined by confocal microscopy (TCS SP2, Leica Microsystems, Germany). The data were collected with sequential scanning to avoid signal overlap, at a resolution of 1.024x1024 pixels, following a 4-6 fold averaging and the optical slices were between 0.3 and 0.5µm. The data sets were processed with LCS Lite software (Leica).

FACS analysis

For FACS analysis, cells were detached using PBS-1mM EDTA and washed with PBS. Cytofix/Cytoperm (BD, Cat.no 554722) was added for 20min at 4^oC and the cells were washed again in Perm/Wash buffer (Cat.no 554723, BD). Subsequently the permeabilized cells were blocked in 5% FBS in Perm/Wash buffer for 15min at 4^oC. When there was no need for intracellular staining the cells were resuspended in MACS buffer (2%FBS and 2mM EDTA in PBS) after being detached and washed and they were stained. Staining was performed directly or indirectly with primary and secondary antibodies or with conjugated antibodies respectively. Time of incubation and temperature varied according to the antibody. Before analysis the cells were incubated in 2% PFA in MACS buffer and counted with a FACSCalibur (BD) instrument.

Live-cell imaging

Each well of a two-well chambered coverglass unit (Lab-Tek, Thermo Scientific) was seeded with $2x10^5$ CD40-U2OS cells and infected at MOI 20 with rHSV-RYC virus in the presence or absence of CD40L (0.5µg/ml) and the PI3K inhibitor LY294002 (25µM). A binding step was performed for 1 hour on ice as described above and the cells were then transferred in a humidified chamber on the microscope stage with 5% CO2 at 37^oC. The cells were observed for at least 8 hours with an epifluorescent Leica DMIRE2 microscope, equipped with a Leica DFC300 FX digital camera and images were acquired with the IM50 software (Leica) and exported as tiff files.

Fractionation

For the fractionation experiments, the cells were collected in PBS with 1mM EDTA and the pellet was incubated for 10min in hypotonic lysis buffer (20mM Hepes pH 7.6, 10mM NaCl, 1.5mM MgCl2, 0.2mM EDTA, 0.1% NP40, 20% glycerol, 1mM DTT and protease inhibitors) at 4^{o}C. Following incubation with the hypotonic buffer, the nuclei were pelleted at 15,600g for 4min at 4^{o}C and the supernatant was collected as the cytoplasmic fraction. The nuclei pellet was washed three times in hypotonic lysis buffer and subsequently the nuclei were incubated with hypertonic lysis buffer (20mM Hepes pH 7.6, 500mM NaCl, 1.5mM MgCl2, 0.2mM EDTA, 0.1% NP40, 20% glycerol, 1mM DTT and protease inhibitors) for 30min at 4^{o}C. The samples were then briefly sonicated (40% amplitude for 15sec at 4^{o}C), centrifuged at 16,100g for 20min at 4^{o}C and the supernatant was kept as the nuclear fraction.

Immunoblotting

Protein extracts were analyzed by immunoblotting. For analysis of whole cell extracts, the cells were washed with cold PBS, collected with 1mM EDTA in PBS and pelleted at 2,500g for 10 minutes. The cells were then incubated for 10min at 4^{o}C with M-PER Mammalian Protein Extraction Reagent (Cat.No 78503, Thermo Scientific) along with protease inhibitors (Cat.No 78415, Thermo Scientific) vortexing mildly every 2 min. The cell extracts were then briefly sonicated (40% amplitude for 15sec at 4^{o}C), centrifuged for 15min at 14,000g at 4^{o}C and the supernatant was kept for analysis.

All protein extracts were quantified with Cayman Protein Determination kit (Cat.No 704002, Cayman). From each sample, 40μg of protein were boiled in SDS gel-loading buffer, separated by electrophoresis and transferred on nitrocellulose membranes. The membranes were subsequently blocked in TBST buffer with 5% (w/vol) dried non-fat milk and incubated overnight at 4^{o}C with the primary antibodies. All antibodies were diluted in TBS-0,1% Tween-20 (vol/vol) containing 1% (w/vol) dried non-fat milk. Following incubation with the primary antibodies, the membranes were thoroughly washed and incubated with the secondary antibodies for 1 hour at room temperature, washed in TBS-T and developed using Luminata Forte Western HRP Substrate (Cat.No WBLUF0100, Millipore) either on film or by the ChemiDoc™ MP System (Cat.No 170-8280, Bio-Rad) with the Image Lab v5.0 software (Bio-Rad).

Methylation profile protocol

Vero cells were plated in p100 dishes and infected with HSV-1 17syn at MOI 1 for 3, 8 and 15 hours. The cells were collected and their DNA was isolated by the PureLink™ Genomic DNA kit for isolation of genomic DNA (Invitrogen, Cat.No K1820-01). In order to isolate genomic DNA from latently infected cells, Vero were infected with the mutant virus dl0C4 at MOI 0,01 for 2-3 days until detection of ICP4 expression on

most cells and prior to the formation of replication centers. A fraction of the latently infected cells was analyzed by FACS for the level of ICP4 expression.

For screening of the methylation status, a customized methylation profiling array by SA Biosciences was used, targeted on the epigenetics related genes HDAC1, HDAC2, HDAC3, HDAC4, HDAC5, HDAC6, HDAC10, HDAC11, DNMT1, DNMT3A, DNMT3B, KDM1, KDM2A, KDM2B, NRF2/GABP, CREB/ATF2, SETD1A, ASH2L, KAT2A, KAT2B, KDM3A, KDM3B, SUV39H1 and WHSC1L1. The array uses methylation sensitive and methylation dependent enzymes (ie requiring or not the presence of methylated cytosines in their recognition sequence) to digest the genome. The genome is mono- or double digested creating four groups of material, ie undigested, digested with a methylation-sensitive enzyme, digested with a methylation-dependent enzyme and double digested. Subsequently, the four groups are subjected to qPCR with primers for CpG sites on the promoters of the desired genes and analysis of the results provides data on the methylation status (Fig 2.1). Analysis of the results is performed on an automated worksheet that takes in consideration the efficiency of digestion and discards data that are not considered trustworthy.

For a more detailed profile of the methylation status, the above conditions of viral infection were repeated and the genomic DNA was subjected to high-throughput methylation profiling by the Illumina Methylation Beadarray. The results were analyzed by means of bioinformatics by Dr. G. Pavlopoulos and Prof. I. Iliopoulos.

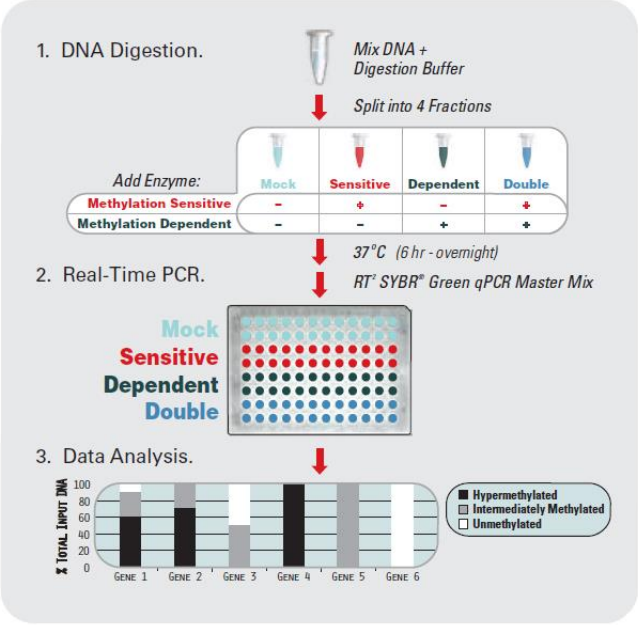

Figure 2. 1: Methylation profiling protocol by SA Biosciences.

Quantitative-PCR

Quantitative PCR was run on a 7500 Fast Real-Time PCR System (Applied Biosystems) using the KAPA SYBR FAST qPCR kit (Cat.No KK4601, KapaBiosystems) according to manufacturer's protocol.

For real-time RT-PCR, we used RNA collected with the NucleoSpin® RNA II (Cat.No 740955.250, MN) and reverse transcribed with PrimeScript™ 1st strand cDNA Synthesis Kit (Takara, Cat.No 6110) with random hexamers following the manufacturer's protocol for qPCR.

For quantification of ICP8 copies, we used DNA from HSV-1 of known titer. HSV-1 was incubated for 1 hour at 60°C in equal volume of virus lysis buffer (VL buffer) containing Tris HCl ph 8.0 10Mm, KCl 50mM, MgCl2 2.5mM, Tween-20 0.45% (v/v) and 60 µg/ml proteinase K. Following incubation at 60°C the virus was incubated for 15min at 95°C to deactivate the proteinase K. DNA from infected cells was extracted using the PureLink™ Genomic DNA Kit (Cat.No K1820-01, Invitrogen).

Primers

Primer List	
18S	F: 5'-CTCAACACGGGAAACCTCAC-3'
	R: 5'-CGCTCCACCAACTAAGAACG-3'
ICP8	F: 5'-CGACGTGCCCTGTAACCTAT-3'
	R: 5'-CTGTTCATGGTCCCGAAGAC-3'
HDAC1	F: 5'-TAAATTCTTGCGCTCCATCC-3'
	R: 5'-TTGCCACAGAACCACCAGTA-3'
HDAC2	F: 5'-TGGTGATGGTGTTGAAGAAG-3'
	R: 5'-CTCATTGGAAAATTGACAGCA-3'
HDAC3	F: 5'-CTCTACTGGTGCTGGGTGGT-3'
	R: 5'-TGTGAAGTCTGGGGCAAAGT-3'
LSD1	F: 5'-CCTCAATAATAAGCCTGTGTCC-3'
	R: 5'-TCTTCCAATGTTCAATCTGCTC-3'
PSMA3	F: 5'-TCAATCGGCACTGGGTATGAC-3'
	R: 5'-ACCCCAAAGACAACACCATC-3'
PSMB1	F: 5'-GCTGCAATGCTGTCTACAATCC-3'
	R: 5'-CCCTTTCCTTCTTCATCAAGTCC-3'
PSMB8	F: 5'-ACCCAGGACACTACAGTTTCTC-3'
	R: 5'-AATTCTGTGGGCTGCATTCC-3'
PSMB9	F: 5'-ACAGCCTTTTGCCATTGGTG-3'
	R: 5'-GCAATAGCGTCTGTGGTGAAG-3'

Plasmids

Plasmid	Reference
phCD40/cDNA	Pullen, SS *et al.* 1999[161]
phCD40 P233G/E235A/T254A cDNA3.1	
pLKO.1 shHDAC1 B4	Bradner, J. E. *et al. 2010* [162]
pLKO.1 shHDAC1 B5	
pLKO.1 shHDAC1 B8	
pLKO.1 shHDAC2 A7	
pLKO.1 shHDAC2 A9	
pLKO.1 shHDAC2 A10	
pSuper shLSD1	Yokoyama, A. *et al.2008* [164]
pSuper shLacZ	
pLKO.1 shHDAC3	Alam, S. *et al.* 2011[163]
pLKO.1 shscrambled	

Antibodies

Primary	**Details**	**Used for:**
anti-HSV-1 **gG** Envelope Protein (7F5)	Santa Cruz Biotechnologies, Cat.No sc-56984	IF, WB
anti-HSV-1 **VP16** MAb LP12	Dr. C. Fraefel[165]	IF, WB
anti-HSV-1 **ICP0**	Virusys Corporation, Cat.No H1A027-100	IF, WB
rabbit anti-**Herpes Simplex Virus Type 1**	DAKO, Cat.No B0114, Lot 016	IF
mouse anti-**actin**	Millipore, Cat.No MAB1501	WB
rabbit anti-**CD40** (H-120)	Santa Cruz Biotechnology, sc-9096	IF, WB
PE anti-human CD270 **(HVEM,** TR2)	Biolegent, Cat. No 318805	FACS
mouse anti-**LC3** (APG8)	Abgent, Cat.No AM1800a	IF, WB
mouse anti-APG5L/**ATG5**	Abcam, Cat.No ab108327	WB
rabbit polyclonal anti-**emerin**	Prof. P. Theodoropoulos[168]	IF
rabbit anti-**H3K79me2**	Cell Signaling, Cat.No 9757	WB
Secondary	**Details**	**Used for:**
Alexa Fluor 488 donkey anti–mouse	Invitrogen, Cat.No A21202	IF, FACS
Alexa Fluor 488 goat anti-rabbit	Invitrogen, Cat.No A11008	IF
Goat anti-rabbit - Cy3	Invitrogen, Cat.No 816115	IF
Goat anti-mouse - Cy3	Invitrogen, Cat.No 816515	IF
CF^{TM}633	Biotium, Cat. No 20121	FACS
Goat anti mouse IgG, Peroxidase Conjugated, H+L	Millipore, Cat.No AP124P	WB
Goat anti rabbit IgG, Horseradish Peroxidase Conjugated, H+L	Millipore, Cat.No AP132P	WB

3. Results

CD40L antiviral effect on HSV-1.

CD40 signaling inhibits production of HSV-1 progeny virions.

It has been previously reported that CD40L has a direct antiviral activity on HSV-1 in vitro[155]. In light of this finding, we set out to investigate the mechanism underlying this phenomenon. To this direction, initially we examined the antiviral activity of CD40L on HSV-1 by analyzing the ability of the virus to produce newly synthesized virions in the presence of CD40L. Our primary experiments were conducted on the BHK hamster cell line, which was transfected with a phCD40 plasmid kndly provided by Dr. Pullen [154] (Fig. 3.1 A). Analysis showed that at 24 h.p.i. (hours post infection) at MOI 1 PFU/cell (multiplicity of infection), cells treated with CD40L produced less viral particles compared to cells treated with vehicle control, and the same was true when we titrated the newly synthesized virions on various time points (Fig. 3.1 B and C). Moreover it was observed that 24 h.p.i. the immediate early protein ICP0 remained nuclear in the presence of CD40L while its normal distribution at 24h.p.i. is cytoplasmic (Fig. 3.2).

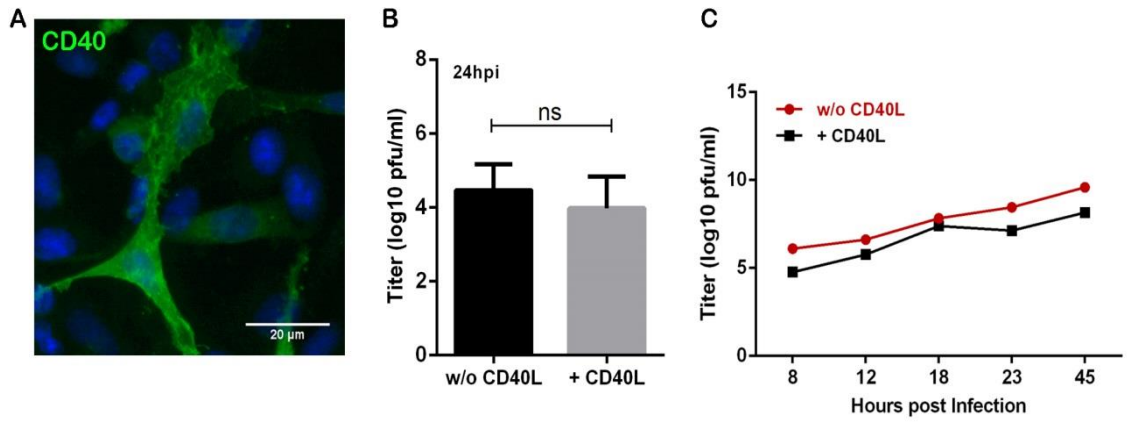

Figure 3.1: HSV-1 titer decreases in the presence of CD40L. (A) BHK cells transfected with CD40. (B) BHK cells transfected with CD40, were pretreated with CD40L (0.5µg/ml) for 30 minutes and then infected with HSV-1 17syn at a multiplicity of 1 PFU per cell, for 24 hours. CD40L was not removed from the medium during the incubation period with the virus. Supernatants of the infected cells were harvested and titrated on BHK cells. The viral titer decreased in the presence of CD40L but not significantly. (C) Growth curves of HSV-1 in the presence or absence of CD40L. BHK cells transfected with CD40 were pretreated with CD40L (0.5µg/ml) for 30 minutes and then infected with HSV-1 17syn at a multiplicity of infection 1. CD40L was not removed from the medium and supernatants were harvested at 8, 12, 18, 23 and 45 hours post infection and they were titrated on BHK cells.

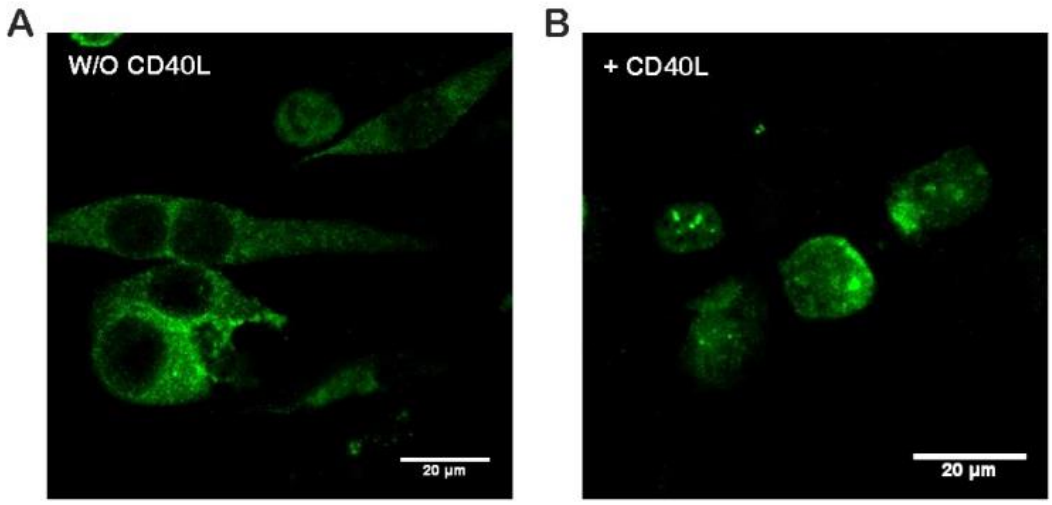

Figure 3.2: Nuclear localization of ICP0 in the presence of CD40L. (A) BHK cells transfected with CD40, were pretreated with CD40L (0.5µg/ml) for 30 minutes and then infected with HSV-1 17syn at a multiplicity of 1 PFU per cell, for 24 hours. The cells were subsequently stained for The ICP0 protein of HSV-1 (green) and visualized by confocal microscopy. ICP0 is depicted at the level of the nucleus in the CD40L-treated cells.

Since data showed a consistently lower production of progeny virions in the presence of CD40L but we could not detect any statistical significance, we went on to construct a stable cell line expressing the CD40 receptor to minimise the variability caused by transfection efficiency. Fot that reason, the permissive to HSV-1 infection, human osteosarcoma cell line U2OS was engineered to express the CD40 receptor (CD40-U2OS). CD40 expression in a stable clone was successfully confirmed by flow cytometry (Fig 3.3 A). CD40-U2OS cells were treated either with recombinant CD40L or vehicle control and subsequently infected with HSV-1 at MOI 1 PFU/cell for 24 hours. Titration assays showed that CD40 ligation inhibited the production of progeny virions from as early as 12 hours post infection and through the 24 hour treatment (Fig. 3.3 B and C).

To further confirm that this effect required CD40 signaling, we established U2OS cell clones stably expressing a P233G/E235A/T254A mutated CD40 receptor (CD40-3x-U2OS) which is incapable of binding TRAFs 1, 2, 3 and 6 to its cytoplasmic tale and is defective in CD40L-induced signal activation[154]. Indeed, treatment of CD40-3x-U2OS with CD40L failed to reduce production of HSV-1 progeny virions (Fig. 3.3 D).

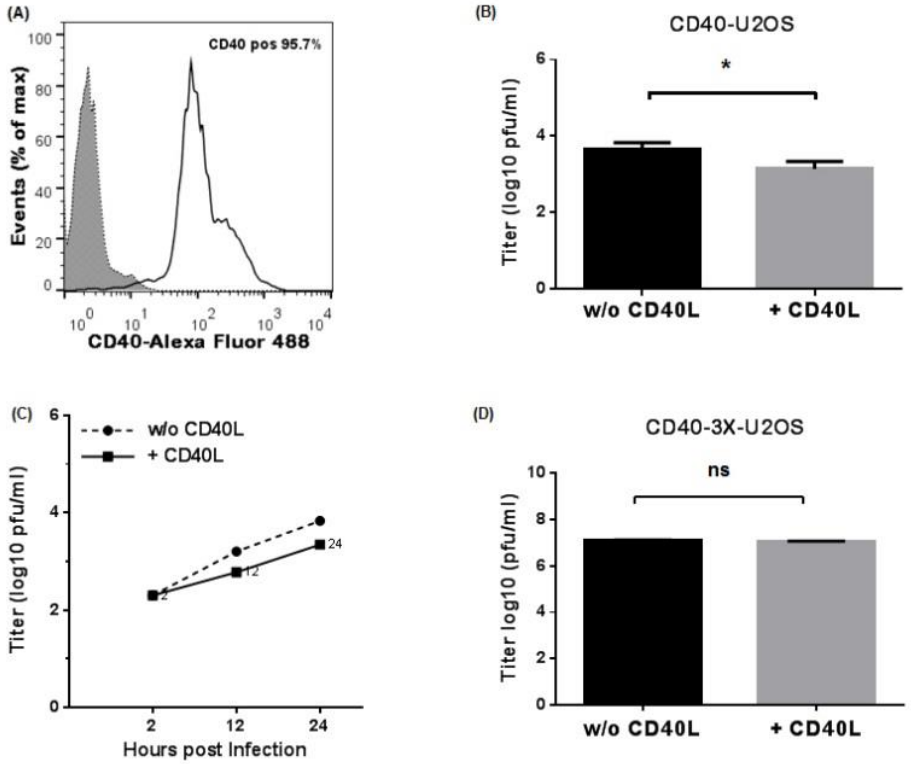

Figure 3.3: HSV-1 titer decreases in the presence of CD40L. (A) U2OS cells were stably transfected with CD40. Purity of the population expressing CD40 was evaluated with FACS for CD40. 95.7% of the cells were found to be CD40 positive. **(B)** CD40-U2OS cells were pretreated with CD40L (0.5μg/ml) for 30 minutes and then infected with HSV-1 17syn at a multiplicity of 1 PFU per cell, for 24 hours. CD40L was not removed from the medium during the incubation period with the virus. Supernatants of the infected cells were harvested and titrated on BHK cells. HSV-1 titer was significantly decreased (P=0.0372) in the presence of CD40L. **(C)** Growth curves of HSV-1 in the presence or absence of CD40L. CD40-U2OS cells were pretreated with CD40L (0.5μg/ml) for 30 minutes and then infected with HSV-1 17syn at a multiplicity of infection 1. CD40L was not removed from the medium and supernatants were harvested at 2, 12 and 24 hours post infection and they were titrated on BHK cells. **(D)** U2OS cells stably transfected with the triple substitution, mutant, CD40 receptor, which prevents binding of any of the TRAFs to its cytoplasmic tail, were pretreated with CD40L (0.5μg/ml) and infected with HSV-1 17syn at a multiplicity of 1 PFU per cell, for 24 hours. Supernatants were harvested and titrated on BHK cells. HSV-1 titer presented no significant variation (P=0.1785). Analysis of statistical significance was performed by unpaired t-test (GraphPad Prism 6.04).

CD40-signaling does not have an apoptotic effect on CD40-U2OS cells.

Neither BHK cells transfected with the CD40 receptor nor CD40-U2OS exhibited apoptotic characteristics macroscopically at 24h.p.i. when the supernatants of the infected cells were collected for titration of HSV-1. CD40L treated cells exhibited the same morphology as the control cells. However, in order to have a further evaluation of the condition of CD40-U2OS cells before embarking on further investigation of the phenotype observed, an MTT assay was conducted following a 24h treatment with CD40L at non-infected cells. The MTT assay showed that there is no difference in the metabolic activity of CD40-U2OS cells treated with CD40L compared to the control (Fig. 3.4).

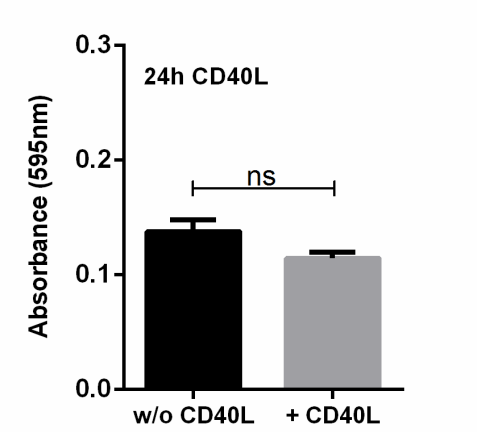

Figure 3.4: CD40L does not cause apoptosis to CD40-U2OS. CD40-U2OS cells were treated with CD40L (0.5μg/ml) for 24 hours and then subjected to an MTT assay.

CD40 signaling does not affect the binding of HSV-1 virions on the cell surface.

In order to identify the stage of infection at which HSV-1 is affected with further consequences on the production of infectious particles, we started from the first virus-host interaction that occurs, ie binding of HSV-1 on the cell surface. To that end, CD40-U2OS cultures were exposed to recombinant CD40L for 30 minutes and were then infected with wild-type HSV-1 at MOI 30 PFU/cell on ice, to prevent entry of the virus in the cells. Subsequently the cells were fixed and stained for the glycoprotein G (gG) of HSV-1, a protein that localizes on the viral envelope. They were also stained with the FM 1-43FX dye to visualize the plasma membrane. The specimens were visualized by confocal microscopy (Fig.3.5 A and B) and gG particles on the surface of the cells were counted using the ImageJ software. No significant differences in the binding of HSV-1 on the cell surface were detected (Fig. 3.5 C), indicating that the effects of CD40 ligation on HSV-1 virion production are not due to reduced binding of the virus to the cell surface.

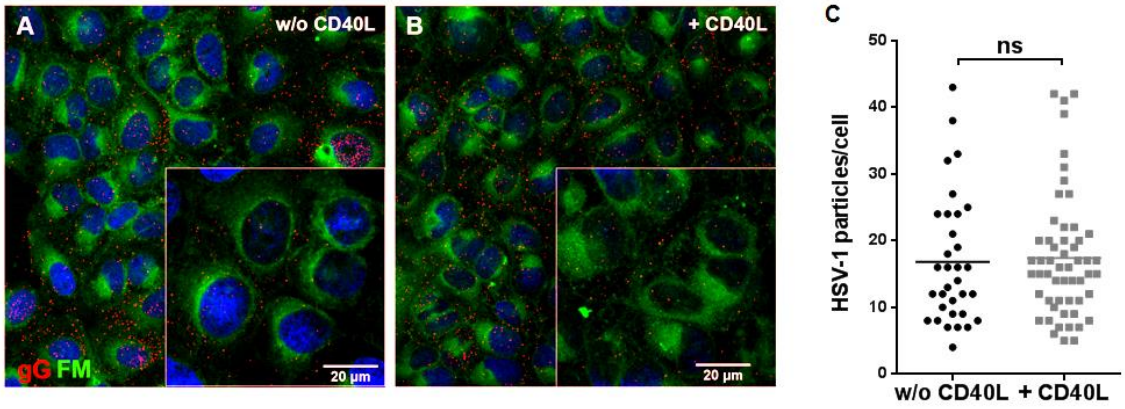

Figure 3.5: Binding of HSV-1 is not affected by CD40 signaling. (A & B) CD40-U2OS cells were treated with CD40L or solvent vehicle for 30 minutes and were then infected with HSV-1 at a multiplicity of 30 PFU/cell for 1.5 hours, on ice. The cells were subsequently fixed at 4°C and stained with FM 1-43FX (green) to label the plasma membrane and for glycoprotein G (red) of HSV-1 to visualize virions entering the cells. **(C)** The number of virions per cell attached to the plasma membrane was counted using the cell counter application of ImageJ. Analysis of statistical significance was performed by an unpaired t-test (GraphPad Prism 6.04). Error bars represent the mean. No statistical significance was observed (p= 0.7794).

Moreover, CD40-U2OS cells were analyzed for cell surface expression of HVEM in the presence and absence of CD40L (Fig. 3.6 A) since HVEM is a primary receptor for binding of HSV-1 on the cell surface. Flow cytometry analysis demonstrated comparable levels of HVEM expression, regardless of CD40 activation. Specifically, 35.3% of the cells expressed HVEM without CD40L treatment and 36.5% after CD40L stimulation. Likewise cells were analyzed for HVEM expression following 24 hours of infection at MOI 1 PFU/cell in the presence or absence of CD40L (Fig. 3.6 B).HSV-1 substantially upregulated the receptor in the infected cells, however, the proportion of HVEM-positive cells was similar both in the absence or presence of CD40L, (78.3% and 71.3%, respectively).

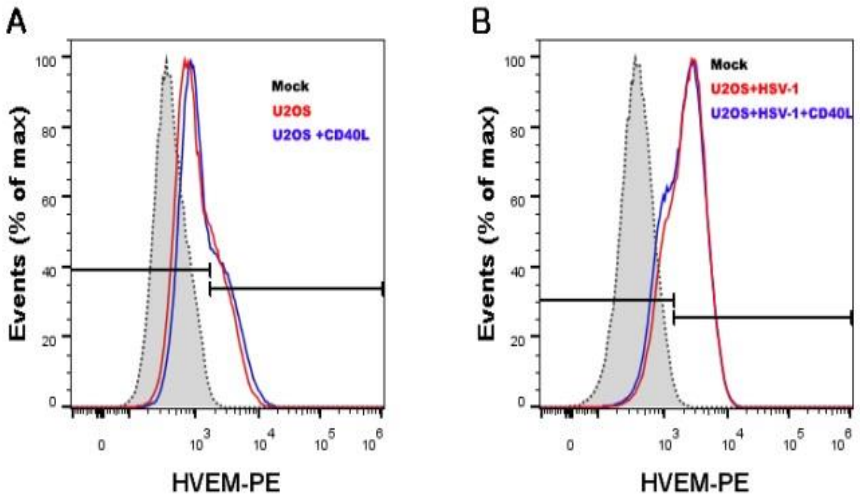

Figure 3.6: Expression of the surface receptor HVEM is not affected by CD40 signaling. The expression of HVEM on the cell surface was monitored by flow cytometry. **(A)** 35.3% of CD40-U2OS were positive for HVEM while in the presence of CD40L the percentage of positive cells was 36.5%. **(B)** The expression of HVEM on the cell surface was also monitored in CD40-U2OS cells infected with HSV-1 at MOI 1 for 24 hours in the presence or absence of CD40L . 78.3% of the infected cells were positive for HVEM while in the presence of CD40L the percentage of positive cells was 71.3%.

CD40L signaling delays the translocation of VP16 to the nucleus.

Since binding of the virus was not affected by CD40 signaling, we sought to investigate whether CD40 ligation impacts on the viral protein VP16, a critical transcriptional activator of the immediate-early gene promoters of HSV-1. As mentioned earlier, VP16 locates in the tegument and forms a complex with the cellular factors HCF-1 and Oct-1 that drive VP16 to the cell nucleus where it initiates transcription of the viral immediate-early genes[169]. Therefore, we monitored the dynamics of this protein in the presence or absence of CD40L. A synchronized infection of CD40-U2OS cells revealed that CD40L hindered the translocation of VP16 from the cytoplasm to the cell nucleus. Specifically, cells were stained for VP16 and the nuclear envelope protein emerin and analyzed by confocal microscopy. At various time points post infection, we could detect fewer VP16 particles in the nuclei of cells treated with CD40L compared to non-treated cells (Fig. 3.7 A & 3B). This observation was further confirmed by western blot analysis of fractionated nuclear and cytoplasmic protein extracts following infection with HSV-1 for 1.5 hours. The results showed reduced VP16 in the nuclei of cells treated with CD40L compared to control cultures (Fig. 3.7 C).

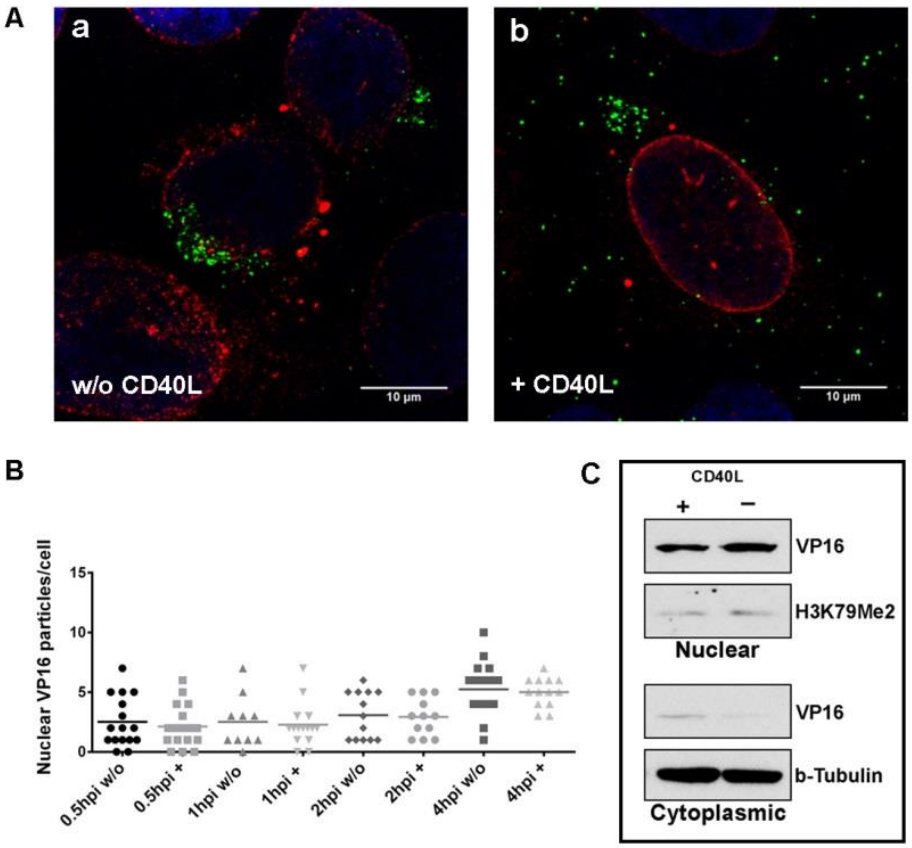

Figure 3.7: Localization of VP16 in relation to the cell nucleus. (A) CD40-U2OS cells were treated with CD40L (0,5µg/ml) or control medium for 30 minutes and were then infected with HSV-1 17syn at a multiplicity of 35 PFU per cell, for 1.5 hours on ice, along with 100µg/ml cycloheximide in order to block translation. The cells were subsequently stained for the tegument protein of HSV-1, VP16 (green) and for emerin (red) in order to visualize VP16 in relation to the nucleus. **(B)** Similarly, CD40-U2OS cells were infected at a multiplicity of 30 PFU per cell in the presence and absence of CD40L and VP16 particles that entered the nucleus were counted at 0.5, 1, 2 and 4 hours post infection (hpi) and are plotted on graph. Statistical analysis was performed by ordinary one-way ANOVA with GraphPad Prism 6.04. Differences of the means were found to be statistically significant ($P<0.0001$). Error bars represent the mean. **(C)** VP16, H3K79Me2 and b-tubulin expression in nuclear and cytoplasmic fractions of CD40-U2OS cells infected with HSV-1 17syn in the presence of CD40L compared to the control at 1.5 hpi. Cells were treated with CD40L (0.5µg/ml) or control medium for 30 minutes and were then infected with HSV-1 17syn at a multiplicity of 30 PFU per cell, for 1.5 hours on ice. Protein extracts were collected and fractioned 1.5 hpi .

In light of these findings, we proceeded to investigate the dynamics of VP16 in association with the dynamics of the virus capsid at early times of infection. To that end, we performed live cell microscopy, utilizing the recombinant virus rHSV-RYC[165] which encodes the fusion proteins VP16-ECFP and VP26-mRFP of the virus tegument and capsid, respectively. CD40-U2OS cells were initially infected on ice and they were subsequently transferred at standard culture conditions and monitored for at least 8 hours. Figure 3.8 A shows representative time points of the infection revealing a delayed onset of the viral lytic cycle upon CD40 signaling. During control HSV-1

infection VP16 was localized perinuclearly at 1 h.p.i. and it was distributed throughout the cytoplasm at 2-5 h.p.i. At approximately 6 h.p.i., VP16 formed small nuclear foci which are indicative of de novo protein synthesis. Markedly, in CD40L-treated cells, VP16 remained perinuclear for approximately 2 hours and did not accumulate in nuclear foci until 8 h.p.i. and thereafter. A similar delay was observed when the VP26 protein was also monitored. VP26 accumulation could be visualized in the nucleus of non-treated cells but not in CD40L-stimulated cells at 8h.p.i. In agreement with the aforementioned observations, there were fewer sites of capsid assembly in cells treated with CD40L at 30 h.p.i. (Fig. 3.8 B).

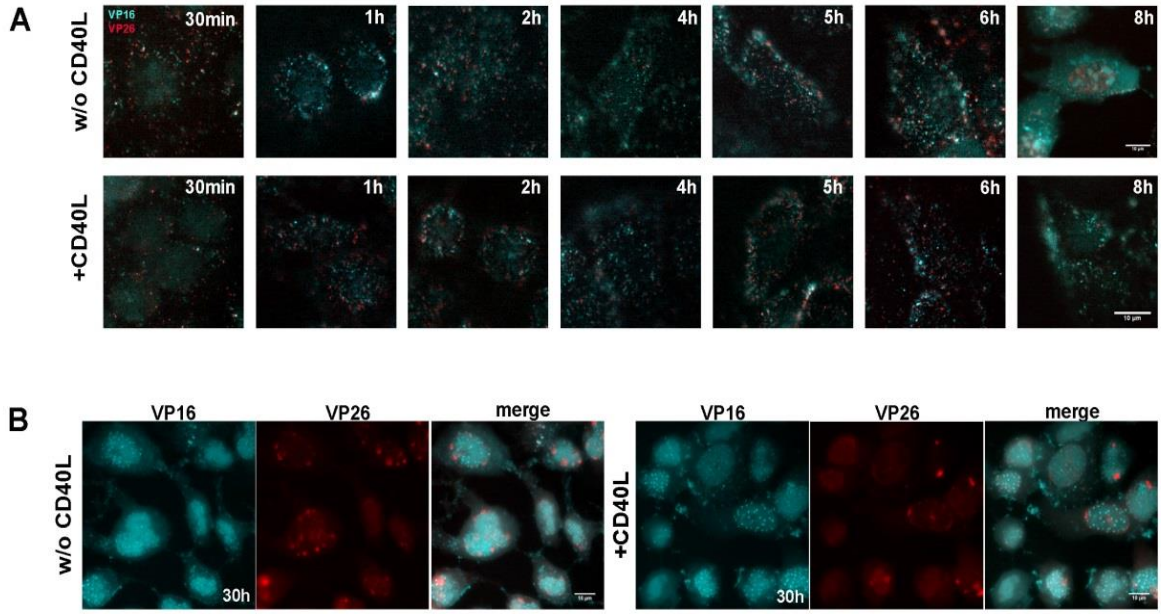

Figure 3.8: Kinetics of HSV-1 in the presence of CD40L. (A) Live imaging of rHSV-RYC infected cells in the presence of CD40L. CD40-U2OS cells were plated in a chambered coverglass unit, treated with CD40L (0,5μg/ml) or control medium for 30 minutes and were then infected with rHSV-RYC at a multiplicity of 20 PFU per cell, for 1.5 hours on ice. The cells were then transferred in a humidified chamber on the microscope stage with 5% CO2 at 37oC and were observed for at least 8 hours. **(B)** CD40-U2OS cells infected with rHSV-RYC (A) as monitored at 30 h.p.i. . Cyan:VP16, Red: VP26

Immediate-early, Early and Late stages of HSV-1 infection during activation of CD40 signaling.

In order to further investigate the events associated with the progression of viral infection we monitored the expression of ICP0, a key regulator of HSV-1 productive infection, the replication of the viral genome through quantification of the ICP8 gene, and late gene expression via monitoring the expression of glycoprotein g. Despite the delayed kinetics of VP16, there was no difference in the expression levels of ICP0, except at 24 hours post infection, when less ICP0 was expressed in cells that had been treated with CD40L (Fig. 3.9 A). To evaluate HSV-1 DNA replication, a qPCR assay was

performed for the ICP8 Early gene to assess the number of HSV-1 DNA copies produced by cells treated with CD40L, compared to those that did not receive any treatment. From as early as 2 h.p.i., we detected a statistically significant reduction of ICP8 copies in the presence of CD40L which increased over time (Fig. 3.9 B). Finally, examination of glycoprotein G (gG) expression in CD40-U2OS cells infected at MOI 1 PFU/cell at 18h.p.i., showed that gG was hardly detectable in cells exposed to CD40L signaling (Fig. 3.9 C).

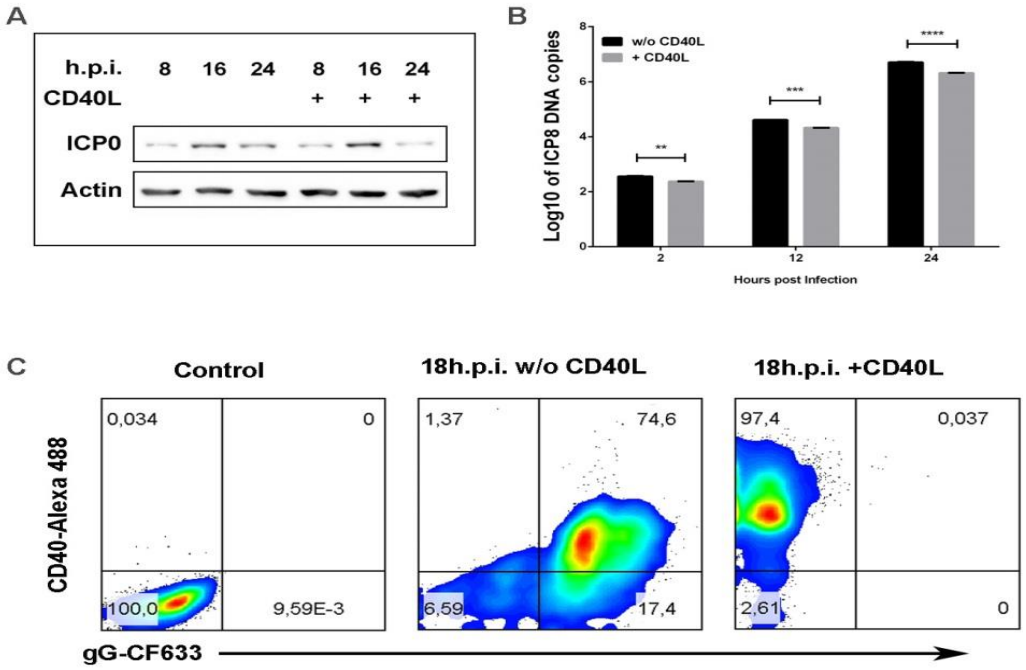

Figure 3.9: Analysis of ICP0 expression, viral DNA replication and glycoprotein synthesis during CD40L signaling. (A) ICP0 expression in CD40-U2OS cells infected with HSV-1 17syn at a multiplicity of 1 PFU/cell in the presence of CD40L, at various points post infection. The cells were treated with CD40L (0.5µg/ml) or control medium for 30 minutes and were then infected with HSV-1 17syn for 8, 16 and 24 hours respectively. Protein extracts were collected and 40µg of protein were analyzed for each time point. **(B)** DNA copies of ICP8 in CD40-U2OS cells infected with HSV-1 17syn at a multiplicity of 1 PFU/cell in the presence of CD40L at various points post infection. The cells were treated with CD40L (0.5µg/ml) or control medium for 30 minutes and were then infected with HSV-1 17syn for 2, 12 and 24 hours respectively. The cells were lysed, DNA was collected and ICP8 copies were quantified by qPCR. For the statistical analysis, an unpaired t-test was performed using GraphPad Prism 6.04. The asterisks indicate statistical significance. ** indicate p=0.001 to 0.01, *** indicate p=0.0001 to 0.001 and **** indicate p<0.0001. **(C)** Glycoprotein G (gG) expression of CD40-U2OS cells infected with HSV-1 17syn at MOI 1 for 18 hours. The cells were treated with CD40L (0.5µg/ml) or control medium for 30 minutes and were then infected with HSV-1 17syn for 18 hours, stained with both CD40 and gG, and analyzed by flow cytometry. (The control panel depicts CD40-U2OS cells stained only with the secondary antibodies).

Visualization of PML nuclear bodies following HSV-1 infection under CD40L signaling.

The effect of CD40L on the production of progeny virus, led us to investigate cellular mechanisms with antiviral properties such as the PML or ND10 bodies[170,171]. PML nuclear bodies associate with the viral genome and they are degraded by the viral protein ICP0[170]. In order to investigate whether there is an upregulation of PML nuclear bodies upon CD40L signaling preventing the replication of the viral genome, CD40-U2OS cells were infected at MOI 1 PFU/ml for several time points following activation of the CD40 pathway and PML integrity was monitored by confocal microscopy in parallel with ICP0 expression. We did not observe any difference (Fig. 3.10) in the rate of PML degradation between CD40L-treated and non-treated cells. PML colocalized with ICP0 while increase of ICP0 expression correlated with a gradual degradation of PML nuclear bodies, regardless of CD40 signaling, highlighting our previous observations that the effect of CD40L on HSV-1 is exerted prior to its localization to the nucleus.

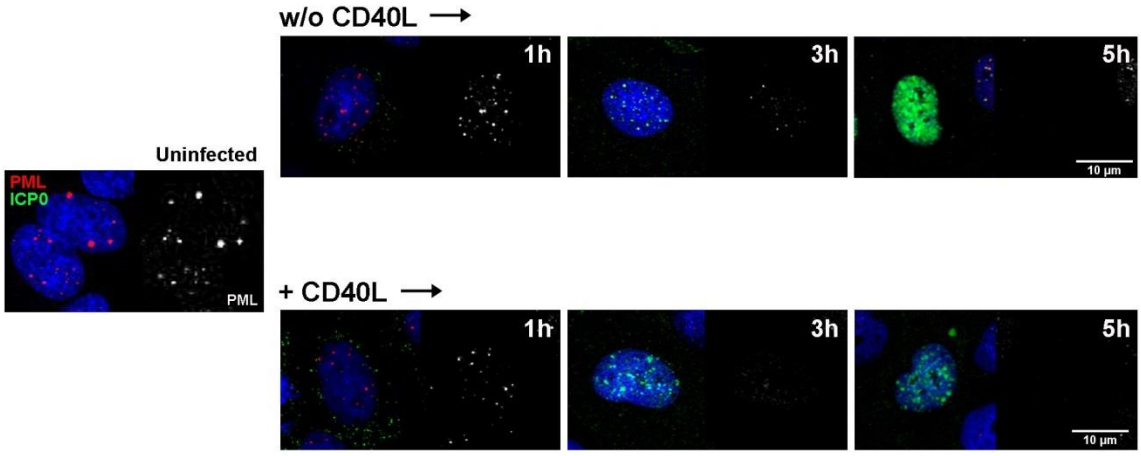

Figure 3.10: Analysis of PML distribution during CD40L signaling in HSV-1 infected cells. PML and ICP0 distribution in CD40-U2OS cells infected with HSV-1 17syn at a multiplicity of 1 PFU/cell in the presence of CD40L, at various points post infection. The cells were treated with CD40L (0.5μg/ml) or control medium for 30 minutes and were then infected with HSV-1 17syn for 1, 3 and 5 hours respectively. They were stained for PML (red) and ICP0 (green) and were visualized by confocal microscopy.

PI3K inhibition reverses the effect of CD40 signaling on HSV-1.

The observed delay in VP16 entry to the nucleus, prompted us to investigate CD40 signaling pathways responsible for the regulation of antiviral responses. In particular, we explored the impact of PI3 kinase which is known to be activated by CD40 ligation in epithelial cells [172] and of autophagy which has been implicated in HSV-1 replication [116,117] and is controlled by PI3 kinase signals. To address this issue, we infected CD40-U2OS with rHSV-RYC in the presence of CD40L, along with the PI3K inhibitor LY294002 which inhibits the autophagosome formation[173] and monitored the dynamics of VP16 and VP26 by live cell microscopy (Fig. 3.11). In LY294002-treated cells, nuclear VP26

foci were clearly visible at 6 h.p.i. whereas in control untreated cultures, VP26 foci were detectable at later time points. Treatment of CD40-U2OS cells with CD40L was able to reverse, in part, the phenotype of LY294002 (Fig. 3.11).

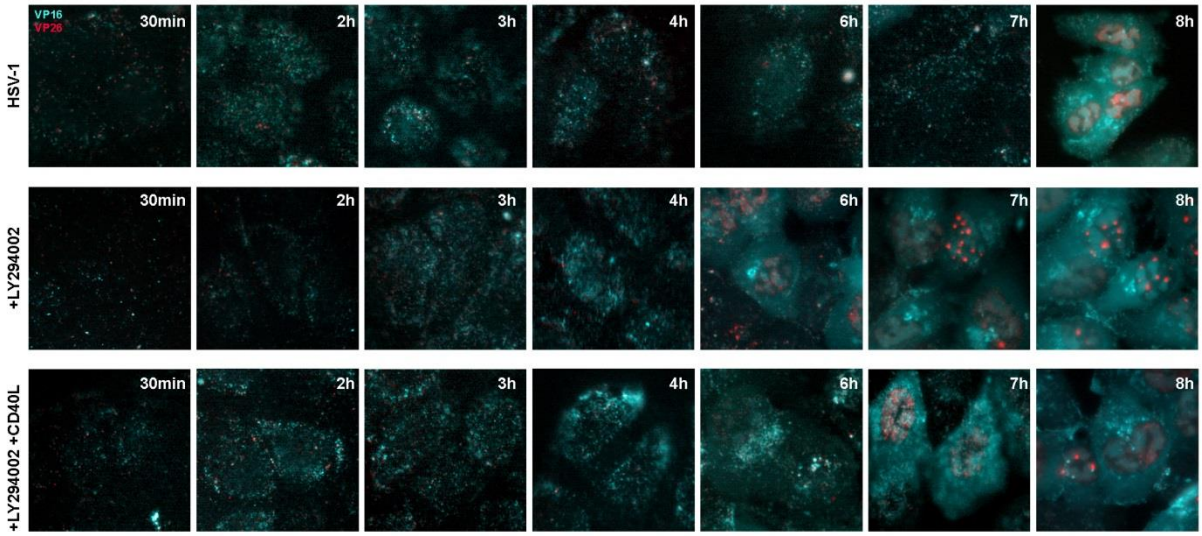

Figure 3.11: Kinetics of HSV-1 in the presence of CD40L and a PI3K inhibitor. Live imaging. CD40-U2OS cells were plated in a chambered coverglass unit, treated with the PI3K inhibitor LY294002 (25μM) for 30 minutes, CD40L (0,5μg/ml) or control medium was added for another 30 minutes and the cells were then infected with rHSV-RYC at a multiplicity of 20 PFU per cell, for 1.5 hours on ice. Following incubation with the virus at 4oC, the cells were transferred in a humidified chamber on the microscope stage with 5% CO2 at 37^{o}C and were monitored for at least 8 hours.

To confirm the timelapse microscopy observations, we examined the production of progeny virions obtained from cells infected at MOI 1 PFU/cell in the presence of LY294002 and/or CD40L, at 24 h.p.i, compared to control infected cells (Fig. 3.12). The results showed a statistically significant difference in the production of progeny virions between cells treated with LY294002 and cells treated with either LY294002 and CD40L or CD40L alone. In contrast, there was no statistically significant difference between the virus produced from the control infection and the virus produced from cells treated with both LY294002 and CD40L, a result which further corroborates the timelapse microscopy findings.

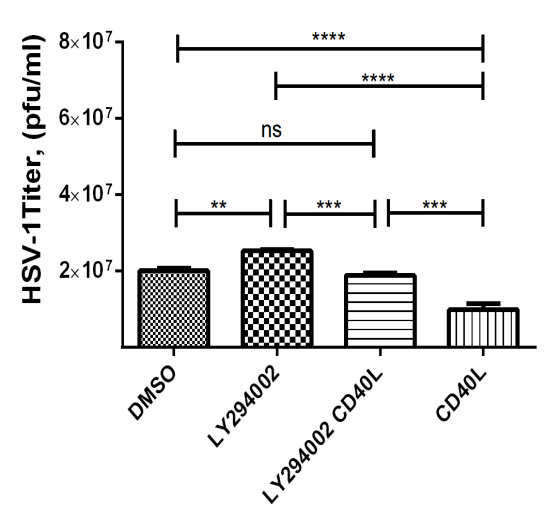

Figure 3.12: Effect of the PI3K inhibitor LY294002 and of CD40L on HSV-1 progeny virus. CD40-U2OS cells were treated with either the PI3K inhibitor LY294002, CD40L or both LY294002 and CD40L. The cells were pretreated with the inhibitor or solvent vehicle for 30 minutes, followed by addition of CD40L (0.5µg/ml) for another 30 minutes. Neither the inhibitor nor the CD40L were removed from the medium for the course of infection. After pretreatments, the cells were infected at a multiplicity of 1 PFU/cell and the supernatants were collected at 24 h.p.i. and were titrated on Vero cells. Titrations are representative of three independent experiments and are shown as means ± SEM. For the statistical analysis, we performed a Repeated Measures one-way ANOVA followed by an uncorrected Fisher's LSD test using GraphPad Prism 6.04. The asterisks indicate statistical significance. ** indicate p=0.001 to 0.01, *** indicate p=0.0001 to 0.001 and **** indicate p<0.0001. ns= not significant.

Next, we investigated the potential association between HSV-1 and LC3 by immunofluorescence analysis since LC3s are involved in the formation of the phagophore. Moreover conversion of LC3 I to LC3 II is indicative of autophagy initiation. CD40-U2OS cells were infected with wild-type HSV-1 at MOI 30 PFU/cell for 1.5 and 3 hours, including a binding step on ice to synchronize the infection. The infected cells were immunostained for all HSV-1 major glycoproteins and at least one core protein, as well as for LC3 isoforms I and II. We observed that HSV-1 exhibited a higher degree of colocalization with LC3 in the presence of CD40L. This colocalization was markedly reduced in the presence of LY294002 while it was partly restored when cells were treated with both LY294002 and CD40L (Fig. 3.13). The association of LC3 foci and HSV-1 was scored and analyzed by ordinary one-way ANOVA at 1.5 and 3 hpi. Differences of the means were found to be statistically significant (P<0.0001) which highlights a strong association between LC3 foci with HSV-1 (Fig. 3.14 A and B).

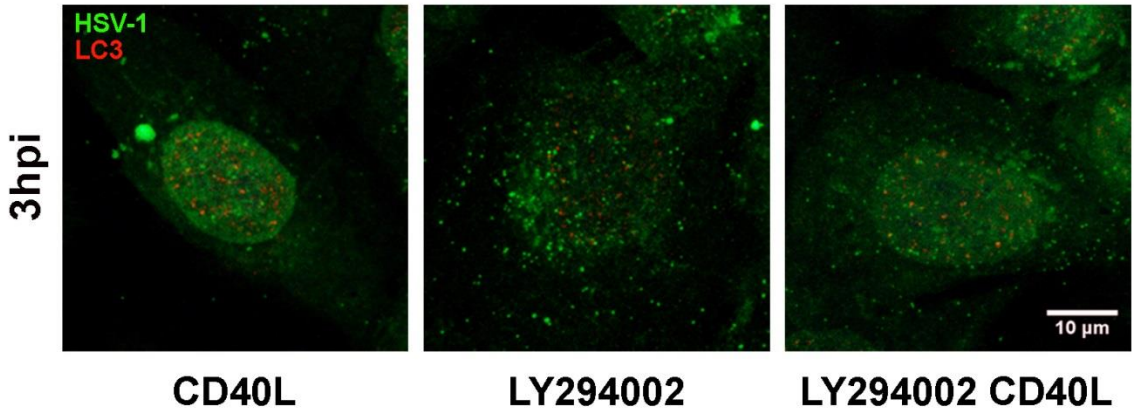

Figure 3.13: Effect of the PI3K inhibitor LY294002 and of CD40L on LC3 localization following HSV-1 infection. CD40-U2OS cells were treated with either the PI3K inhibitor LY294002, CD40L or both LY294002 and CD40L. The cells were pretreated with the inhibitor or solvent vehicle for 30 minutes, followed by addition of CD40L (0.5μg/ml) for another 30 minutes. Neither the inhibitor nor the CD40L were removed from the medium for the course of infection. After pretreatments, the cells were infected at a multiplicity of 30 PFU/cell while a binding step was also added. The cells were stained for HSV-1 with a rabbit anti-HSV type-1 antibody (green) and were also stained for LC3 isoforms I and II (red). Images were obtained by confocal microscopy.

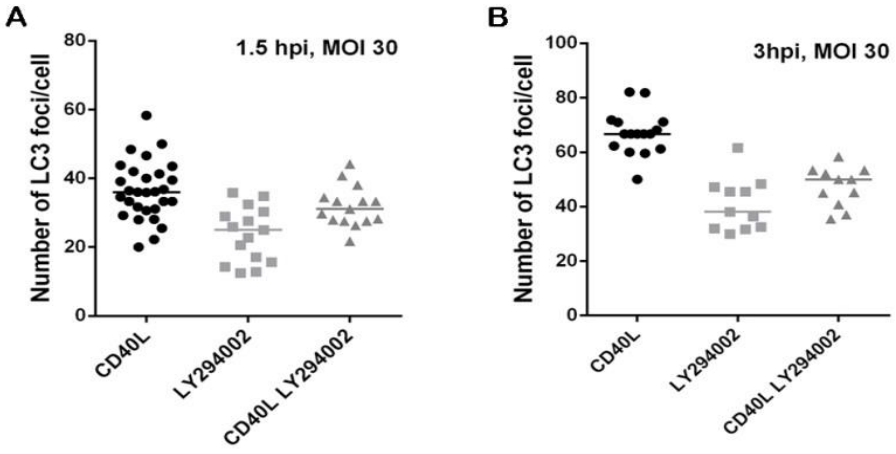

Figure 3.14: Perinuclear colocalization of LC3 with HSV-1. The number of LC3 foci per cell that colocalized with HSV-1 at 1.5 and 3 hpi was counted from images obtained after confocal microscopy of the experiment described on Fig. 3.13, using the ImageJ cell counter application. Statistical analysis was performed by ordinary one-way ANOVA with GraphPad Prism 6.04. Differences of the means were found to be statistically significant ($p<0.0001$). Error bars represent the median.

Spautin-1 does not reverse the effect of CD40L on HSV-1 replication.

Based on the aforementioned findings which pointed to the direction of autophagy, we proceeded to investigate whether the specific and potent autophagy inhibitor (spautin-1) has also an effect on the production of progeny virions. To address this issue, we treated CD40-U2OS cells with spautin-1 in the presence or absence of CD40L and assessed progeny virions production 24 h.p.i.. Interestingly, spautin-1

significantly inhibited the production of progeny virions compared to the control infection and its effect was found to be comparable to the inhibitory effect of CD40L on HSV-1 (Fig. 3.15). Treatment of CD40-U2OS cells with CD40L in combination with spautin-1 did not inhibit virion production beyond the effect of each compound alone (Fig. 3.15), suggesting that CD40L exerts its effect via a pathway upstream of Beclin-1 or p53, which are both inhibited by spautin-1[174].

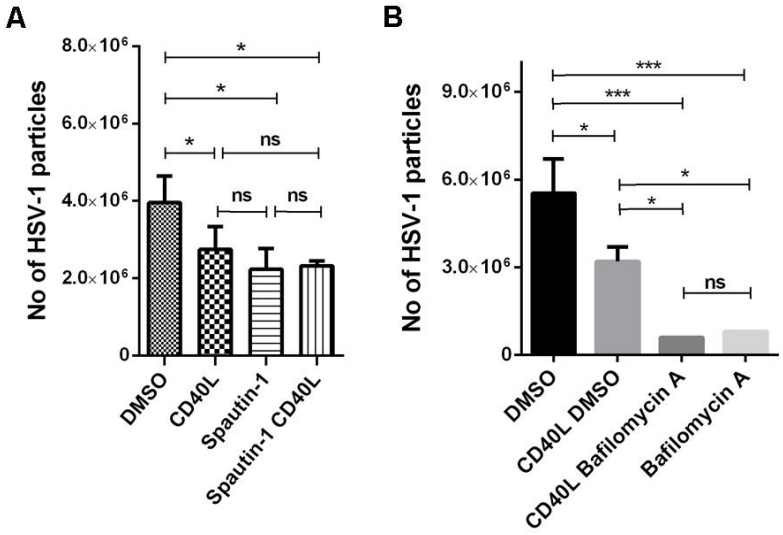

Figure 3.15: Effect of the autophagy-related inhibitors Spautin-1 and Bafilomycin HSV-1 progeny virus. CD40-U2OS cells were either treated with the specific autophagy inhibitor Spautin-1, Bafilomycin A, CD40L, or a combination of an inhibitor and CD40L. Whenever both an inhibitor and CD40L were used, the cells were pretreated with the inhibitor for 30 minutes, followed by addition of CD40L (0.5µg/ml) for another 30 minutes. Neither the inhibitors nor the CD40L were removed from the medium for the course of infection. After pretreatments, the cells were infected at a multiplicity of 1 PFU/cell and the supernatants were collected at 24 h.p.i. and were titrated on Vero cells **(A)** Titration of HSV-1 17syn treated with DMSO, CD40L, Spautin-1 (10µM), or with both Spautin-1 and CD40L. **(B)** Titration of HSV-1 17syn treated with DMSO, CD40L, Bafilomycin A (100nM), or with both Bafilomycin A and CD40L. The data are representative of three independent experiments and are shown as means ± SEM. For the statistical analysis, we performed a Repeated Measures one-way ANOVA followed by an uncorrected Fisher's LSD test using GraphPad Prism 6.04. The asterisks indicate statistical significance. * indicates p= 0.01 to 0.05, ** indicate p=0.001 to 0.01, *** indicate p=0.0001 to 0.001 and ns= not significant.

Bafilomycin A1 blocks HSV-1 propagation irrespective of CD40 signaling.

Since LY294002 and Spautin-1 had opposing effects on HSV-1 infection we also used Bafilomycin A1. Bafilomycin A1 is an inhibitor of the vacuolar H+ ATPase (V-ATPase) and prevents acidification of the lysosome[175]. It is commonly used as an inhibitor of autophagy since it inhibits autophagosome-lysosome fusion[176]. Since Bafilomycin is able to decrease the production of progeny HSV-1 virions[72] we first established that the virus enters the cell and that the infection proceeds, through fluorescence microscopy. For assessment of its effect upon CD40L signaling, CD40-U2OS cells were treated with Bafilomycin A1 in combination with CD40L and the progeny HSV-1 virus collected at 24h.p.i. was titrated. We found that HSV-1 was significantly blocked

regardless of the presence of CD40L (Fig 3.15) suggesting that acidification of the lysosome is crucial to HSV-1 progression of infection.

JNK is not required for CD40-mediated suppression of progeny virion production.

CD40 ligation also induces the JNK pathway[177] which has been implicated in autophagy induction[178]. For that reason and since the results we obtained were inconclusive in respect of autophagy, we utilized the JNK inhibitor SP600125. We incubated CD40-U2OS cells with SP600125 in combination with CD40L and spautin-1. The cells were subsequently infected with wild-type HSV-1 at MOI 1 PFU/cell for 24 hours and the progeny virions produced were determined by plaque assay. We found that the SP600125 inhibitor caused a marked decrease in the production of progeny virus equal to that caused by CD40L and that inhibition of JNK with parallel activation of the CD40 pathway caused an even greater effect (Fig 3.16) suggesting that JNK and CD40L have opposite effects as to the inhibition of HSV-1 progeny production.

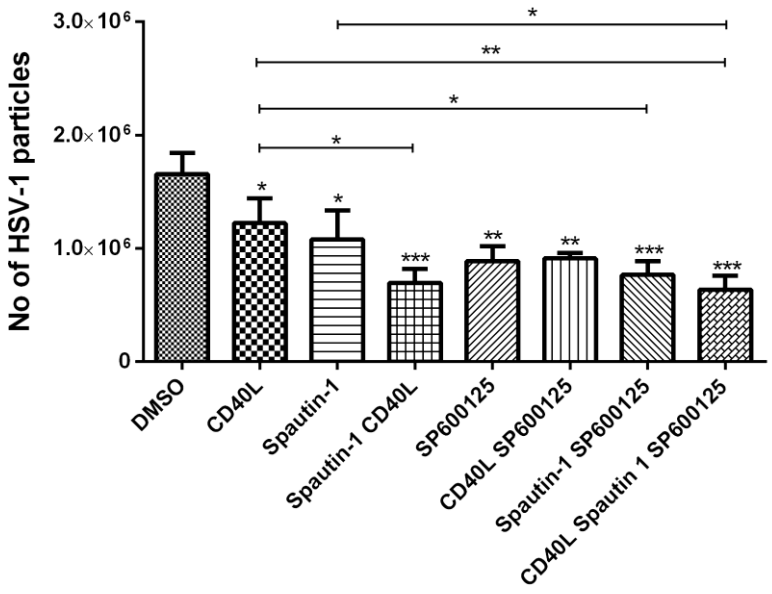

Figure 3.16: The effect of Spautin-1, SP600125 and CD40L on HSV-1 progeny virus. Titration of HSV-1 17syn treated with DMSO, CD40L, Spautin-1, SP600125 (7.5μM) or a combination of them. CD40-U2OS cells were either treated with the specific autophagy inhibitor Spautin-1, the JNK inhibitor SP600125, CD40L, or a combination of the above inhibitors and CD40L. Whenever both an inhibitor(s) and CD40L were used, the cells were pretreated with the inhibitor(s) for 30 minutes, followed by addition of CD40L (0.5μg/ml) for another 30 minutes. Neither the inhibitors nor the CD40L were removed from the medium for the course of infection. After pretreatments, the cells were infected at a multiplicity of 1 PFU/cell and the supernatants were collected at 24 h.p.i. and were titrated on Vero cells. The data are representative of three independent experiments and are shown as means ± SEM. For the statistical analysis, we performed a Repeated Measures one-way ANOVA followed by an uncorrected Fisher's LSD test using GraphPad Prism 6.04. The asterisks indicate statistical significance. * indicates p= 0.01 to 0.05, ** indicate p=0.001 to 0.01, and *** indicate p=0.0001 to 0.001 .

Interestingly, CD40L in combination with SP600125 leads to a decrease in LC3 II/LC3 I ratio and the same is true for spautin-1 (Fig. 3.17 A and B). Moreover, we confirmed that in the presence of CD40L, there is induction of LC3 II, independently of HSV-1 infection (Fig 3.17 A). Intriguingly, CD40 activation favors LC3 I over LC3 II and the LC3 II/LC3 I ratio decreases in the presence of CD40L.

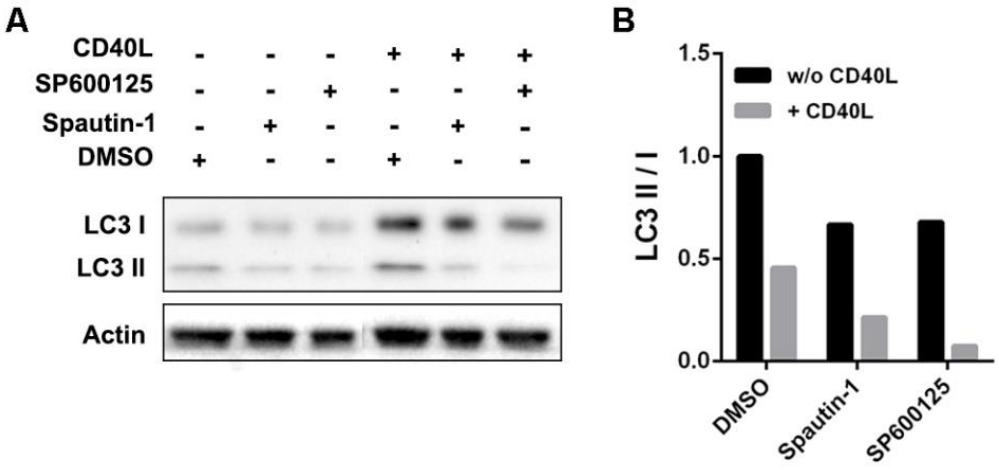

Figure 3.17: **LC3 I and II expression (A)** LC3 I and II expression in CD40-U2OS cells treated with Spautin-1, SP600125, CD40L or vehicle solvent as well as in cells treated with both the inhibitors and CD40L (0,5μg/ml) for 24 hours. **(B)** Quantification of LC3 II/I ration after being normalized to actin from the western blot depicted on **(A)** using the Image Lab 5.0 software.

Silencing of Atg5 attenuates production of progeny virions.

Atg5 constitutes a key component for the formation of the autophagic vesicle. Atg5 associates covalently with Atg12 forming an E3-like enzyme which forms a complex with Atg16. The Atg5-Atg12/Atg16 complex leads to the lipidation of LC3 I, with the lipid phosphatidylethanolamine (PE) to form LC3 II at the site of expansion of the autophagic membrane[179]. In addition, Atg5 is essential to the cytoplasm-to-vacuole-transport (Cvt) pathway in yeast[179,180]. We transfected CD40-U2OS cells with siAtg5 and control siRNA for 48 hours and subsequently treated the cells with CD40L (0.5μg/ml) or vehicle solvent and assessed the production of progeny virus collected 24 h.p.i. We found that silencing of Atg5 led to a significant decrease in the production of progeny virions as compared to the control. Moreover, CD40L further inhibited HSV-1 production in combination with Atg5 silencing (Fig. 3.18). All of the above data confirm that CD40L does not exert its antiviral effect through autophagy but rather through a PI3K dependent mechanism.

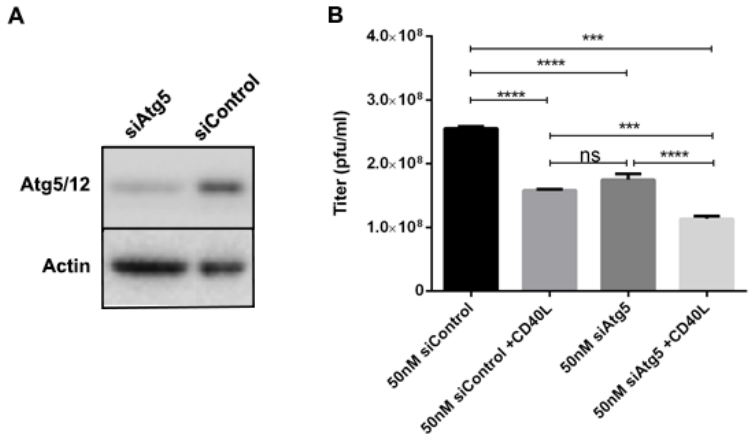

Figure 3. 18: Knockdown of Atg5 attenuated HSV-1 progeny virus. CD40-U2OS cells were transfected with siAtg5 or siControl RNA and remained in culture for 48 hours. They were subsequently treated with CD40L (0,5µg/ml) for 30min and were then infected with HSV-1 for 24 hours at MOI 1. (A) Cell extracts were collected and analyzed for Atg5 expression by western blot. (B) Titration of HSV-1 17syn treated with CD40L in CD40-U2OS cells transfected with siControl or siAtg5. Titration was performed on Vero cells. The data are representative of three independent experiments and are shown as means ± SEM. For the statistical analysis, we performed a Repeated Measures one-way ANOVA followed by an uncorrected Fisher's LSD test using GraphPad Prism 6.04. The asterisks indicate statistical significance. *** indicate p=0.0001 to 0.001 and **** indicate p<0.0001. ns= not significant.

Epigenetic phenomena during HSV-1 infection.

Characterization of the lytic and latent state of HSV-1.

Epigenetic phenomena related to HSV-1 infection are being studied for more than a decade. It has been established that transition from a lytic to a latent infection and vice versa constitutes an epigenetic event and it is a field of active research. Therefore, we set out to investigate DNA methylation in a group of genes coding for epigenetic factors (e.g. methylation enzymes, acetylation enzymes, etc) and its impact on the progression of HSV-1 lytic and latent infection. To this end, we used the permissive to HSV-1 infection Vero cell line. To determine the appropriate time points characteristic of the *α*, *β* and *γ* phases of HSV-1 infection we infected cells at MOI 1 PFU/cell for various time points with the wild type virus HSV-1 17syn and stained for the ICP0, ICP8 and gG viral proteins respectively. At 3 h.p.i. ICP0 was detected but not in replication compartments. At 8.h.p.i. there was colocalization of DNA with ICP8 and at 15h.p.i. gG aggregated around the nucleus and in the cytoplasm (Fig. 3.19). Thus, the methylation study was performed at 3 h.p.i. for the *α*, at 8 h.p.i. for the *β* and at 15 h.p.i. for the *γ* phase of the infection.

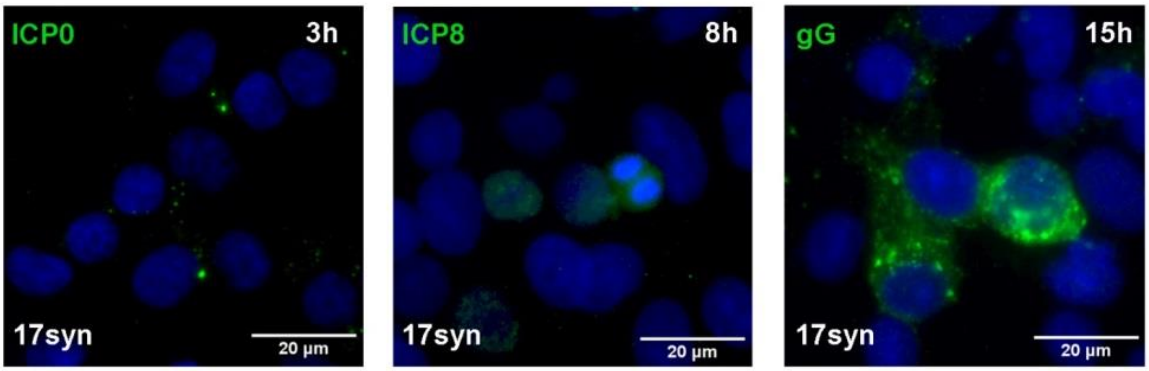

Figure 3.19: Progress of HSV-1 infection in time. Vero cells were infected at a multiplicity of 1 PFU/cell with HSV-1 17syn and stained for HSV-1 with ICP0 at 3hpi (green), ICP8 at 8hpi (green) or gG at 15hpi (green).

In order to achieve a latent infection we utilized the mutant virus dl0c4[181] which lacks ICP0, carries a CFP tag on ICP4 and constitutes an established system for simulation of latent infection. Vero were infected at MOI 0.01 PFU/cell for 2-3 days until there was detection of ICP4 fluorescence in the majority of cells and prior to the formation of replication compartments (Fig. 3.20 A). Latent population isolation was based on microscopic observation of ICP4 expression and its distribution in the nucleus; however, it was further verified by FACS analysis. Cells infected at a higher MOI exhibited two peaks of fluorescence due to the coexistence of a lytic and latent population and were used as a control to evaluate the fraction of latent cells in the sample that would be analyzed for DNA methylation (Fig 3.20 B and C).

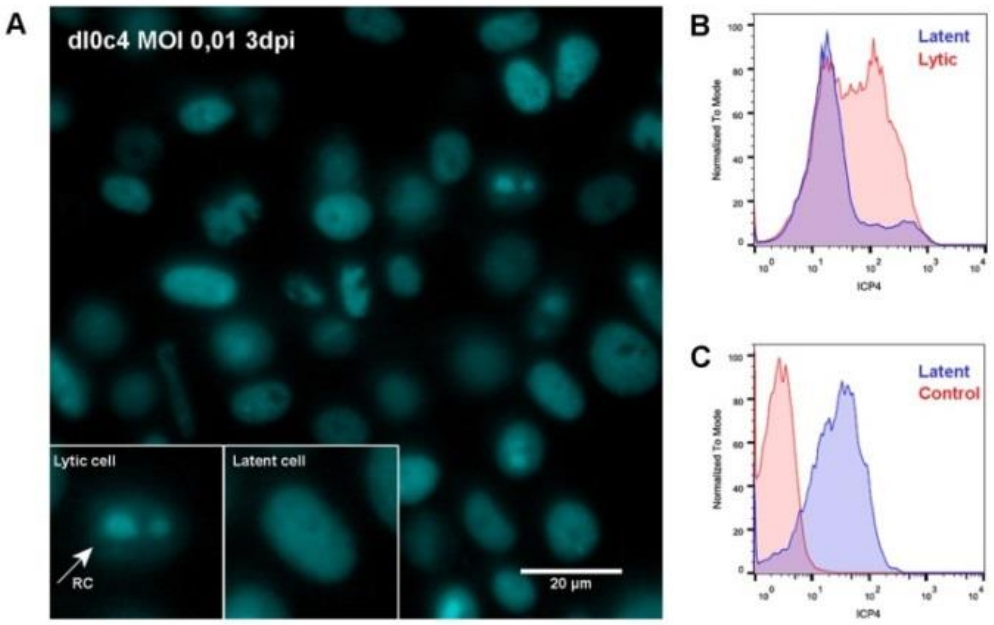

Figure 3. 20: **Establishment of the latent infection *in vitro* system. (A)** Vero cells were infected at a multiplicity of 0,01 PFU/cell with dl0c4 and ICP4 (cyan) was observed at approximately 3 days post infection. In the culture coexisted two populations, latent and a number of lytic cells. The left inset depicts a lytic cell that has developed replication compartments (RC) and the right inset depocts a latent cell where ICP4 is expressed but there are no replication compartments. **(B)** Vero cells were latently infected (MOI 0.01 for ~3days) and lytically infected (MOI 1 for 24 hours) with dl0c4 to determine the fluorescence profile of each population. The level of ICP4 expression in the two samples was monitored by flow cytometry. **(C)** Vero cells were latently infected with dl0c4 for verification of its fluorescence profile. The level of ICP4 expression was monitored by flow cytometry.

Methylation profiling during lytic and latent infection.

In order to identify the methylation profile of the genes depicted on Table 3.1 consisting of histone deacetylases and acetyltransferaces, DNA methyltransferases, lysine specific demethylases, histone-lysine N-methyltransferases and transcriptional regulators, we collected DNA from Vero cells following infection. For lytic infection, Vero cells were infected at MOI 1 PFU/cell with the wild type virus HSV-1 17syn for 3, 8 and 15 hours, respectively. For a latent infection Vero cells were infected for approximately 2-3 days at MOI 0.01 PFU/cell with the mutant HSV-1 virus dl0c4. Among the 24 genes tested, variation in the methylation profile was identified in 6, while the methylation profile of 10 of the genes tested was not affected by infection. Finally, 8 genes failed to produce any results due to technical reasons.

Table 3.1: Genes tested for methylation profile at their promoter region.

Histone Deacetylases	DNA methyltransferaces	Lysine specific demethylases
HDAC1	DNMT1	KDM1
HDAC2	DNMT3A	KDM2A
HDAC3	DNMT3B	KDM2B
HDAC4	Transcriptional regulators	KDM3A
HDAC5	CREB/ATF2	KDM3B
HDAC6	NRF2/GABP	Histone-lysine N-methyltransferases
HDAC10	Histone acetyltransferases	SUV39H1
HDAC11	KAT2A	WHSC1L1
	KAT2B	SETD1A
		ASH2L
Legent		
Variation in methylation upon HSV-1 infection		
No variation im methylation upon HSV-1 infection		
Technical failure		

Analysis of the methylation profile revealed that the histone deacetylases HDAC2, 3 and 10 were mainly unmethylated both in the control samples and during infection. Interestingly, at 3h.p.i. there was a shift towards intermediate methylation (Fig. 3.21).

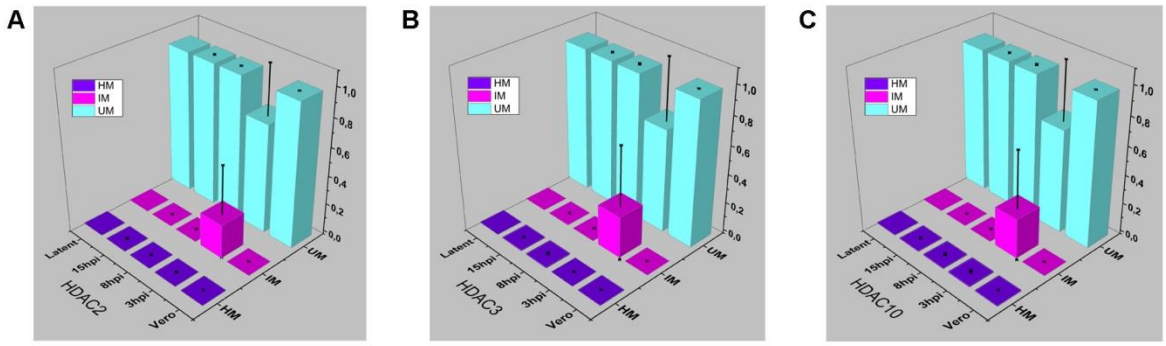

Figure 3.21: Mehtylation profiling of HDAC1, HDAC2 and HDAC10 gene promoters during HSV-1 lytic infection. Vero cells were infected at a multiplicity of 1 PFU/cell with HSV-1 17syn for 3, 8 and 15 hours or with dl0c4 at a multiplicity of 0.01 PFU/cell. DNA was collected at appropriate time points and was subjected to methylation profiling (Methylation profiling array, SA Biosciences). Analysis detects three methylation profiles of the specified promoters, namely the hypermethylated state, the intermediately methylated state and the unmethylated state. The data are representative of three independent experiments and are shown as means ± SD.

The lysine specific demethylase, LSD1 or KDM1 was also unmethylated both at steady state and during infection with the exception of a shift towards intermediate methylation at 8h.p.i.. The histone acetyltransferase KAT2A on the contrary was hypermethylated in all conditions apart from 3 h.p.i. when it was to some extent hypomethylated. Lastly, the DNA methyltransferace DNMT3A exhibited a greater fluctuation between the unmethylated and methylated state of its promoter in the course of infection (Fig. 3.22). In general, the latent state exhibits a methylation status similar to that of the control sample while most of the differences are identified at 3h.p.i., the immediate early phase of HSV-1 and at 8h.p.i. the early phase.

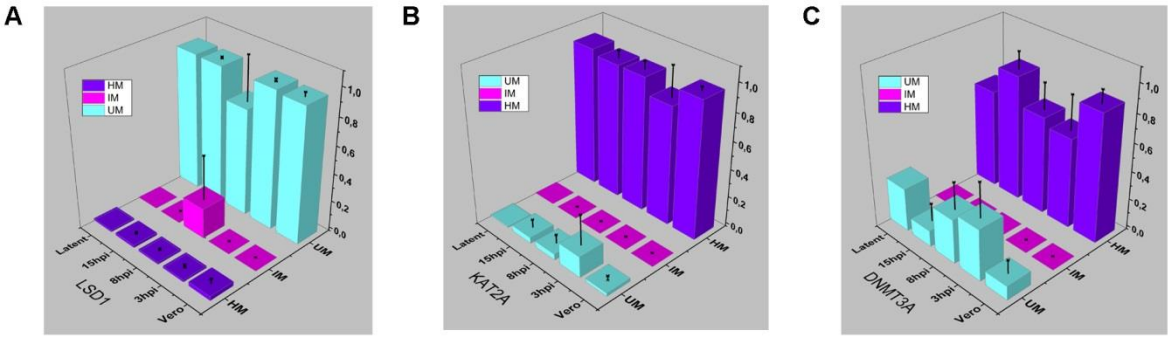

Figure 3.22: Mehtylation profiling of LSD1, KAT2 and DNMT3A gene promoters during HSV-1 lytic infection. Vero cells were infected at a multiplicity of 1 PFU/cell with HSV-1 17syn for 3, 8 and 15 hours or with dl0c4 at a multiplicity of 0.01 PFU/cell. DNA was collected at appropriate time points and was subjected to methylation profiling (Methylation profiling array, SA Biosciences). Analysis detects three methylation profiles of the specified promoters, namely the hypermethylated state, the intermediately methylated state and the unmethylated state. The data are representative of three independent experiments and are shown as means ± SD.

Expression pattern of HDAC 1, HDAC2, HDAC3 and LSD1 in the course of HSV-1 lytic infection.

Following the above observations, we set out to investigate the expression profile of HDAC1, HDAC2, HDAC3 and LSD1. Concerning HDAC1, we had some indications from the methylation profiling assay but due to failure to detect its profile at the steady state we could not evaluate it. In order to evaluate the expression of the above enzymes during lytic infection we collected RNA from Vero cells infected at MOI 1 PFU/cell for 3, 8 and 15 hours respectively and performed RT-qPCR. HDAC1 was significantly decreased at 8 and 15 h.p.i., while HDAC2 was significantly decreased for the course of infection. Interestingly, it was particularly reduced at the immediate-early and late phases of infection. HDAC3 expression on the other hand, was markedly decreased during the course of the infection and the same was observed for the LSD1 gene (Fig. 3.23).

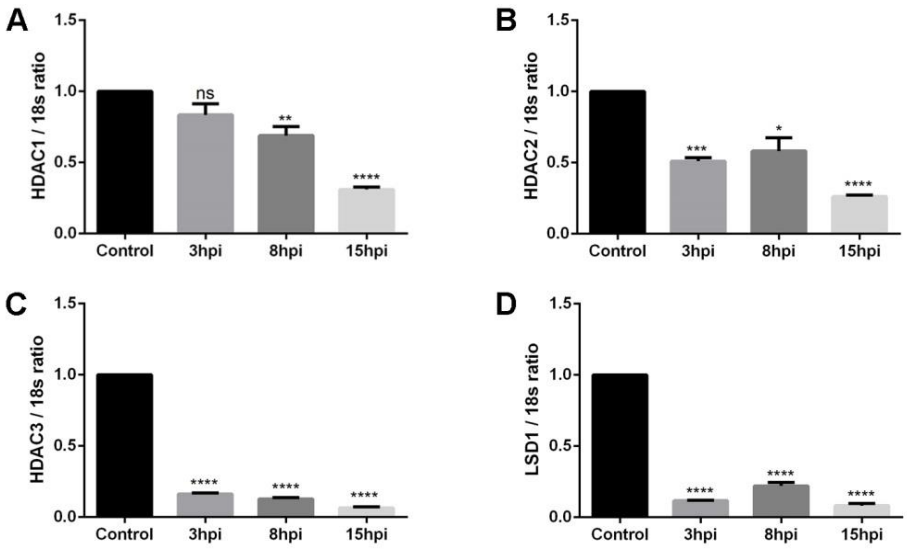

Figure 3. 23: Relative expression of HDAC, HDAC2, HDAC3 and LSD1 during productive HSV-1 infection. Vero cells were infected at a multiplicity of 1 PFU/cell with HSV-1 17syn for 3, 8 and 15 hours, RNA was collected and subjected to qPCR (relative standard curve method). The data are representative of three independent experiments and are shown as means ± SEM. For the statistical analysis, we performed an unpaired t-test using GraphPad Prism 6.04. The asterisks indicate statistical significance. ** indicate p=0.001 to 0.01, *** indicate p=0.0001 to 0.001 **** indicate p<0.0001 and ns= not significant.

HSV-1 propagation in cell lines silenced for HDAC1, HDAC2, HDAC3 and LSD1.

Next, we went on to evaluate viral replication on cell lines silenced independently for HDAC1, HDAC2, HDAC3 or LSD1. Vero cells were transduced with the appropriate lentiviruses expressing shRNA cassettes, targeting the aforementioned genes. The positively transduced cells were selected with puromycin. Expression of the respective genes was evaluated by RT-qPCR. Among all clones created for HDAC1 and HDAC2 knockdown, Vero shHDAC1 B8 and Vero shHDAC2 A7 were used for the viral replication assays (Fig. 3.24).

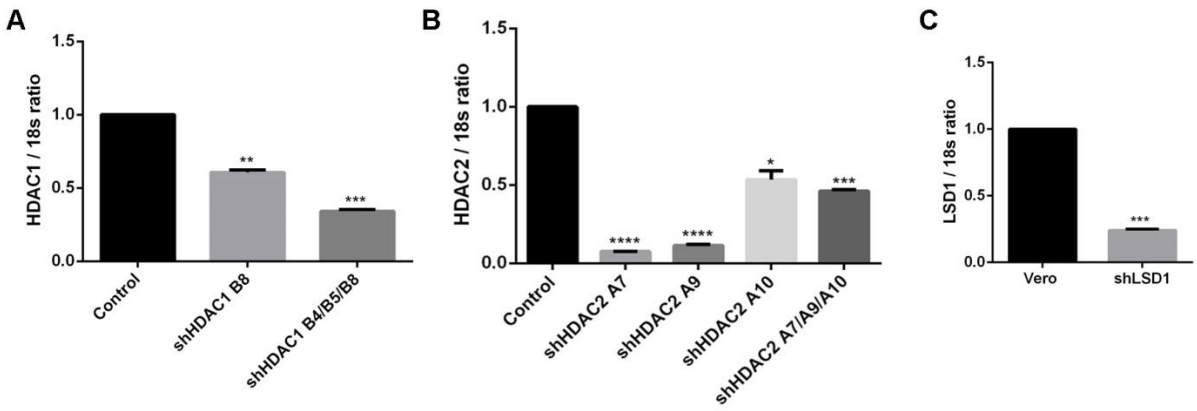

Figure 3.24: Evaluation of silenced Vero cell lines. Vero cells were silenced for HDAC1, HDAC2 and LSD1 with various shRNA lentiviral clones and were subjected to RT-qPCR for evaluation of the silencing level achieved (relative standard curve method). The data are representative of three independent experiments and are shown as means ± SEM. For the statistical analysis, we performed an unpaired t-test. For the statistical analysis, we performed an unpaired t-test using GraphPad Prism 6.04. The asterisks indicate statistical significance. * indicates P ≤ 0.05, ** indicate p=0.001 to 0.01, *** indicate p=0.0001 to 0.001, **** indicate p<0.0001 and ns= not significant.

Infection of the silenced cell lines was performed at MOI 1 PFU/ml for 24 hours and supernatants were titrated on Vero cells. Production of progeny virions was not significantly different in HDAC1 knockdown Vero cells. On the contrary, silencing of HDAC2 caused a marked increase in the production of HSV-1 progeny virions while silencing of HDAC3 and LSD1 caused a significant decrease in the propagation of the virus (Fig. 3.25)

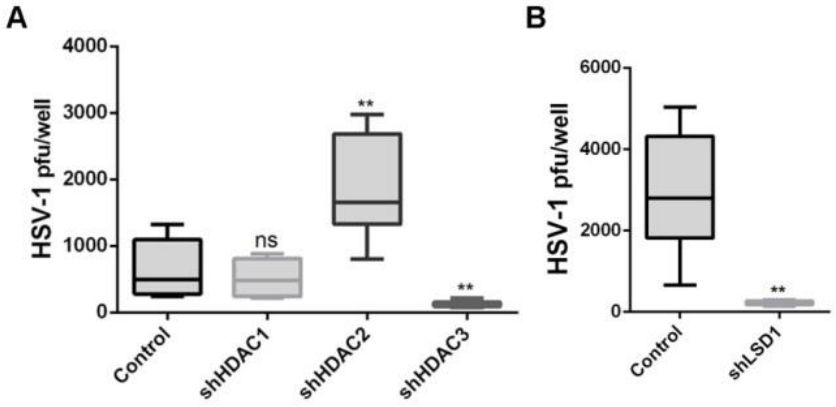

Figure 3.25: Vero cells silenced for HDAC1, HDAC2, HDAC3 or LSD1 were infected at a multiplicity of 1 PFU/cell with HSV-1 17syn for 24 hours and titrated on Vero cells. The data are representative of three independent experiments and are shown as means ± SEM. For the statistical analysis, we performed an unpaired t-test. For the statistical analysis, we performed an unpaired t-test using GraphPad Prism 6.04. The asterisks indicate statistical significance. ** indicate p=0.001 to 0.01 and ns= not significant.

High throughput methylation profiling.

Characterization of the methylation status in the course of infection and during latency produced a massive amount of data that will give rise to the investigation of many aspects of HSV-1 infection. Bioinformatic analysis revealed many pathways that are modified which are associated with various physiological procedures of the cell as well as neurological diseases. Interestingly, genes associated with Huntington's disease were found to be significantly affected in all phases of viral infection, lytic or latent. Regarding the above 24 studied genes, HDAC1 gene promoter was found to be significantly hypomethylated at 3 and 8 hours post infection while HDAC2 HDAC3 and LSD1 did not exhibit any significant change. Moreover, the body of the HDAC4 gene was also found to be significantly hypomethylated for the course of infection in lytic and latent cells as compared to the steady state of HDAC4 methylation on Vero cells.

4. Discussion

Herpes Simplex Virus type-1 was studied using two different approaches to infection. Specifically, we studied the effect of the activation of the host CD40L pathway on HSV-1 infection. Furthermore, we also studied the effect of the virus on host genes associated with a particular regulatory mechanism, such as the DNA methylation. Both approaches aimed at identifying antiviral mechanisms that could be utilized against herpesviral infection.

Effect of CD40L on HSV-1 lytic infection.

In this study, we demonstrate that CD40 signaling confers direct antiviral effects on HSV-1 by negatively regulating the lytic cycle of the virus. This effect is specifically attributed to CD40-mediated signals, as expression of a mutated receptor that lacks the binding sites of TRAFs 1, 2, 3, 6 and 5 failed to protect U2OS cells from HSV-1 infection upon CD40L treatment. We have also shown that CD40 ligation does not affect the binding of HSV-1 to the cell membrane but causes a delay in the translocation of the viral tegument protein VP16 from the cytoplasm to the nucleus. As VP16 is largely responsible for the transactivation of immediate-early viral genes which are required to evade the host cell response to HSV-1 infection, the observed effects of CD40L on VP16 localization extend our understanding of the direct anti-viral properties of the CD40 pathway.

Furthermore, CD40 signaling was found to delay the trafficking of the viral capsid protein VP26 from the cytoplasm to the nucleus. As VP26 is a Late protein, the observation that VP26 lingers to the cytoplasm at the initiation of infection suggests that the delivery of the viral capsid is disturbed. The immediate-early protein ICP0 has been found to decrease at 24 hpi. The fact that we do not observe a decreased expression of ICP0 throughout the entire course of the infection is likely due to the fact that U2OS cells can substitute the functionality of ICP0 [167]. Congruent with these findings, the DNA copies of the virus are significantly decreased as early as 2 hpi while glycoprotein G (gG) synthesis in CD40L treated cells is almost completely abolished at late times of the infection.

The aforementioned observations coupled with the reported effects of CD40L on autophagy [150,182,183] prompted us to investigate whether this process is implicated in CD40-mediated anti-viral responses. To that end, we explored a variety of pharmacological inhibitors to block autophagy including the pan-class I/II/III PI3K inhibitor LY294002 that affects autophagosome formation, spautin-1 that leads to degradation of Beclin-1 and the JNK inhibitor SP600125 which induces the downregulation of Beclin-1. We observed that PI3K inhibition by LY294002 reversed the effect of CD40 ligation on progeny virion production (Fig. 3.12). Furthermore, LC3, a protein involved in the formation of autophagosomes, exhibited perinuclear colocalization with HSV-1 under CD40 signaling which was abrogated in the presence of LY294002. In contrast, spautin-1 and SP600125 did not reverse the CD40-mediated anti-HSV-1 effect (Fig. 3.16). Similar results were obtained when a genetic approach

was applied to inhibit autophagy by silencing Atg5 (Fig. 3.18). Intriguingly, suppression of autophagy by spautin-1, SP600125 or Atg5 siRNA inhibited virion production in the absence of CD40 ligation (Fig. 3.15, 3.16 and 3.18).

Collectively, these data suggest that the antiviral properties of CD40L are not mediated through autophagy but depend on the PI3K signaling pathway. When autophagy is upregulated, lysosomes move towards the perinuclear area to fuse with the autophagosomes that are being formed [184]. Interestingly, lysosomes have been shown to localize at the periphery of the cell, when autophagosome synthesis is downregulated and this is associated with increased mTORC1 activity regulated by Akt [184], a downstream target of PI3K. In terms of HSV-1, the virus mobilizes along microtubules to the nucleus, either as a naked capsid [185] or inside vacuoles such as endosomes [186,187], highlighting the importance of vesicular trafficking for HSV-1 infection. Because PI3-kinase regulates membrane trafficking [188], it is likely that the activation of this pathway by CD40L modifies a vesicle trafficking event that is important for the delivery of HSV-1 to the nuclear membrane. The class III PI3K Vsp34, that is also part of the Beclin-1 complex, is critical for the formation of vesicles in the multivesicular bodies (MVPs) and for endocytic recycling [189,190]. However, the operation of other host cell mechanisms that are accountable for the protective properties of CD40L cannot be excluded. It is worth mentioning that in neuronal culture systems PI3K signaling inhibition leads to reactivation of HSV-1 [191,192] and that a recent study strongly associated neonatal encephalitis with active autophagy in the brain of both mice and human specimens [193].

In conclusion, this study demonstrates that CD40 signaling exerts direct anti-viral effects by blocking the progress of HSV-1 lytic cycle. The finding that this phenomenon depends on PI3K signals but not autophagy raises the possibility that the CD40-TRAF-PI3K axis operates by impeding vesicular trafficking within the infected cell resulting in a delay in the trafficking of HSV-1 or its subvirion components to the nuclear membrane of the host.

Epigenetic phenomena during HSV-1 lytic and latent infection.

Epigenetic analysis of HSV-1 has been an active field of research for the last 10-20 years since it has been shown that epigenetic regulation is of key importance to the transition from a lytic to a latent infection[83]. DNA methylation is not the silencing mechanism inflicted on HSV-1[194,195]. Rather, silencing and reactivation of HSV-1 is regulated by methylation and acetylation of histones that assemble on the viral DNA following its entry in the nucleus. The tegument protein VP16 has been shown to reduce the association of histones with IE gene promoters and also to promote euchromatin modifications on histones that associate with lytic genes[59]. Moreover, ICP0 contributes to the derepression of the viral genome and its association with acetylated histones[138]. Thus, during lytic infection HSV-1 is associated with chromatin

bearing euchromatin modifications such as methylation of lysine 4 on histone H3 (H3K4me3) and acetylation of lysines 9 and 14 on histone H3 (H3K9 and H3K14)[196]. On the contrary, during latency, the lytic genes are associated with heterochromatin while LAT, the only viral region active during latency bears H3K9 and H3K14 acetylation[195]. Moreover, LAT induces H3K9me2 on lytic genes, a methylation mark that is characteristic of heterochromatin, and reduces HEK4me2 that is characteristic of euchromatin[197].

In this study, we attempted to identify changes in the methylation status of host genes in the course of infection. The genes under investigation code for "epigenetic" factors, mostly enzymes involved in the infliction of epigenetic phenomena. Moreover, we sought to unravel any phenomena that would differentiate lytic from latent infection. To that end we examined 24 genes, specifically HDAC1, HDAC2, HDAC3, HDAC4, HDAC5, HDAC6, HDAC10, HDAC11, DNMT1, DNMT3A, DNMT3B, KDM1, KDM2A, KDM2B, NRF2/GABP, CREB/ATF2, SETD1A, ASH2L, KAT2A, KAT2B, KDM3A, KDM3B, SUV39H1 and WHSC1L1. In order to study the promoters of those genes, we first identified the appropriate time points for immediate-early (IE), early (E) and late (L) infection in Vero cells. For a latent infection, we used a well-established *in vitro* system that utilizes the mutant HSV-1 virus dl0c4. The latter lacks a major regulator of infection, ICP0, and it also carries an ECFP tag fused to the immediate-early protein ICP4, allowing microscopy monitoring. The latent infection required intense observation of the infected cultures in order to identify the time point at which ICP4 was expressed in most cells and prior to the formation of replication compartments in a proportion of infected cells.

PCR-array analysis showed that among the 24 genes tested, HDAC2, HDAC3, HDAC10, DNMT3A, KDM1 and KAT2A exhibited a variation in DNA methylation in the course of infection. There was no variation in the methylation profile of 10 genes while 8 failed to produce any results due to technical reasons (Table 3.1).

In more detail, HDAC2, HDAC3 and HDAC10 revealed a similar methylation pattern. Specifically, HDAC2, HDAC3 and HDAC10 promoters were mainly unmethylated for the course of infection. However, at 3hpi, 25% of promoters exhibited an intermediate methylation pattern. HDAC2, HDAC3 and HDAC10, they all deacetylate lysine residues on the N-terminal part of the core histones (H2A, H2B, H3 and H4)[144]. Interestingly, HDAC10 can interact both with HDAC2 and HDAC3[198,199]. LSD1 also known as KDM1, was also unmethylated in most conditions, apart from the Early phase (8hpi) that it also exhibited an intermediate pattern of methylation on its promoter. On the contrary, the two other promoters, namely KAT2A and DNMT3A, were mainly hypermethylated. KAT2A lost its hypermethylation on about 15% of its promoters at the IE phase (3hpi) while DNMT3A lost its hypermethylation on about 30% of its promoters both at the IE and E phases (3 and 8hpi) and during latency.

It should be noted that there was a great variation in the methylation profile for the above 6 gene promoters from one experiment to the other. All experiments were

performed in triplicates and the 24 genes were analyzed simultaneously. However, for the 10 gene promoters that gave no variation the percentage of methylation detected was very consistent. Moreover, mock infected Vero cells at steady state also gave very consistent methylation levels with a standard deviation of 0.01%-2%. For that reason, the variation in methylation on these 6 genes is probably the result of specific virus-host interactions.

Overall, fluctuation in the methylation state of promoters during the lytic infection is observed mainly at the Immediate-Early (3 hpi) and Early (8 hpi) state of infection while latently infected cells exhibit almost an identical methylation profile to the cell's steady state methylation. This result is consistent with the fact that during latency, the viral genome is occupied by histones and is mainly inactive[83] thus requiring a more extensive approach to identify crucial changes it may inflict in the methylation pattern of the host. Moreover, this result highlights the credibility of the *in vitro* system used for latency in this study.

Following up on the data, we went on to further analyze HDAC1, HDAC2, HDAC3 and LSD1 in the context of HSV-1 lytic infection. We analyzed the expression of these enzymes as well as the impact of their silencing on HSV-1 production of progeny virions.

HDAC1 exhibited a decreasing expression in the course of infection with a significant drop arising at 8hpi and continuing to 15hpi. However, knockdown of HDAC1 did not have a significant impact on HSV-1 propagation *in vitro*.

HDAC2 expression was also significantly lower, particularly at 3hpi and 15hpi. The decrease of its expression at 3hpi is consistent with the increased methylation detected on its promoter at 3hpi. Moreover, silencing of HDAC2 led to a significant elevation in the production of HSV-1 virions.

Regarding HDAC3, its expression was markedly decreased at all phases of lytic infection, although it was mainly unmethylated. Interestingly, HDAC3 expression at 3hpi is significantly increased compared to 8hpi and 15hpi which correlates with an elevation of its methylation status at 3hpi. Silencing of HDAC3 led to a decreased viral titer.

The same phenomenon was observed for LSD1. Specifically, its expression decreased during infection compared to the control uninfected cells. However, compared to 3 and 15hpi, LSD1 expression was significantly elevated at 8hpi which correlated with an increase in the methylation of its promoter. Silencing of LSD1 caused a marked decrease on HSV-1 progeny virion production. This result was in agreement with data from Liang, Y. *et al* that also showed that depletion of LSD1 or inhibition of its activity results in a block to viral gene expression. This group also showed that depletion of LSD-1 led to the accumulation of repressive chromatin on HSV-1[200].

Concerning DNA methylation, it is usually associated with silencing of genes. In accordance, intermediate methylation has been associated with an intermediate

levels of transcription and has been identified not only on promoters but also on enhancers, exons and DNase sensitive sites[201]. Interestingly, it has also been observed in various situations, that methylation of a promoter region can lead to upregulation of expression[202–204]. In the context of this study we cannot reach a conclusion yet as to which mechanism characterizes each gene. However, it is intriguing that all histone deacetylases studied are mainly unmethylated and only acquire an intermediate methylation.

Finally, high-throughput methylation analysis also highlighted HDAC1 as a significantly hypomethylated promoter at 3hpi and at 8hpi. Moreover, the gene body of HDAC4, defined as the transcribed region including introns and exons, was also found to be significantly hypomethylated for the course of infection in lytic and latent cells compared to the steady state of HDAC4 methylation on Vero cells. There were no data for HDAC2, HDAC3 and LSD1. However, this may require additional analysis.

A common denominator of HDAC1, HDAC2, HDAC3, HDAC4 and HDAC10 is the transcriptional repressor complex N-CoR/SMRT. SMRT can recruit both class I and class II deacetylases[205]. N-CoR has been found to form a variety of complexes with histone deacetylases and it can associate with HDAC1, HDAC2 and HDAC3[206]. In addition SMRT forms a complex with HDAC2 and HDAC10[199]. N-CoR and SMRT also forms a complex that contains HDAC4[207]. Moreover N-CoR mediates HDAC4 and HDAC3 interaction which allows for activation of HDAC4 by HDAC3[208].

However, HDAC1 and HDAC2 form another complex, namely the HDAC1/2 CoREST/LSD1/REST repressor complex which has been shown to be manipulated by HSV-1 in order to suppress and activate genes[209]. LSD1 can act both as an activator through H3K9 demethylation or as a repressor through H3K4 demethylation. At the initial steps of infection the VP16-HCF-1-Oct1 transactivator complex recruits LSD1 to the IE promoters in order to relieve the silencing marks of the viral genome. Subsequently, the viral protein ICP0 dissociates HDACs from the complex to keep the IE promoters active[81]. The fact that its primary function is to repress neuronal genes in non-neuronal cells constitutes the HDAC1/2 CoREST/LSD1/REST repressor complex particularly important in the context of HSV-1 infection[209].

DNMT3A has been recently shown to interact with viral tegument and capsid proteins while silencing of DNMT3A led to reduction of the viral titer. This is in agreement with our results showing that while DNMT3A is hypermethylated in uninfected cells it becomes[210] hypomethylated at 3 and 8 hpi.

Collectively, these data suggest that the progress of HSV-1 infection is regulated to some extent through manipulation of methylation on the genes of histone deacetylases and possibly through an as yet unidentified mechanism of DNA methylation that is the result of virus-host interaction.

5.Bibliography

1. King, A., Lefkowitz, E., Adams, M. J. & Carstens, E. B. *Virus Taxonomy*. *1st Edition* (2011). doi:ISBN 9780123846846

2. Preston, C. M. & Efstathiou, S. Molecular basis of HSV latency and reactivation. (2007). at <http://www.ncbi.nlm.nih.gov/books/NBK47421/>

3. Looker, K. J. & Garnett, G. P. A systematic review of the epidemiology and interaction of herpes simplex virus types 1 and 2. *Sex. Transm. Infect.* **81,** 103–7 (2005).

4. Bradley, H., Markowitz, L. E., Gibson, T. & McQuillan, G. M. Seroprevalence of herpes simplex virus types 1 and 2-United States, 1999-2010. *J. Infect. Dis.* **209,** 325–333 (2014).

5. Timbury, M. C. & Edmond, E. Herpesviruses. *J. Clin. Pathol.* **32,** 859–881 (1979).

6. Wozniak, M. A., Mee, A. P. & Itzhaki, R. F. Herpes simplex virus type 1 DNA is located within Alzheimer ' s disease amyloid plaques. *J Pathol.* **1,** 131–138 (2009).

7. Itzhaki, R. F. & Wozniak, M. A. Herpes Simplex Virus Type 1 in Alzheimer ' s Disease : The Enemy Within. *J. Alzheimers. Dis.* **13,** 393–405 (2008).

8. Carter, C. J. Interactions between the products of the Herpes simplex genome and Alzheimer's disease susceptibility genes: relevance to pathological-signalling cascades. *Neurochem. Int.* **52,** 920–34 (2008).

9. Knipe, D. M. & Howley, P. M. *Fields Virology*. (Lippincott Williams & Wilkins, 2013).

10. Arduino, P. G. & Porter, S. R. Herpes Simplex Virus Type 1 infection: overview on relevant clinico-pathological features. *J. Oral Pathol. Med.* **37,** 107–21 (2008).

11. Smith, J. S., Robinson, N. J., Thomas, C. A. & Elisa, T. Age-Specific Prevalence of Infection with Herpes Simplex Virus Types 2 and 1 : A Global Review.

12. Davison, A. J. Overview of classification - Human Herpesviruses - NCBI Bookshelf. at <http://www.ncbi.nlm.nih.gov/books/NBK47406/?report=reader>

13. Davison, A. J. *et al.* The order Herpesvirales. *Arch. Virol.* **154,** 171–7 (2009).

14. Knipe, D. M. & Howley, P. M. Fields Virology. (2001).

15. Hulo, C. *et al.* ViralZone: A knowledge resource to understand virus diversity. *Nucleic Acids Res.* **39,** 576–582 (2011).

16. Davison, A. J. Evolution of the herpesviruses. *Vet. Microbiol.* **86,** 69–88 (2002).

17. McGeoch, D. J., Rixon, F. J. & Davison, A. J. Topics in herpesvirus genomics and evolution. *Virus Res.* **117,** 90–104 (2006).

18. Furlong, D., Swift, H. & Roizman, B. Arrangement of herpesvirus deoxyribonucleic acid in the core. *J. Virol.* **10,** 1071–1074 (1972).

19. Zhou, Z. H., Chen, D. H., Jakana, J., Rixon, F. J. & Chiu, W. Visualization of tegument-capsid interactions and DNA in intact herpes simplex virus type 1 virions. *J. Virol.* **73,** 3210–3218 (1999).

20. Booy, F. P. *et al.* Liquid-crystalline, phage-like packing of encapsidated DNA in herpes simplex virus. *Cell* **64,** 1007–1015 (1991).

21. Gibson, W. & Roizman, B. Compartmentalization of spermine and spermidine in the herpes simplex virion. *Proc. Natl. Acad. Sci. U. S. A.* **68,** 2818–2821 (1971).

22. Bauer, D. W., Huffman, J. B., Homa, F. L. & Evilevitch, A. Herpes virus genome, the pressure is on. *J. Am. Chem. Soc.* **135,** 11216–11221 (2013).

23. Grünewald, K. *et al.* Three-dimensional structure of herpes simplex virus from cryo-electron tomography. *Science* **302,** 1396–8 (2003).

24. Newcomb, W. W. *et al.* The UL6 Gene Product Forms the Portal for Entry of DNA into the Herpes Simplex Virus Capsid. *J. Virol.* **75,** 10923 (2001).

25. Brown, J. C. & Newcomb, W. W. Herpesvirus capsid assembly: Insights from structural analysis. *Curr. Opin. Virol.* **1,** 142–149 (2011).

26. Rochat Ryan H. , Corey W. Hecksel, W. C. Cryo-EM techniques to resolve the structure of HSV-1 capsid-associated components. *Methods Mol. Biol.* **1144,** 265–281 (2014).

27. Newcomb, W. W. *et al.* Assembly of the herpes simplex virus procapsid from purified components and identification of small complexes containing the major capsid and scaffolding proteins. *J. Virol.* **73,** 4239–4250 (1999).

28. Newcomb, W. W., Homa, F. L. & Brown, J. C. Involvement of the Portal at an Early Step in Herpes Simplex Virus Capsid Assembly. *J Virol* **79,** 10540–10546 (2005).

29. Spencer, J. V *et al.* Structure of the herpes simplex virus capsid: peptide A862-H880 of the major capsid protein is displayed on the rim of the capsomer protrusions. *Virology* **228,** 229–235 (1997).

30. Radtke, K. *et al.* Plus- and minus-end directed microtubule motors bind simultaneously to herpes simplex virus capsids using different inner tegument structures. *PLoS Pathog.* **6,** 1–20 (2010).

31. Newcomb, W. W. & Brown, J. C. Structure and capsid association of the herpesvirus large tegument protein UL36. *J. Virol.* **84,** 9408–9414 (2010).

32. Meckes, D. G. & Wills, J. W. Structural rearrangement within an enveloped virus upon binding to the host cell. *J. Virol.* **82,** 10429–35 (2008).

33. Wolfstein, A. *et al.* The inner tegument promotes herpes simplex virus capsid motility along microtubules in vitro. *Traffic* **7,** 227–37 (2006).

34. Kelly, B. J., Fraefel, C., Cunningham, A. L. & Diefenbach, R. J. Functional roles of the tegument proteins of herpes simplex virus type 1. *Virus Res.* **145,** 173–186 (2009).

35. Roizman, B. The structure and isomerization of herpes simplex virus genomes. *Cell* **16,** 481–494 (1979).

36. Campadelli-Fiume, G., Menotti, L., Avitabile, E. & Gianni, T. Viral and cellular contributions to herpes simplex virus entry into the cell. *Curr. Opin. Virol.* **2,** 28–36 (2012).

37. Akhtar, J. & Shukla, D. Viral entry mechanisms: cellular and viral mediators of herpes simplex virus entry. *FEBS J.* **276,** 7228–36 (2009).

38. Cocchi, F., Menotti, L., Mirandola, P. & Lopez, M. The Ectodomain of a Novel Member of the Immunoglobulin Subfamily Related to the Poliovirus Receptor Has the Attributes of a Bona Fide Receptor for Herpes Simplex Virus Types 1 and 2 in Human Cells. **72,** 9992–10002 (1998).

39. Geraghty, R. J., Krurnmenacher, C., Cohen, G. H., Eisenberg, R. J. & Spear, P. G. Entry of alphaherpesviruses mediated by poliovirus receptor-related protein 1 and poliovirus receptor. *Science (80-.).* **280,** 1618–1620 (1998).

40. Montgomery, R. I., Warner, M. S., Lum, B. J. & Spear, P. G. Herpes Simplex Virus-1 Entry into Cells Mediated by a Novel Member of the TNF/NGF Receptor Family. *Cell* **87,** 427–436 (1996).

41. Shukla, D. *et al.* A novel role for 3-O-sulfated heparan sulfate in herpes simplex virus 1 entry. *Cell* **99,** 13–22 (1999).

42. Tiwari, V. *et al.* Role for 3-O-sulfated heparan sulfate as the receptor for herpes simplex virus type 1 entry into primary human corneal fibroblasts. *J. Virol.* **80,** 8970–8980 (2006).

43. Gianni, T., Gatta, V. & Campadelli-Fiume, G. {alpha}V{beta}3-integrin routes herpes simplex virus to an entry pathway dependent on cholesterol-rich lipid rafts and dynamin2. *Proc. Natl. Acad. Sci. U. S. A.* **107,** 22260–22265 (2010).

44. Satoh, T. *et al.* PILRalpha is a herpes simplex virus-1 entry coreceptor that associates with glycoprotein B. *Cell* **132,** 935–44 (2008).

45. Warner, M. S. *et al.* A cell surface protein with herpesvirus entry activity (HveB) confers susceptibility to infection by mutants of herpes simplex virus type 1, herpes simplex virus type 2, and pseudorabies virus. *Virology* **246,** 179–189 (1998).

46. Kopp, S. J. *et al.* Infection of neurons and encephalitis after intracranial inoculation of herpes simplex virus requires the entry receptor nectin-1. *Proc. Natl. Acad. Sci. U. S. A.* **106,** 17916–17920 (2009).

47. Simpson, S. a *et al.* Nectin-1/HveC Mediates herpes simplex virus type 1 entry into primary human sensory neurons and fibroblasts. *J. Neurovirol.* **11,** 208–218 (2005).

48. Richart, S. M. *et al.* Entry of herpes simplex virus type 1 into primary sensory neurons in vitro is mediated by nectin-1/HveC. *J. Virol.* **77,** 3307 (2003).

49. Lee, G. E., Murray, J. W., Wolkoff, A. W. & Wilson, D. W. Reconstitution of herpes simplex virus microtubule-dependent trafficking in vitro. *J. Virol.* **80,** 4264–75 (2006).

50. Mues, M. B., Cheshenko, N., Wilson, D. W., Gunther-Cummins, L. & Herold, B. C. *Dynasore disrupts trafficking of HSV proteins*. *Journal of Virology* **2974,** (2015).

51. Abaitua, F., Hollinshead, M., Bolstad, M., Crump, C. M. & O'Hare, P. A Nuclear Localization Signal in Herpesvirus Protein VP1-2 Is Essential for Infection via Capsid Routing to the Nuclear Pore. *J. Virol.* **86,** 8998–9014 (2012).

52. Delboy, M. G., Roller, D. G. & Nicola, A. V. Cellular proteasome activity facilitates herpes simplex virus entry at a postpenetration step. *J. Virol.* **82,** 3381–90 (2008).

53. Ojala, P. M., Sodeik, B., Ebersold, M. W., Kutay, U. & Helenius, a. Herpes Simplex Virus Type 1 Entry into Host Cells: Reconstitution of Capsid Binding and Uncoating at the Nuclear Pore Complex In Vitro. *Mol. Cell. Biol.* **20,** 4922–4931 (2000).

54. Anderson, F. *et al.* Targeting of Viral Capsids to Nuclear Pores in a Cell-Free Reconstitution System. *Traffic* **15,** 1266–1281 (2014).

55. Meyring-Wösten, A., Hafezi, W., Kühn, J., Liashkovich, I. & Shahin, V. Nano-visualization of viral DNA breaching the nucleocytoplasmic barrier. *J. Control. Release* **173,** 96–101 (2014).

56. Jovasevic, V., Liang, L. & Roizman, B. Proteolytic cleavage of VP1-2 is required for release of herpes simplex virus 1 DNA into the nucleus. *J. Virol.* **82,** 3311–9 (2008).

57. Silva, L., Oh, H. S. & Chang, L. Roles of the Nuclear Lamina in Stable Nuclear Association and Assembly of a Herpesviral Transactivator Complex on Viral. (2012). doi:10.1128/mBio.00300-11.Editor

58. Kutluay, S. B. & Triezenberg, S. J. Regulation of histone deposition on the herpes simplex virus type 1 genome during lytic infection. *J. Virol.* **83,** 5835–5845 (2009).

59. Herrera, F. J. & Triezenberg, S. J. VP16-dependent association of chromatin-modifying coactivators and underrepresentation of histones at immediate-early gene promoters during herpes simplex virus infection. *J. Virol.* **78,** 9689–9696 (2004).

60. Strang, B. L. & Stow, N. D. Circularization of the Herpes Simplex Virus Type 1 Genome upon Lytic Infection. *Society* **79,** 12487–12494 (2005).

61. Sourvinos, G. & Everett, R. D. Visualization of parental HSV-1 genomes and replication compartments in association with ND10 in live infected cells. **21,** 4989–4997 (2002).

62. Everett, R. D. *et al.* Formation of Nuclear Foci of the Herpes Simplex Virus Type 1 Regulatory Protein ICP4 at Early Times of Infection : Localization , Dynamics , Recruitment of ICP27 , and Evidence for the De Novo Induction of ND10-Like Complexes. **78,** 1903–1917 (2004).

63. Everett, R. D. & Murray, J. ND10 Components Relocate to Sites Associated with Herpes Simplex Virus Type 1 Nucleoprotein Complexes during Virus Infection. **79,** 5078–5089 (2005).

64. Park, J., Lammers, F., Herr, W. & Song, J.-J. HCF-1 self-association via an interdigitated Fn3 structure facilitates transcriptional regulatory complex formation. *Proc. Natl. Acad. Sci.* **109,** 17430–17435 (2012).

65. Lehman, I. R. & Boehmer, P. E. Replication of Herpes Simplex Virus DNA. *J. Biol. Chem.* **274,** 28059–28062 (1999).

66. Newcomb, W. W., Cockrell, S. K., Homa, F. L. & Brown, J. C. Polarized DNA Ejection from the Herpesvirus Capsid. *J. Mol. Biol.* **392,** 885–894 (2009).

67. McVoy, M. a, Nixon, D. E., Hur, J. K. & Adler, S. P. The ends on herpesvirus DNA replicative concatemers contain pac2 cis cleavage/packaging elements and their formation is controlled by terminal cis sequences. *J. Virol.* **74,** 1587–1592 (2000).

68. Hofemeister, H. & O'Hare, P. Nuclear pore composition and gating in herpes simplex virus-infected cells. *J. Virol.* **82,** 8392–8399 (2008).

69. Wild, P. *et al.* Exploring the nuclear envelope of herpes simplex virus 1-infected cells by high-resolution microscopy. *J. Virol.* **83,** 408–419 (2009).

70. Reynolds, A. E. *et al.* U(L)31 and U(L)34 proteins of herpes simplex virus type 1 form a complex that accumulates at the nuclear rim and is required for envelopment of nucleocapsids. *J Virol.* **75,** 8803–8817 (2001).

71. Loret, S., Guay, G. & Lippé, R. Comprehensive characterization of extracellular herpes simplex virus type 1 virions. *J. Virol.* **82,** 8605–8618 (2008).

72. Harley, C. a, Dasgupta, a & Wilson, D. W. Characterization of herpes simplex virus-containing organelles by subcellular fractionation: role for organelle acidification in assembly of infectious particles. *J. Virol.* **75,** 1236–1251 (2001).

73. Van Genderen, I. L., Brandimarti, R., Torrisi, M. R., Campadelli, G. & van Meer, G. The phospholipid composition of extracellular herpes simplex virions differs from that of host cell nuclei. *Virology* **200,** 831–836 (1994).

74. Whiteley, a, Bruun, B., Minson, T. & Browne, H. Effects of targeting herpes simplex virus type 1 gD to the endoplasmic reticulum and trans-Golgi network. *J. Virol.* **73,** 9515–9520 (1999).

75. Skepper, J. N., Whiteley, a, Browne, H. & Minson, a. Herpes simplex virus nucleocapsids mature to progeny virions by an envelopment --> deenvelopment --> reenvelopment pathway. *J. Virol.* **75,** 5697–5702 (2001).

76. Campadelli-Fiume, G. *The egress of alphaherpesviruses from the cell. Human Herpesviruses: Biology, Therapy, and Immunoprophylaxis* (Cambridge University Press, 2007). at <http://www.ncbi.nlm.nih.gov/books/NBK47427/>

77. Deshmane, S. L. & Fraser, N. W. During latency, herpes simplex virus type 1 DNA is associated with nucleosomes in a chromatin structure. *J. Virol.* **63,** 943–947 (1989).

78. Amelio, A. L., McAnany, P. K. & Bloom, D. C. A chromatin insulator-like element in the herpes simplex virus type 1 latency-associated transcript region binds CCCTC-binding factor and displays enhancer-blocking and silencing activities. *J. Virol.* **80,** 2358–2368 (2006).

79. Cliffe, A. R., Garber, D. a & Knipe, D. M. Transcription of the herpes simplex virus latency-associated transcript promotes the formation of facultative heterochromatin on lytic promoters. *J. Virol.* **83,** 8182–90 (2009).

80. Frazier, D. P., Cox, D., Godshalk, E. M. & Schaffer, P. a. Identification of cis-acting sequences in the promoter of the herpes simplex virus type 1 latency-associated transcripts required for activation by nerve growth factor and sodium butyrate in PC12 cells. *J. Virol.* **70,** 7433–7444 (1996).

81. Gu, H., Liang, Y., Mandel, G. & Roizman, B. Components of the REST CoREST histone deacetylase repressor complex are disrupted , modified , and translocated in HSV-1-infected cells. 1–6 (2005).

82. Gu, H. & Roizman, B. Herpes simplex virus-infected cell protein 0 blocks the silencing of viral DNA by dissociating histone deacetylases from the CoREST-REST complex. *Proc. Natl. Acad. Sci. U. S. A.* **104,** 17134–9 (2007).

83. Knipe, D. M. & Cliffe, A. Chromatin control of herpes simplex virus lytic and latent infection. *Nat. Rev. Microbiol.* **6,** 211–21 (2008).

84. Wertheim, J. O., Smith, M. D., Smith, D. M., Scheffler, K. & Kosakovsky Pond, S. L. Evolutionary origins of human herpes simplex viruses 1 and 2. *Mol. Biol. Evol.* **31,** 2356–64 (2014).

85. Zhou, G. & Roizman, B. Cation-independent mannose 6-phosphate receptor blocks apoptosis induced by herpes simplex virus 1 mutants lacking glycoprotein D and is likely the target of antiapoptotic activity of the glycoprotein. *J. Virol.* **76,** 6197–6204 (2002).

86. Jerome, K. R. *et al.* Herpes simplex virus inhibits apoptosis through the action of two genes, Us5 and Us3. *J. Virol.* **73,** 8950–8957 (1999).

87. Zhou, G., Galvan, V., Campadelli-Fiume, G. & Roizman, B. Glycoprotein D or J delivered in trans blocks apoptosis in SK-N-SH cells induced by a herpes simplex virus 1 mutant lacking intact genes expressing both glycoproteins. *J. Virol.* **74,** 11782–11791 (2000).

88. Aubert, M. *et al.* The antiapoptotic herpes simplex virus glycoprotein J localizes to multiple cellular organelles and induces reactive oxygen species formation. *J. Virol.* **82,** 617–629 (2008).

89. Mcnearney, T. A., Odell, C., Holers, V. M., Spear, P. G. & Atkinson, J. P. Herpes simplex virus glycoproteins gC-1 and gC-2 bind to the third component of complement and provide protection against complement-mediated neutralization of viral infectivity. **166,** (1987).

90. Harris SL, Frank I, Yee A, Cohen GH, Eisenberg RJ, F. H. Glycoprotein C of Herpes Simplex Virus Type 1 Prevents Complement-Mediated Cell Lysis and Virus Neutralization. *J Infect Dis* **162,** 331–337 (1990).

91. Friedman, H. M. *et al.* Immune evasion properties of herpes simplex virus type 1 glycoprotein gC. *J. Virol.* **70,** 4253–4260 (1996).

92. Page, H. G. & Read, G. S. The virion host shutoff endonuclease (UL41) of herpes simplex virus interacts with the cellular cap-binding complex eIF4F. *J. Virol.* **84,** 6886–6890 (2010).

93. Taddeo, B. & Roizman, B. The virion host shutoff protein (UL41) of herpes simplex virus 1 is an endoribonuclease with a substrate specificity similar to that of RNase A. *J. Virol.* **80,** 9341–9345 (2006).

94. Barzilai, A., Barzilai, A., Frenkel, N. & Frenkel, N. The herpes simplex virus type 1 vhs-UL41 gene secures viral replication by temporarily evading apoptotic cellular response to infection: Vhs-UL41 activity might require interactions with elements of cellular mRNA degradation machinery. *Microbiology* **80,** 505–513 (2006).

95. Cotter, C. R. *et al.* The virion host shut-off (vhs) protein blocks a TLR-independent pathway of herpes simplex virus type 1 recognition in human and mouse dendritic cells. *PLoS One* **5,** e8684 (2010).

96. Samady, L. *et al.* Deletion of the virion host shutoff protein (vhs) from herpes simplex virus (HSV) relieves the viral block to dendritic cell activation: potential of vhs- HSV vectors for dendritic cell-mediated immunotherapy. *J. Virol.* **77,** 3768–3776 (2003).

97. Shen, G. *et al.* Herpes Simplex Virus 1 Counteracts Viperin via Its Virion Host Shutoff Protein UL41. *J. Virol.* **88,** JVI.01380–14– (2014).

98. Yao, F. & Courtney, R. J. Association of ICP0 but not ICP27 with purified virions of herpes simplex virus type 1. *J. Virol.* **66,** 2709–2716 (1992).

99. Orzalli, M. H., DeLuca, N. a & Knipe, D. M. Nuclear IFI16 induction of IRF-3 signaling during herpesviral infection and degradation of IFI16 by the viral ICP0 protein. *Proc. Natl. Acad. Sci. U. S. A.* **109,** E3008–17 (2012).

100. Paladino, P., Collins, S. E. & Mossman, K. L. Cellular localization of the herpes simplex virus ICP0 protein dictates its ability to block IRF3-mediated innate immune responses. *PLoS One* **5,** e10428 (2010).

101. Daubeuf, S. *et al.* HSV ICP0 recruits USP7 to modulate TLR-mediated innate response. *Blood* **113,** 3264–75 (2009).

102. Lilley, C. E. *et al.* A viral E3 ligase targets RNF8 and RNF168 to control histone ubiquitination and DNA damage responses. *EMBO J.* **29,** 943–955 (2010).

103. Lilley, C. E., Chaurushiya, M. S., Boutell, C., Everett, R. D. & Weitzman, M. D. The intrinsic antiviral defense to incoming HSV-1 genomes includes specific DNA repair proteins and is counteracted by the viral protein ICP0. *PLoS Pathog.* **7,** (2011).

104. Conwell, S. E., White, A. E., Harper, J. W. & Knipe, D. M. Identification of TRIM27 as a Novel Degradation Target of Herpes Simplex Virus 1 ICP0. *J. Virol.* **89,** 220–229 (2015).

105. Sandri-Goldin, R. M. ICP27 mediates HSV RNA export by shuttling through a leucine-rich nuclear export signal and binding vital intronless RNAs through an RGG motif. *Genes Dev.* **12,** 868–879 (1998).

106. Bryant, H. E., Wadd, S. E., Lamond, a I., Silverstein, S. J. & Clements, J. B. Herpes simplex virus IE63 (ICP27) protein interacts with spliceosome-associated protein 145 and inhibits splicing prior to the first catalytic step. *J. Virol.* **75,** 4376–4385 (2001).

107. Chen, I. B., Sciabica, K. S. & Sandri-goldin, R. M. ICP27 Interacts with the RNA Export Factor Aly / REF To Direct Herpes Simplex Virus Type 1 Intronless mRNAs to the TAP Export Pathway. **76,** 12877–12889 (2002).

108. Nojima, T. *et al.* Herpesvirus protein ICP27 switches PML isoform by altering mRNA splicing. *Nucleic Acids Res.* **37,** 6515–6527 (2009).

109. Song, B., Yeh, K. C., Liu, J. & Knipe, D. M. Herpes simplex virus gene products required for viral inhibition of expression of G1-phase functions. *Virology* **290,** 320–8 (2001).

110. Johnson, K. E., Song, B. & Knipe, D. M. Role for herpes simplex virus 1 ICP27 in the inhibition of type I interferon signaling. *Virology* **374,** 487–94 (2008).

111. Kim, J. C. *et al.* HSV-1 ICP27 suppresses NF-kappaB activity by stabilizing IkappaBalpha. *FEBS Lett.* **582,** 2371–6 (2008).

112. Zaborowska, J. *et al.* Herpes Simplex Virus 1 (HSV-1) ICP22 Protein Directly Interacts with Cyclin-Dependent Kinase (CDK)9 to Inhibit RNA Polymerase II Transcription Elongation. *PLoS One* **9,** e107654 (2014).

113. Cells, S. V., Orlando, J. S., Astor, T. L., Rundle, S. a & Schaffer, P. a. The products of the Herpes Simplex Virus Type 1 immediate-early US1/US1.5 genes downregulate levels of S-phase-specific cyclins and facilitate virus replication in S-phase Vero cells. **80,** 4005–4016 (2006).

114. Ahn, K. *et al.* Molecular mechanism and species specificity of TAP inhibition by herpes simplex virus ICP47. *EMBO J.* **15,** 3247–3255 (1996).

115. Duguay, B. a & Smiley, J. R. Mitochondrial nucleases ENDOG and EXOG participate in mitochondrial DNA depletion initiated by herpes simplex virus 1 UL12.5. *J. Virol.* **87,** 11787–97 (2013).

116. McKnight, N. C. *et al.* Beclin 1 Is Required for Neuron Viability and Regulates Endosome Pathways via the UVRAG-VPS34 Complex. *PLoS Genet.* **10,** e1004626 (2014).

117. Orvedahl, A. *et al.* HSV-1 ICP34.5 confers neurovirulence by targeting the Beclin 1 autophagy protein. *Cell Host Microbe* **1,** 23–35 (2007).

118. Tang, S. *et al.* An acutely and latently expressed herpes simplex virus 2 viral microRNA inhibits expression of ICP34.5, a viral neurovirulence factor. *Proc. Natl. Acad. Sci. U. S. A.* **105,** 10931–6 (2008).

119. Tang, S., Patel, A. & Krause, P. R. Novel less-abundant viral microRNAs encoded by herpes simplex virus 2 latency-associated transcript and their roles in regulating ICP34.5 and ICP0 mRNAs. *J. Virol.* **83,** 1433–42 (2009).

120. Verpooten, D., Ma, Y., Hou, S., Yan, Z. & He, B. Control of TANK-binding kinase 1-mediated signaling by the gamma(1)34.5 protein of herpes simplex virus 1. *J. Biol. Chem.* **284,** 1097–105 (2009).

121. He, B., Gross, M. & Roizman, B. The gamma134.5 protein of herpes simplex virus 1 has the structural and functional attributes of a protein phosphatase 1 regulatory subunit and is present in a high molecular weight complex with the enzyme in infected cells. *J. Biol. Chem.* **273,** 20737–20743 (1998).

122. Li, Y. *et al.* ICP34.5 protein of herpes simplex virus facilitates the initiation of protein translation by bridging eukaryotic initiation factor 2α (eIF2α) and protein phosphatase 1. *J. Biol. Chem.* **286,** 24785–24792 (2011).

123. Nascimento, R., Dias, J. D. & Parkhouse, R. M. E. The conserved UL24 family of human alpha, beta and gamma herpesviruses induces cell cycle arrest and inactivation of the cyclinB/cdc2 complex. *Arch. Virol.* **154,** 1143–1149 (2009).

124. Rao, P. *et al.* Herpes simplex virus 1 glycoprotein B and US3 collaborate to inhibit CD1d antigen presentation and NKT cell function. *J. Virol.* **85,** 8093–8104 (2011).

125. Leopardi, R., Van Sant, C. & Roizman, B. The herpes simplex virus 1 protein kinase US3 is required for protection from apoptosis induced by the virus. *Proc. Natl. Acad. Sci. U. S. A.* **94,** 7891–7896 (1997).

126. Mori I, Goshima F, Koshizuka T, Koide N, Sugiyama T, Yoshida T, Yokochi T, Kimura Y, N. Y. The US3 protein kinase of herpes simplex virus attenuates the activation of the c-Jun N-terminal protein kinase signal transduction pathway in infected piriform cortex neurons of C57BL/6 mice. *Neurosci. Lett.* **351,** 201–205 (2003).

127. Ndjamen, B., Farley, A. H., Lee, T., Fraser, S. E. & Bjorkman, P. J. The Herpes Virus Fc Receptor gE-gI Mediates Antibody Bipolar Bridging to Clear Viral Antigens from the Cell Surface. *PLoS Pathog.* **10,** (2014).

128. Ng, T. I., Ogle, W. O. & Roizman, B. UL13 protein kinase of herpes simplex virus 1 complexes with glycoprotein E and mediates the phosphorylation of the viral Fc receptor: glycoproteins E and I. *Virology* **241,** 37–48 (1998).

129. Javouhey, E., Gibert, B., Arrigo, A.-P., Diaz, J. J. & Diaz-Latoud, C. Protection against heat and staurosporine mediated apoptosis by the HSV-1 US11 protein. *Virology* **376,** 31–41 (2008).

130. Lussignol, M. *et al.* The herpes simplex virus 1 Us11 protein inhibits autophagy through its interaction with the protein kinase PKR. *J. Virol.* **87,** 859–71 (2013).

131. Wilson, A. G. Epigenetic Regulation of Gene Expression in the Inflammatory Response and Relevance to Common Diseases. *J. Periodontol.* **79,** 1514–1519 (2008).

132. Bird, A. Introduction Perceptions of epigenetics. *Nature* **447,** 396–398 (2007).

133. Hoffmann, A., Zimmermann, C. a. & Spengler, D. Molecular epigenetic switches in neurodevelopment in health and disease. *Front. Behav. Neurosci.* **9,** 1–15 (2015).

134. Hutchinson, F. Summary : Epigenetics — from Phenomenon to Field. *Cold Spring Harb Symp Quant Biol* **69,** 507–519 (2004).

135. Knipe, D. M. Nuclear sensing of viral DNA, epigenetic regulation of herpes simplex virus infection, and innate immunity. *Virology* **479-480,** 153–159 (2015).

136. Everett, R. D. ICP0, a regulator of herpes simplex virus during lytic and latent infection. *BioEssays* **22,** 761–770 (2000).

137. Cliffe, A. R. & Knipe, D. M. Herpes simplex virus ICP0 promotes both histone removal and acetylation on viral DNA during lytic infection. *J. Virol.* **82,** 12030–8 (2008).

138. Coleman, H. M. *et al.* Histone modifications associated with herpes simplex virus type 1 genomes during quiescence and following ICP0-mediated de-repression. *J. Gen. Virol.* **89,** 68–77 (2008).

139. Orvedahl, A. & Levine, B. Autophagy and viral neurovirulence. **10,** 1747–1756 (2008).

140. Schmid, D. & Münz, C. Innate and adaptive immunity through autophagy. *Immunity* **27,** 11–21 (2007).

141. Levine, B. & Deretic, V. Unveiling the roles of autophagy in innate and adaptive immunity. *Nat. Rev. Immunol.* **7,** 767–77 (2007).

142. Sumpter R Jr, L. B. Autophagy and Innate Immunity: Triggering, Targeting and Tuning. *Semin Cell Dev Biol.* **21,** 699–711 (2010).

143. Lamb, C. a, Yoshimori, T. & Tooze, S. a. The autophagosome: origins unknown, biogenesis complex. *Nat. Rev. Mol. Cell Biol.* **14,** 759–74 (2013).

144. Consortium, T. U. UniProt: a hub for protein information. *Nucleic Acids Res.* **43,** D204–D212 (2014).

145. Clark, E. A. & Ledbettert, J. A. Activation of human B cells mediated through two distinct cell surface differentiation antigens , Bp35 and Bp5O. **83,** 4494–4498 (1986).

146. Ferrari, S. *et al.* Mutations of CD40 gene cause an autosomal recessive form of immunodeficiency with hyper IgM. *Proc. Natl. Acad. Sci. U. S. A.* **98,** 12614–9 (2001).

147. Kooten, C. Van, Banchereau, J. & Gene, C. D. L. CD40-CD40 ligand. **67,** (2000).

148. Libby, P. The CD40 / CD154 receptor / ligand dyad. **58,** 4–43 (2001).

149. Furman, M. I. *et al.* Release of soluble CD40L from platelets is regulated by glycoprotein IIb/IIIa and actin polymerization. *J. Am. Coll. Cardiol.* **43,** 2319–25 (2004).

150. Van Grol, J., Muniz-Feliciano, L., Portillo, J.-A. C., Bonilha, V. L. & Subauste, C. S. CD40 induces anti-Toxoplasma gondii activity in nonhematopoietic cells dependent on autophagy proteins. *Infect. Immun.* **81,** 2002–11 (2013).

151. Lee, W. *et al.* Molecular analysis of a large cohort of patients with the hyper immunoglobulin M (IgM) syndrome. **105,** 1881–1890 (2005).

152. Fanslow WC, Srinivasan S, Paxton R, Gibson MG, Spriggs MK, A. R. Structural characteristics of CD40 ligand that determine biological function. *Semin Immunol.* (1994).

153. Elgueta, R. *et al.* Molecular mechanism and function of CD40/CD40L engagement in the immune system. *Immunol. Rev.* **229,** 152–72 (2009).

154. Pullen, S. S. *et al.* High-affinity interactions of tumor necrosis factor receptor-associated factors (TRAFs) and CD40 require TRAF trimerization and CD40 multimerization. *Biochemistry* **38,** 10168–77 (1999).

155. Ruby J, Bluethmann H, Aguet M, R. I. CD40 ligand has potent antiviral activity. *Nat Med.* (1995).

156. Beland, B. J. L. *et al.* Recombinant CD40L Treatment Protects Allogeneic Murine Bone Marrow Transplant Recipients From Death Caused by Herpes Simplex Virus-1 Infection. **92,** 4472–4478 (1998).

157. Edelmann, K. H. & Wilson, C. B. Role of CD28/CD80-86 and CD40/CD154 costimulatory interactions in host defense to primary herpes simplex virus infection. *J. Virol.* **75,** 612–21 (2001).

158. Winkelstein JA, Marino MC, Ochs H, Fuleihan R, Scholl PR, Geha R, Stiehm ER, C. M. The X-linked hyper-IgM syndrome: clinical and immunologic features of 79 patients. *Med.* **82,** 373–84 (2003).

159. García-Pérez, M. a *et al.* Mutations of CD40 ligand in two patients with hyper-IgM syndrome. *Immunobiology* **207,** 285–294 (2003).

160. Kawabe, T., Hasegawa, Y., Hashimoto, N. & Nishiyama, Y. Critical involvement of CD40 in protection against herpes simplex virus infection in a murine model of genital herpes Brief Report. 187–194 (2002).

161. Pullen, S. S., Dang, T. T. A., Crute, J. J. & Kehry, M. R. CD40 Signaling through Tumor Necrosis Factor Receptor-associated Factors (TRAFs). **274,** 14246–14254 (1999).

162. Bradner, J. E. *et al.* Chemical genetic strategy identifies histone deacetylase 1 (HDAC1) and HDAC2 as therapeutic targets in sickle cell disease. *Proc. Natl. Acad. Sci. U. S. A.* **107,** 12617–22 (2010).

163. Alam, S. *et al.* Galectin-9 protein expression in endothelial cells is positively regulated by histone deacetylase 3. *J. Biol. Chem.* **286,** 44211–44217 (2011).

164. Yokoyama, A., Takezawa, S., Schüle, R., Kitagawa, H. & Kato, S. Transrepressive function of TLX requires the histone demethylase LSD1. *Mol. Cell. Biol.* **28,** 3995–4003 (2008).

165. De Oliveira, A. P. *et al.* Live visualization of herpes simplex virus type 1 compartment dynamics. *J. Virol.* **82,** 4974–90 (2008).

166. Harland, J. & Brown, S. M. in *Methods in Molecular Medicine* **10,** 1–8

167. Schaffer, P. A. An activity specified by the osteosarcoma line U2OS can substitute functionally for ICP0 , a major regulatory protein of herpes simplex virus type 1 . (1995).

168. Polioudaki, H., Kastrinaki, M.-C., Papadaki, H. a & Theodoropoulos, P. a. Microtubule-interacting drugs induce moderate and reversible damage to human bone marrow mesenchymal stem cells. *Cell Prolif.* **42,** 434–47 (2009).

169. Wysocka, J. & Herr, W. The herpes simplex virus VP16-induced complex: the makings of a regulatory switch. *Trends Biochem Sci* **28,** 294–304 (2003).

170. Everett, R. D. *et al.* PML contributes to a cellular mechanism of repression of herpes simplex virus type 1 infection that is inactivated by ICP0. *J. Virol.* **80,** 7995–8005 (2006).

171. Tavalai, N., Papior, P., Rechter, S., Leis, M. & Stamminger, T. Evidence for a role of the cellular ND10 protein PML in mediating intrinsic immunity against human cytomegalovirus infections. *J. Virol.* **80,** 8006–8018 (2006).

172. Davies, C. C., Mason, J., Wakelam, M. J. O., Young, L. S. & Eliopoulos, A. G. Inhibition of phosphatidylinositol 3-kinase- and ERK MAPK-regulated protein synthesis reveals the pro-apoptotic properties of CD40 ligation in carcinoma cells. *J. Biol. Chem.* **279,** 1010–9 (2004).

173. Blommaart, E. F. C., Krause, U., Schellens, J. P. M., Vreeling-sindelarova, H. & Meijer, A. J. The phosphatidylinositol 3-kinase inhibitors wortmannin and LY 294002 inhibit autophagy in isolated rat hepatocytes. **246,** 240–246 (1997).

174. Liu, J. *et al.* Beclin1 controls the levels of p53 by regulating the deubiquitination activity of USP10 and USP13. *Cell* **147,** 223–34 (2011).

175. Yoshimori, T., Yamamoto, A., Moriyama, Y., Futai, M. & Tashiro, Y. Bafilomycin A1, a specific inhibitor of vacuolar-type H(+)-ATPase, inhibits acidification and protein degradation in lysosomes of cultured cells. *J Biol Chem* **266,** 17707–17712 (1991).

176. Yamamoto, a *et al.* Bafilomycin A1 prevents maturation of autophagic vacuoles by inhibiting fusion between autophagosomes and lysosomes in rat hepatoma cell line, H-4-II-E cells. *Cell Struct. Funct.* **23,** 33–42 (1998).

177. Davies, C. C., Mak, T. W., Young, L. S. & Eliopoulos, A. G. TRAF6 is required for TRAF2-dependent CD40 signal transduction in nonhemopoietic cells. *Mol. Cell. Biol.* **25,** 9806–19 (2005).

178. Li, D. D. *et al.* The pivotal role of c-Jun NH2-terminal kinase-mediated Beclin 1 expression during anticancer agents-induced autophagy in cancer cells. *Oncogene* **28,** 886–898 (2009).

179. Hanada, T. *et al.* The Atg12-Atg5 conjugate has a novel E3-like activity for protein lipidation in autophagy. *J. Biol. Chem.* **282,** 37298–37302 (2007).

180. Romanov, J. *et al.* Mechanism and functions of membrane binding by the Atg5-Atg12/Atg16 complex during autophagosome formation. *EMBO J.* **31,** 4304–17 (2012).

181. Everett, R. D., Boutell, C., Orr, A. & Al, E. E. T. Phenotype of a Herpes Simplex Virus Type 1 Mutant That Fails To Express Immediate-Early Regulatory Protein ICP0. **78,** 1763–1774 (2004).

182. Andrade, R. M., Wessendarp, M., Gubbels, M.-J., Striepen, B. & Subauste, C. S. CD40 induces macrophage anti-Toxoplasma gondii activity by triggering autophagy-dependent fusion of pathogen-containing vacuoles and lysosomes. *J. Clin. Invest.* **116,** 2366–77 (2006).

183. Portillo, J.-A. C. *et al.* The CD40-autophagy pathway is needed for host protection despite IFN-γ-dependent immunity and CD40 induces autophagy via control of P21 levels. *PLoS One* **5,** e14472 (2010).

184. Korolchuk, V. I. *et al.* Lysosomal positioning coordinates cellular nutrient responses. *Nat. Cell Biol.* **13,** 453–60 (2011).

185. Sodeik, B., Ebersold, M. W. & Helenius, A. Microtubule-mediated Transport of Incoming Herpes Simplex Virus 1 Capsids to the Nucleus. **136,** 1007–1021 (1997).

186. Nicola, a. V., McEvoy, a. M. & Straus, S. E. Roles for Endocytosis and Low pH in Herpes Simplex Virus Entry into HeLa and Chinese Hamster Ovary Cells. *J. Virol.* **77,** 5324–5332 (2003).

187. Nicola, A. V, Hou, J., Major, E. O. & Straus, S. E. Herpes simplex virus type 1 enters human epidermal keratinocytes, but not neurons, via a pH-dependent endocytic pathway. *J. Virol.* **79,** 7609–16 (2005).

188. Vanhaesebroeck, B., Guillermet-Guibert, J., Graupera, M. & Bilanges, B. The emerging mechanisms of isoform-specific PI3K signalling. *Nat. Rev. Mol. Cell Biol.* **11,** 329–41 (2010).

189. Carpentier, S. *et al.* Class III phosphoinositide 3-kinase/VPS34 and dynamin are critical for apical endocytic recycling. *Traffic* **14,** 933–48 (2013).

190. Futter, C. E., Collinson, L. M., Backer, J. M. & Hopkins, C. R. Human VPS34 is required for internal vesicle formation within multivesicular endosomes. *J. Cell Biol.* **155,** 1251–64 (2001).

191. Kim, J. Y., Mandarino, A., Chao, M. V, Mohr, I. & Wilson, A. C. Transient reversal of episome silencing precedes VP16-dependent transcription during reactivation of latent HSV-1 in neurons. *PLoS Pathog.* **8,** e1002540 (2012).

192. Camarena, V. *et al.* Nature and duration of growth factor signaling through receptor tyrosine kinases regulates HSV-1 latency in neurons. *Cell Host Microbe* **8,** 320–30 (2010).

193. Wilcox, D. R., Wadhwani, N. R., Longnecker, R. & Muller, W. J. Differential Reliance on Autophagy for Protection from HSV Encephalitis between Newborns and Adults. *PLoS Pathog.* **11,** e1004580 (2015).

194. Dressler, G. R., Rock, D. L. & Fraser, N. W. Latent herpes simplex virus type 1 DNA is not extensively methylated in vivo. *J. Gen. Virol.* **68 (Pt 6),** 1761–1765 (1987).

195. Kubat, N. J., Tran, R. K., McAnany, P. & Bloom, D. C. Specific Histone Tail Modification and Not DNA Methylation Is a Determinant of Herpes Simplex Virus Type 1 Latent Gene Expression. *J. Virol.* **78,** 1139–1149 (2004).

196. Kent, J. R. *et al.* During Lytic Infection Herpes Simplex Virus Type 1 Is Associated with Histones Bearing Modifications That Correlate with Active Transcription. *J. Virol.* **78,** 10178–10186 (2004).

197. Wang, Q.-Y. *et al.* Herpesviral latency-associated transcript gene promotes assembly of heterochromatin on viral lytic-gene promoters in latent infection. *Proc. Natl. Acad. Sci. U. S. A.* **102,** 16055–16059 (2005).

198. Tong, J. J., Liu, J., Bertos, N. R. & Yang, X.-J. Identification of HDAC10, a novel class II human histone deacetylase containing a leucine-rich domain. *Nucleic Acids Res.* **30,** 1114–1123 (2002).

199. Fischer, D. D. *et al.* Isolation and characterization of a novel class II histone deacetylase, HDAC10. *J. Biol. Chem.* **277,** 6656–6666 (2002).

200. Liang, Y., Vogel, J. L., Narayanan, A., Peng, H. & Kristie, T. M. Inhibition of the histone demethylase LSD1 blocks alpha-herpesvirus lytic replication and reactivation from latency. *Nat. Med.* **15,** 1312–7 (2009).

201. Elliott, G. *et al.* Intermediate DNA methylation is a conserved signature of genome regulation. *Nat. Commun.* **6,** 6363 (2015).

202. Hantusch, B., Kalt, R., Krieger, S., Puri, C. & Kerjaschki, D. Sp1/Sp3 and DNA-methylation contribute to basal transcriptional activation of human podoplanin in MG63 versus Saos-2 osteoblastic cells. *BMC Mol. Biol.* **8,** 20 (2007).

203. Tanaka, K., Appella, E. & Jay, G. Developmental activation of the H-2K gene is correlated with an increase in DNA methylation. *Cell* **35,** 457–465 (1983).

204. Bahar Halpern, K., Vana, T. & Walker, M. D. Paradoxical role of DNA methylation in activation of FoxA2 gene expression during endoderm development. *J. Biol. Chem.* (2014). doi:10.1074/jbc.M114.573469

205. Kao, H., Downes, M., Ordentlich, P. & Evans, R. M. Isolation of a novel histone deacetylase reveals that class I and class II deacetylases promote SMRT-mediated repression. 55–66 (2000). doi:10.1101/gad.14.1.55

206. Heinzel, T. *et al.* A complex containing N-CoR, mSin3 and histone deacetylase mediates transcriptional repression. *Nature* **387,** 43–48 (1997).

207. Huang, E. Y. *et al.* Nuclear receptor corepressors partner with class II histone deacetylases in a Sin3-independent repression pathway. *Genes Dev.* **14,** 45–54 (2000).

208. Fischle, W. *et al.* Enzymatic activity associated with class II HDACs is dependent on a multiprotein complex containing HDAC3 and SMRT/N-CoR. *Mol. Cell* **9,** 45–57 (2002).

209. Roizman, B. The checkpoints of viral gene expression in productive and latent infection: the role of the HDAC/CoREST/LSD1/REST repressor complex. *J. Virol.* **85,** 7474–82 (2011).

210. Rowles DL, Tsai YC, Greco TM, Lin AE, Li M, Yeh J, C. I. DNA methyltransferase DNMT3A associates with viral proteins and impacts HSV-1 infection. *Proteomics* 1–45 (2015). doi:10.1002/pmic.201500035

Appendix *(Vlahava et al., 2015)*

Cellular Signalling 27 (2015) 1253–1263

Contents lists available at ScienceDirect

Cellular Signalling

journal homepage: www.elsevier.com/locate/cellsig

CD40 ligand exhibits a direct antiviral effect on Herpes Simplex Virus type-1 infection via a PI3K-dependent, autophagy-independent mechanism

Virginia-Maria Vlahava [a], Aristides G. Eliopoulos [b,c], George Sourvinos [a,*]

[a] Laboratory of Clinical Virology, Medical School, University of Crete, Heraklion, Crete, Greece
[b] Molecular and Cellular Biology Laboratory, Medical School, University of Crete, Heraklion, Crete, Greece
[c] Institute of Molecular Biology & Biotechnology, FORTH, Heraklion, Crete, Greece

ARTICLE INFO

Article history:
Received 4 February 2015
Accepted 3 March 2015
Available online 10 March 2015

Keywords:
HSV-1
CD40 ligand
PIK3K
VP16
Autophagy
Atg5

ABSTRACT

The interaction between CD40 and its ligand, CD40L/CD154, is crucial for the efficient initiation and regulation of immune responses against viruses. Herpes Simplex Virus type-1 (HSV-1) is a neurotropic virus capable of manipulating host responses and exploiting host proteins to establish productive infection. Herein we have examined the impact of CD40L-mediated CD40 activation on HSV-1 replication in U2OS cells stably expressing the CD40 receptor. Treatment of these cells with CD40L significantly reduced the HSV-1 progeny virus compared to non-treated cells. The activation of CD40 signaling did not affect the binding of HSV-1 virions on the cell surface but rather delayed the translocation of VP16 to the nucleus, affecting all stages of viral life cycle. Using pharmacological inhibitors and RNAi we show that inhibition of PI3 kinase but not autophagy reverses the effects of CD40L on HSV-1 replication. Collectively, these data demonstrate that CD40 activation exerts a direct inhibitory effect on HSV-1, initiating from the very early stages of the infection by exploiting PI3 kinase-dependent but autophagy-independent mechanisms.

1. Introduction

Herpes Simplex Virus type-1 (HSV-1) is a neurotropic virus that is regarded as a serious threat, causing clinical manifestations both in immunocompetent individuals and in patients with immune deficiency, transplant recipients and neonates [1,2]. HSV-1 has been coevolving with humans since their speciation [3] and has adapted to the cell's immune response alternating from a lytic to a latent state depending on the dynamics of the cellular environment. HSV-1 is a double-stranded DNA virus that belongs to the alpha subfamily of *Herpesviridae*. Structurally, it comprises of an envelope, a proteinaceous layer that is called tegument and a capsid that surrounds the viral DNA. The lytic cycle follows three sequential phases of viral gene transcription, the immediate-early (IE), the early (E) and the late (L) with each phase being subjected to regulation by the previous one. HSV-1 enters the cell by fusion of the envelope with the cell membrane, by endocytosis or both [4]. Upon viral entry in the cell, the tegument protein VP16 forms a complex with the host transcription factors HCF-1 and Oct-1 [5]. This transactivator complex binds to the IE gene promoters of the virus enabling their transcription. The IE gene products in turn act as transcription factors for the E genes and contribute to the evasion of the innate immune response. Furthermore, HSV-1 enters sensory neurons that innervate the infected dermatome and it is translocated to the neuronal nucleus where it initially replicates. The replication is terminated soon after infection but the viral DNA persists in the neurons as episome and reactivates upon stress stimuli [6].

HSV-1 infection triggers complex immune responses of the host which involve fine-tuned interactions between innate signaling pathways and adaptive immune responses, playing a crucial role at early times of infection and spread (reviewed in [7]). Several lines of evidence suggest that CD40L exhibits antiviral properties against HSV-1 in vivo [8–11]. Notably, patients with X-linked hyper-IgM syndrome, an immune deficiency syndrome caused by mutations in the CD40L gene, are more susceptible to herpetic infections [12,13]. CD40 is expressed on B cells, antigen presenting cells (APCs), fibroblasts, epithelial and endothelial cells as well as neurons [14,15], while CD40L is expressed on activated T and B cells and platelets and it also circulates in a soluble form [15]. CD40 signaling on B cells causes isotype switching and differentiation to plasma cells and memory B cells [15]. On APCs, CD40 interaction with its ligand causes the production of cytokines and costimulatory molecules and enhances cross presentation [16]. The CD40 pathway also protects against opportunistic pathogens such as *Toxoplasma gondii*, an effect attributed to the CD40-mediated activation of the autophagy machinery [17–20]. Interestingly, patients with X-linked hyper-IgM syndrome are also susceptible to encephalitis

* Corresponding author at: Laboratory of Virology, Faculty of Medicine, University of Crete, Heraklion 71003, Crete, Greece. Tel./fax: +30 2810 394 835.
E-mail address: sourvino@med.uoc.gr (G. Sourvinos).

http://dx.doi.org/10.1016/j.cellsig.2015.03.002
0898-6568/

caused by *T. gondii* [21] further highlighting the importance of CD40–CD40L signaling in humoral and adaptive immunity.

The ability of CD40L to control HSV-1 is supported by findings in various mouse models. Thus, CD40 deficient mice exhibit impaired survival upon HSV-1 infection [11] and poor clearance of avirulent HSV-1 administered intravaginally [10]. Moreover, in a murine model of posttransplant infection by HSV-1, mice that had undergone bone marrow transplantation and developed graft versus host disease (GVHD) exhibited increased mortality rates from herpetic encephalitis which was attenuated by CD40L administration [9]. While the induction of anti-viral immune responses represents a major route by which CD40L controls HSV-1, a previous study has also indicated direct effects of CD40 activation in susceptibility to HSV-1 infection in L929 cells [8] but the mechanisms involved remain unexplored.

Autophagy is a highly conserved cellular mechanism with multiple functions. Apart from recycling nutrients for the cell, it is also involved in pathogen removal and antigen presentation [22–24]. Blocking autophagy is an essential step in the progression of HSV-1 lytic cycle in neurons. Via the neurovirulence factor ICP34.5, HSV-1 can block autophagy in neurons by binding to Beclin-1, a major autophagosome component essential for neuron survival [25], and inhibiting its autophagy function [26]. Moreover, HSV-1 carrying a mutation in the ICP34.5 gene exhibited impaired ability to cause encephalitis in mice [26]. Emphasizing the importance of ICP34.5 to neurovirulence is the fact that ICP34.5 is regulated by viral microRNAs encoded by the latency-associated transcript (LAT) of both HSV-1 and HSV-2 [27,28]. The late HSV-1 protein US11 has also been implicated in the HSV-1-associated autophagy through modulation of RKR which functions upstream of Beclin-1 [29].

The signaling pathways involved in the regulation of autophagy are only beginning to emerge. The PI3K/AKT/mTOR represents a major pathway involved in autophagy that interacts with MAPK, insulin, nutrient availability, hypoxia and ROS-mediated signals to initiate or halt autophagy [30]. mTORC1 negatively regulates autophagy via the ULK complex. Inactivation of mTORC1 leads to the release of the ULK complex and interaction with the PI3K complex (Beclin-1–Vps34) which is responsible for initiating autophagosome nucleation [31]. Vps34 is also involved in endosome recycling and phagocytosis [32,33]. Furthermore, activated mTORC1 prevents endosome maturation [34] and colocalizes with lysosomes at the cell periphery which correlates with decreased autophagosome synthesis and autophagosome–lysosome fusion [35]. Other mechanisms, such as Ca^{2+} signaling can also regulate autophagy [36].

In the present study, we set out to investigate the mechanism underlying this protective effect of CD40L on HSV-1 propagation. Our data demonstrate that CD40L impacts on the very early stages of HSV-1 infection, affecting the successful nuclear translocation of VP16 and consequently, the subsequent steps of viral life cycle. Data presented herein also show that CD40 engagement activates the PI3K pathway to inhibit HSV-1 propagation by an autophagy-independent mechanism.

2. Materials & methods

2.1. Cells and viruses

The CD40-U2OS cells were derived after stable transfection of the U2OS cell line with phCD40 [37]. Half a microgram of phCD40/cDNA was transfected into 1×10^5 U2OS cells using TurboFect™ in vitro Transfection Reagent (Fermentas) according to the manufacturer's protocol. Transfected cells were selected with 500 μg/ml geneticin (GIBCO) and resistant cells were maintained in complete DMEM (10% (vol/vol) FBS, penicillin (100 units/ml), and streptomycin (100 μg/ml)) supplemented with geneticin (500 μg/ml). CD40 expression of the CD40-U2OS cells was evaluated by flow cytometry. The CD40-3x-U2OS cells were derived after stable transfection of U2OS with the triple substitution phCD40 P233G/E235A/T254A [37] which bears mutations that prevent binding of any of the TRAFs (TRAFs 1, 2, 3, 6 and 5) to the cytoplasmic tail of CD40. Both phCD40/cDNA and phCD40 P233G/E235A/T254A cDNA3.1 were kindly provided by Dr. S. Pullen, Boehringer Ingelheim Pharmaceuticals, Inc.

Vero and BHK cells were used for propagation of viruses and titration of viruses and supernatants collected from experimental conditions. Vero cells were maintained in complete DMEM and BHK cells were maintained in complete Glasgow MEM BHK 21 (GMEM) (10% (vol/vol) New Born Calf Serum (NBCS), penicillin (100 unit/ml), streptomycin (100 μg/ml) and 10% Tryptose Phosphate Broth (TPB)).

The wild-type virus used was HSV-1 strain 17syn. The rHSV-RYC [38] virus containing three fluorescent tags (RFP-VP26, YFP-gH and CFP-VP16) was kindly provided by Dr. C. Fraefel. The virus stocks were propagated and titrated either on BHK or Vero cells according to standard protocols [39].

2.2. Inhibitors and recombinant molecules

The inhibitors used for the experiments were the PI3K inhibitor LY294002 (PHZ1144, Invitrogen) at a final concentration of 25 μM, the JNK inhibitor SP600125 (420119, CalBiochem) at a final concentration of 7.5 μM, the Specific Autophagy Inhibitor (Spautin-1, SML0440 SIGMA) at a final concentration of 10 μM and the vacuolar H + ATPase (V-ATPase) inhibitor Bafilomycin A1 at a final concentration of 100 nm. All inhibitors were diluted in dimethyl sulfoxide (DMSO). For the induction of the CD40 pathway, we used recombinant soluble human CD40L (BMS308/2, Bender MedSystems) at a final concentration 0.5 μg/ml diluted in PBS. For all inhibitors as wells as for CD40L, MTT assays were performed to determine the optimal dilutions that would not affect cell viability.

2.3. Gene silencing

CD40-U2OS cells were transfected with either ATG5 siRNA (sc-41445, Santa Cruz) or control siRNA-A (sc-37007, Santa Cruz) at a final concentration of 50 nm using TurboFect™ in vitro Transfection Reagent (Fermentas) according to the manufacturer's protocol. At 48 h post-transfection, the cells were infected with HSV-1.

2.4. Treatments and HSV-1 infections

CD40-U2OS cells or CD40-3x-U2OS cells were first treated for 30 min with the appropriate inhibitors, then for another 30 min with CD40L and HSV-1 was added last, at a multiplicity of infection (MOI) of 1 PFU/cell or at variable multiplicities depending on the experiment. CD40L and any inhibitors added were not removed from the medium for the course of infection. For experiments requiring synchronized entrance of the virus in the cells, a binding step was added. Specifically, after treatment with CD40L, the cells were incubated on ice for 5 min and then the virus was added on the cells and was allowed to bind on the cell surface for 1–1.5 h. Subsequently, cells were transferred in a humidified incubator at 37 °C and 5% CO_2 for the required time depending on the experiment.

2.5. Immunofluorescence and FACS analysis

For immunofluorescence, 1×10^5 CD40-U2OS cells were plated on glass coverslips placed in 24-well plates. The conditioned medium was aspirated, and the cells were washed with PBS, fixed with formaldehyde (4% [vol/vol] in PBS containing 2% sucrose) and permeabilized with Permeabilization Solution (Cat. No 5115, Millipore). The coverslips were incubated for 1 h with primary antibodies diluted in PBS containing 1% (vol/vol) fetal bovine serum at room temperature and they were subsequently washed in the same buffer twice before incubation with the secondary antibodies. Incubation with the secondary antibodies was performed likewise. The primary antibodies used were anti-HSV-

1 gG Envelope Protein (7F5) (Cat. No sc-56984, Santa Cruz Biotechnologies) 1:100, anti-HSV-1 VP16 MAb LP1 [38], 1:10, rabbit polyclonal anti-emerin [40], 1:150, mouse anti-LC3 (APG8) (Cat. No AM1800a, Abgent) 1:200, and rabbit anti-Herpes Simplex Virus type 1 (Cat. No B0114, DAKO) 1:100. The secondary antibodies used were Alexa Fluor 488 donkey anti-mouse (Cat. No A21202, Invitrogen), Alexa Fluor 488 goat anti-rabbit (Cat. No A11008, Invitrogen), goat anti-rabbit — Cy3 (Cat. No 816115, Invitrogen) and goat anti-mouse Cy3 (Cat. No 816515, Invitrogen). The nuclei were stained with TO-PRO-3 (Cat. No T3605, Invitrogen) at a dilution of 1:1000 in PBS. In order to visualize the binding of the virus on the cells we also used the FM 1-43FX (Cat. No F35355, Invitrogen) dye for labeling of the plasma membrane according to the manufacturer's instructions. The cells were mounted in Ibidi Mounting Medium (Cat. No 50001, Ibidi) and examined by confocal microscopy (TCS SP2, Leica Microsystems, Germany). The data were collected with sequential scanning to avoid signal overlap, at a resolution of 1024 × 1024 pixels, after a 4–6 fold averaging and the optical slices were between 0.3 and 0.5 μm. The data sets were processed with LCS Lite software (Leica).

For FACS analysis, the cells were stained with rabbit anti-CD40 (H-120) (sc-9096; Santa Cruz Biotechnology), anti-HSV-1 gG Envelope Protein (7F5) (Cat. No sc-56984, Santa Cruz Biotechnologies), PE anti-human CD270 (HVEM, TR2) (Cat. No 318805, Biolegent), anti-mouse CF™633 (Cat. No 20121, Biotium), and anti-rabbit Alexa Fluor 488 (Invitrogen) and were counted with a FACSCalibur (BD).

2.6. Live-cell microscopy

Each well of a two-well chambered coverglass unit (Lab-Tek, Thermo Scientific) was seeded with 2×10^5 CD40-U2OS cells and infected at MOI 20 PFU/cell with rHSV-RYC [38] virus in the presence or absence of CD40L (0.5 μg/ml) and the PI3K inhibitor LY294002 (25 μM). A binding step was performed for 1 h on ice as described above and the cells were then transferred in a humidified chamber on the microscope stage with 5% CO_2 at 37 °C. The cells were observed for at least 8 h with an epifluorescent Leica DMIRE2 microscope, equipped with a Leica DFC300 FX digital camera and images were acquired with the IM50 software (Leica) and exported as tiff files.

2.7. Western blot

Protein extracts were analyzed by Western blot. For whole cell extracts, the cells were washed with cold PBS, collected with 1 mM EDTA in PBS and pelleted at 2500 *g* for 10 min. The cells were then incubated for 10 min at 4 °C with M-PER Mammalian Protein Extraction Reagent (Cat. No 78503, Thermo Scientific) along with protease inhibitors (Cat. No 78415, Thermo Scientific) vortexing mildly every 2 min. The cell extracts were then briefly sonicated (40% amplitude for 15 s at 4 °C), centrifuged for 15 min at 14,000 *g* at 4 °C and the supernatant was kept for analysis. For the fractionation experiments, the cells were also collected in PBS with 1 mM EDTA as described above and the pellet was incubated for 10 min in hypotonic lysis buffer (20 mM Hepes pH 7.6, 10 mM NaCl, 1.5 mM $MgCl_2$, 0.2 mM EDTA, 0.1% NP40, 20% glycerol, 1 mM DTT and protease inhibitors) at 4 °C. Following incubation with the hypotonic buffer, the nuclei were pelleted at 15,600 *g* for 4 min at 4 °C and the supernatant was collected as the cytoplasmic fraction. The nuclei pellet was washed three times in hypotonic lysis buffer and subsequently the nuclei were incubated with hypertonic lysis buffer (20 mM Hepes pH 7.6, 500 mM NaCl, 1.5 mM $MgCl_2$, 0.2 mM EDTA, 0.1% NP40, 20% glycerol, 1 mM DTT and protease inhibitors) for 30 min at 4 °C. The samples were then briefly sonicated (40% amplitude for 15 s at 4 °C), and centrifuged at 16,100 *g* for 20 min at 4 °C and the supernatant was kept as the nuclear fraction. All protein extracts were quantified with Cayman Protein Determination kit (Cat. No 704002, Cayman). From each sample, 40 μg of protein was boiled in SDS gel-loading buffer, separated by electrophoresis and transferred on nitrocellulose membranes. The membranes were subsequently blocked in TBS-T buffer with 5% (w/vol) dried non-fat milk and incubated overnight at 4 °C with the primary antibodies. The primary antibodies used for immunoblotting were anti-HSV-1 VP16 MAb LP1 [38] 1:100, anti-HSV-1 ICP0 1:8000 (Cat. No H1A027-100, Virusys Corporation), mouse anti-actin 1:2000 (Cat. No MAB1501, Millipore), rabbit anti-H3K79me2 1:500 (Cat. No 9757, Cell Signaling) and mouse anti-APG5L/ATG5 1:1000 (Cat. No ab108327, Abcam). All antibodies were diluted in TBS-0.1% Tween-20 (vol/vol) containing 1% (w/vol) dried non-fat milk. Following incubation with the primary antibodies, the membranes were thoroughly washed and incubated with the secondary antibodies for 1 h at room temperature, washed in TBS-T and developed using Luminata Forte Western HRP Substrate (Cat. No WBLUF0100, Millipore) either on film or by the ChemiDoc™ MP System (Cat. No 170-8280, Bio-Rad) with the Image Lab v5.0 software (Bio-Rad).

2.8. Quantitative-PCR

Quantitative PCR was run on a 7500 Fast Real-Time PCR System (Applied Biosystems) using the KAPA SYBR FAST qPCR kit (Cat. No KK4601, KapaBiosystems). The ICP8 primers used were 5′-CGACGTGC CCTGTAACCTAT-3′ (forward) and 5′-CTGTTCATGGTCCCGAAGAC-3′ (reverse). In order to quantify ICP8 copies, we used DNA from HSV-1 of known titer. HSV-1 was incubated for 1 h at 60 °C in equal volume of virus lysis buffer (VL buffer) containing Tris HCl pH 8.0 10 Mm, KCl 50 mM, $MgCl_2$ 2.5 mM, Tween-20 0.45% (v/v) and 60 μg/ml proteinase K. Following incubation at 60 °C the virus was incubated for 15 min at 95 °C to deactivate the proteinase K. DNA from infected cells was extracted using the PureLink™ Genomic DNA Kit (Cat. No K1820-01, Invitrogen).

3. Results

3.1. CD40 signaling inhibits production of HSV-1 progeny virions

It has been previously reported that CD40L has a direct antiviral activity on HSV-1 in vitro [8]. In light of this finding, we set out to investigate the mechanism underlying this phenomenon using the permissive to HSV-1 infection, human osteosarcoma cell line U2OS engineered to express the CD40 receptor (CD40-U2OS). CD40 expression in a stable clone was successfully confirmed by flow cytometry (Fig. 1A). To determine whether CD40 ligation confers anti-viral effects in this model, CD40-U2OS cells were treated either with recombinant CD40L or vehicle control and subsequently infected with HSV-1 at MOI 1 PFU/cell for 24 h. Titration assays showed that CD40 ligation inhibited the production of progeny virions from as early as 12 h post-infection and through the 24 hour treatment (Fig. 1B and C). To further confirm that this effect required CD40 signaling, indeed, we established U2OS cell clones stably expressing a P233G/E235A/T254A mutated CD40 receptor (CD40-3x-U2OS) which is incapable of binding TRAFs 1, 2, 3, 6 and 5 to its cytoplasmic tale and is defective in CD40L-induced signal activation [37]. Treatment of CD40-3x-U2OS with CD40L failed to reduce production of HSV-1 progeny virions.

3.2. CD40 signaling does not affect the binding of HSV-1 virions on the cell surface

Having established that CD40 signaling affects the HSV-1 progeny virus, we proceeded to identify the mechanism underlying this effect. To that end, we first investigated whether CD40L could inhibit the binding of HSV-1 virions to the cell surface. CD40-U2OS cultures were exposed to recombinant CD40L for 30 min and were then infected with wild-type HSV-1 at MOI 30 PFU/cell for 1.5 h on ice, to prevent entry of the virus in the cells. Subsequently the cells were fixed and stained for the glycoprotein G (gG) of HSV-1 and with the FM 1-43FX dye to

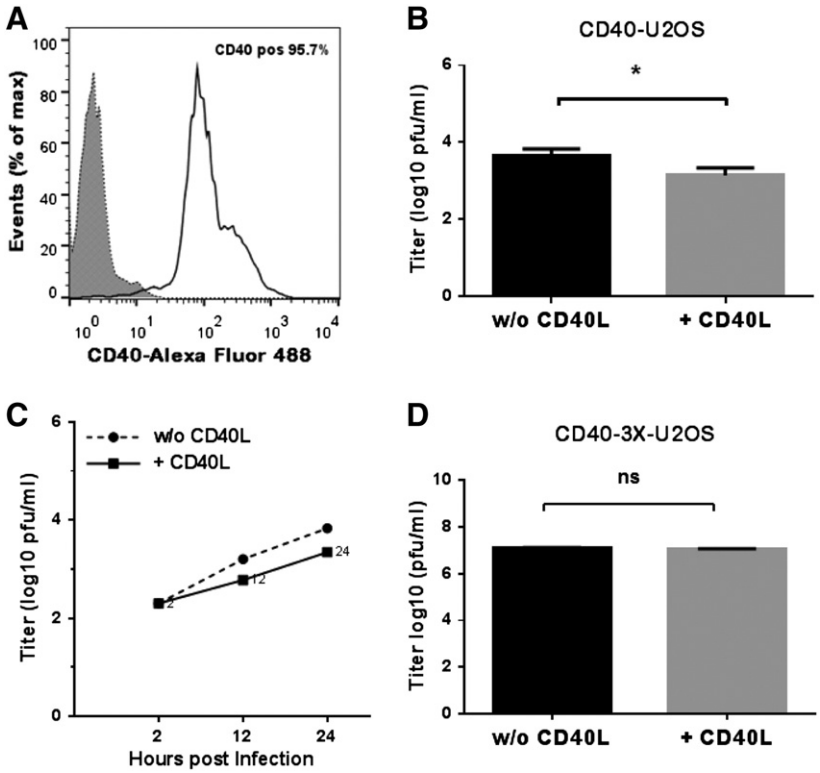

Fig. 1. HSV-1 titer decreases in the presence of CD40L. (A) U2OS cells were stably transfected with CD40. Purity of the population expressing CD40 was evaluated using flow cytometry. 95.7% of the cells were found to be CD40 positive. (B) CD40-U2OS cells were pretreated with CD40L (0.5 μg/ml) for 30 min and then infected with HSV-1 at a multiplicity of 1 PFU/ cell, for 24 h. CD40L was not removed from the medium during the incubation period with the virus. Supernatants of the infected cells were harvested and titrated on BHK cells. HSV-1 titer was significantly decreased ($P = 0.0372$) in the presence of CD40L. (C) Growth curves of HSV-1 in the presence or absence of CD40L. CD40-U2OS cells were pretreated with CD40L (0.5 μg/ml) for 30 min and then infected with HSV-1 at a MOI 1 PFU/cell. CD40L was not removed from the medium and supernatants were harvested at 2, 12 and 24 h.p.i. and they were titrated on BHK cells. (D) U2OS cells stably transfected with the triple substitution P233G/E235A/T254A CD40 receptor, which prevents binding of any of the TRAFs to its cytoplasmic tail, were pretreated with CD40L (0.5 μg/ml) and infected with HSV-1 at MOI 1 PFU/cell, for 24 h. Supernatants were harvested and titrated on BHK cells. HSV-1 titer presented no significant variation ($P = 0.1785$). Analysis of statistical significance was performed by unpaired t-test (GraphPad Prism 6.04).

visualize the plasma membrane. The specimens were examined by confocal microscopy (Fig. 2A and B) and gG particles on the surface of the cells were counted using the ImageJ software. No significant differences in the binding of HSV-1 on the cell surface were detected (Fig. 2B), indicating that the effects of CD40 ligation on HSV-1 virion production are not due to reduced binding of the virus to the cell surface. Moreover, CD40-U2OS cells were analyzed for cell surface expression of HVEM in the presence and absence of CD40L (Fig. 2D) and likewise after 24 hour infection at MOI 1 PFU/cell (Fig. 2E). Flow cytometric analysis demonstrated comparable levels of HVEM expression, regardless of CD40 activation. Specifically, 35.3% of the cells expressed HVEM without CD40L treatment and 36.5% after CD40L stimulation. HSV-1 substantially upregulated the receptor in the infected cells, however, the proportion of HVEM-positive cells was similar both in the absence or presence of CD40L (78.3% and 71.3%, respectively).

3.3. CD40L signaling delays the translocation of VP16 to the nucleus

As the binding of the virus was not affected by CD40 signaling, we sought to investigate whether CD40 ligation impacts on the viral protein VP16, a critical transcriptional activator of the immediate-early gene promoters of HSV-1 [41]. VP16 forms a complex with the cellular factors HCF-1 and Oct-1 that drive VP16 to the cell nucleus where it initiates transcription of the viral immediate-early genes [5]. Therefore, we monitored the dynamics of this protein in the presence or absence of CD40L. A synchronized infection of CD40-U2OS cells revealed that CD40L hindered the translocation of VP16 from the cytoplasm to the cell nucleus. Specifically, cells were stained for VP16 and the nuclear envelope protein emerin and analyzed by confocal microscopy. At various time points post-infection, we could detect fewer VP16 particles in the nuclei of cells treated with CD40L compared to non-treated cells (Fig. 3A & B). This observation was further confirmed by Western blot analysis of fractionated nuclear and cytoplasmic protein extracts following infection with HSV-1 for 1.5 h. The results showed reduced VP16 in the nuclei of cells treated with CD40L compared to control cultures (Fig. 3C).

In light of these findings, we proceeded to investigate the dynamics of VP16 in association with the dynamics of the virus capsid at early times of infection. To that end, we performed live cell microscopy, utilizing the recombinant virus rHSV-RYC [38] which encodes the fusion proteins VP16-ECFP and VP26-mRFP of the virus tegument and capsid, respectively. CD40-U2OS cells were initially infected on ice and they were subsequently transferred at standard culture conditions and monitored for at least 8 h. Fig. 4A shows representative time points of the infection revealing a delayed onset of the viral lytic cycle upon CD40 signaling. VP16 was localized perinuclearly at 1 h.p.i. (hours post-infection) and it was distributed throughout the cytoplasm at 2–5 h.p.i. At approximately 6 h.p.i., VP16 formed small nuclear foci which are indicative of de novo protein synthesis. Markedly, in CD40L-treated cells, VP16 remained perinuclear for approximately 2 h and did not accumulate in nuclear foci until 8 h.p.i. and thereafter. A similar delay was observed when the VP26 protein was also monitored. VP26 accumulation could be visualized in the nucleus of non-treated but not in CD40L-stimulated cells at 8 h.p.i. In agreement with the aforementioned observations, there were fewer sites of capsid assembly in cells treated with CD40L at 30 h.p.i. (Fig. 4B).

3.4. Immediate-early, early and late stages of HSV-1 infection during activation of CD40 signaling

To further elucidate the HSV-1-related events which are associated with CD40 signaling, we proceeded to investigate the kinetics of ICP0,

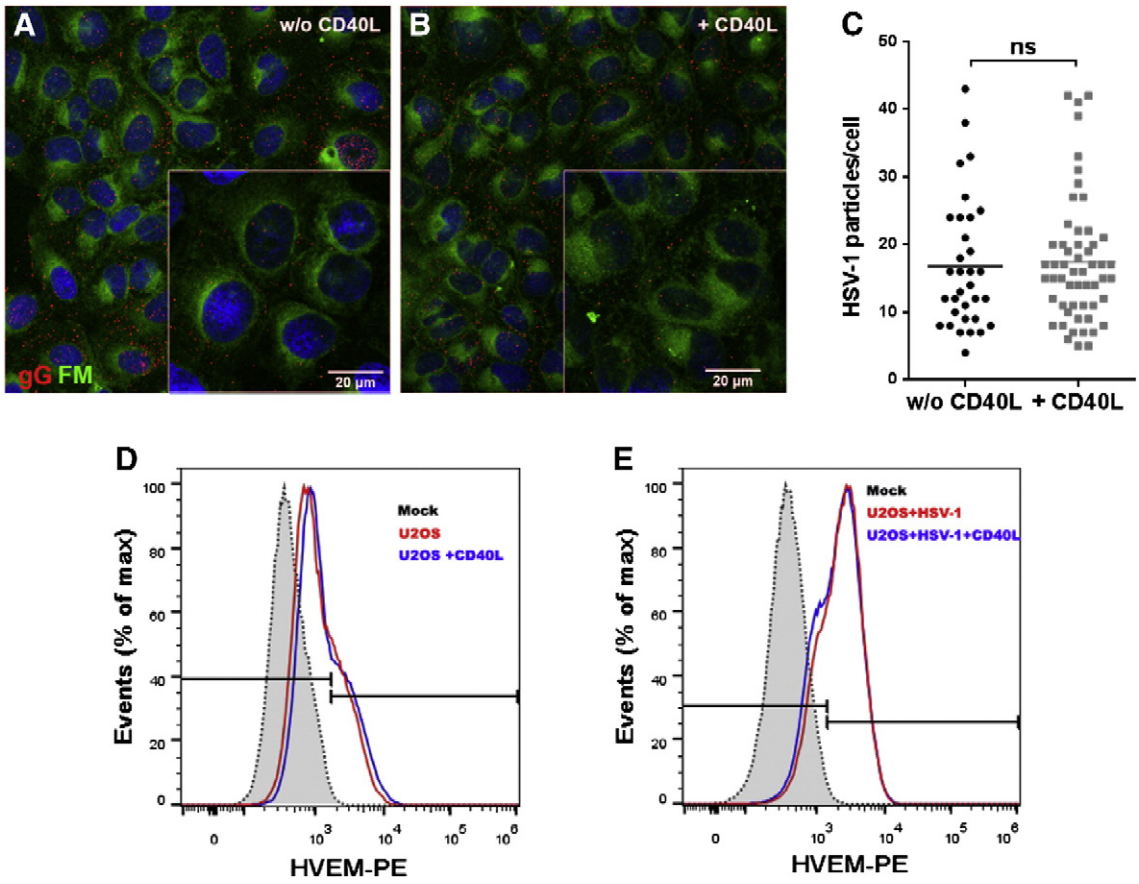

Fig. 2. Binding of HSV-1 is not affected by CD40 signaling nor the expression of the surface receptor HVEM. (A & B) CD40-U2OS cells were treated with CD40L or solvent vehicle for 30 min and were then infected with HSV-1 at MOI 30 PFU/cell for 1.5 h, on ice. The cells were subsequently fixed at 4 °C and stained with FM 1-43FX (green) to label the plasma membrane and for glycoprotein G (red) of HSV-1 to visualize virions entering the cells. (C) The number of virions per cell attached to the plasma membrane was counted using the cell counter application of ImageJ. Analysis of statistical significance was performed by an unpaired t-test (GraphPad Prism 6.04). Error bars represent the mean. No statistical significance was observed ($P = 0.7794$). (D) The expression of HVEM on the cell surface of the CD40-U2OS cells was monitored by flow cytometry. (E) The expression of HVEM on the cell surface was also monitored in CD40-U2OS cells infected with HSV-1 at MOI 1 PFU/cell for 24 h in the presence or absence of CD40L.

a key-regulator of HSV-1 productive infection. CD40-U2OS cells were infected at MOI 1 PFU/cell and protein extracts were harvested at various time points post-infection. Despite the delayed kinetics of VP16, there was no difference in the expression levels of ICP0, except at 24 h post-infection, when less ICP0 was expressed in cells that had been treated with CD40L (Fig. 5A). We next sought to determine the impact of CD40L on HSV-1 DNA replication. For that purpose, a qPCR assay was performed using primers for the ICP8 early gene to assess the number of HSV-1 DNA copies produced by cells treated with CD40L, compared to those that did not receive any treatment. From as early as 2 h.p.i., we detected a statistically significant reduction of ICP8 copies in the presence of CD40L which increased over time (Fig. 5B). Finally, the expression of glycoprotein G (gG) in CD40-U2OS cells infected at MOI 1 PFU/cell was examined, as a marker of late gene expression. At 18 h.p.i., gG was hardly detectable in CD40-U2OS cells exposed to CD40L signaling (Fig. 5C).

3.5. PI3K inhibition reverses the effect of CD40 signaling on HSV-1

The observed delay in VP16 entry to the nucleus, along with the decreased production of progeny virus, led us to investigate CD40 signaling pathways responsible for the regulation of antiviral responses. In particular, we explored the impact of PI3 kinase which is known to be activated by CD40 ligation in epithelial cells [42] and of autophagy which has been implicated in HSV-1 replication [25,26] and is controlled by PI3 kinase signals. To address this issue, we infected CD40-U2OS with rHSV-RYC in the presence of CD40L, along with the PI3K inhibitor LY294002 which inhibits the autophagosome formation [43] and monitored the dynamics of VP16 and VP26 by live cell microscopy (Fig. 6). In LY294002-treated cells, nuclear VP26 foci were clearly visible at 6 h.p.i. whereas in control untreated cultures, VP26 foci were detectable at later time points. Treatment of CD40-U2OS cells with CD40L along with LY294002 was able to reverse, in part, the phenotype of LY294002 (Fig. 6).

To confirm the timelapse microscopy observations, we examined the production of progeny virions at 24 h.p.i., obtained from cells infected at MOI 1 PFU/cell in the presence of LY294002 and/or CD40L compared to control infected cells (Fig. 7A). The results showed a statistically significant difference in the production of progeny virions between cells treated with LY294002 and cells treated with either LY294002 and CD40L or CD40L alone. In contrast, there was no statistically significant difference between the virus produced from the control infection and the virus produced from cells treated with both LY294002 and CD40L, a result which further corroborates the timelapse microscopy findings.

The potential association between HSV-1 and LC3 was next investigated by immunofluorescence analysis. CD40-U2OS cells were infected with wild-type HSV-1 at MOI 30 PFU/cell for 1.5 and 3 h, including a binding step on ice to synchronize the infection. The infected cells were immunostained for all HSV-1 major glycoproteins and at least one core protein, as well as for LC3 isoforms I and II. LC3s are involved in the formation of the phagophore and conversion of LC3 I to LC3 II is indicative of autophagy initiation. We observed that HSV-1 exhibited a higher degree of colocalization with LC3 in the presence of CD40L (Fig. 7B). This colocalization was markedly reduced in the presence of

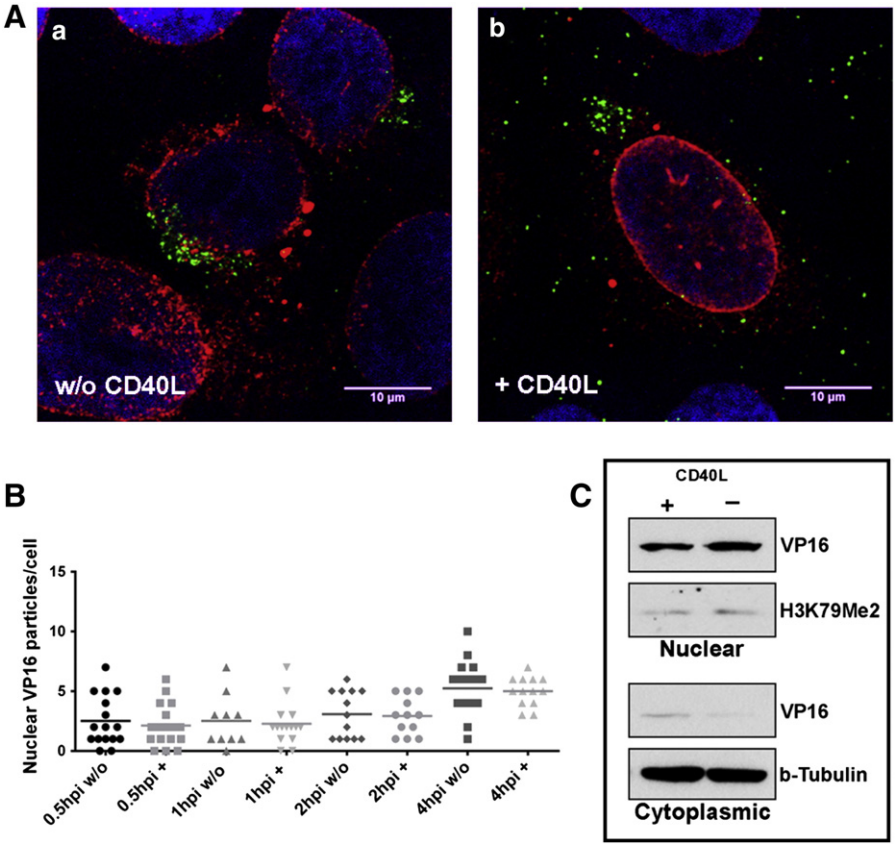

Fig. 3. Localization of VP16 in relation to the cell nucleus. (A). CD40-U2OS cells were treated with CD40L (0.5 μg/ml) or control medium for 30 min and were then infected with HSV-1 at MOI 35 PFU/cell, for 1.5 h on ice, along with 100 μg/ml cycloheximide in order to block translation. The cells were subsequently stained for the tegument protein of HSV-1, VP16 (green) and for emerin (red) in order to visualize VP16 in relation to the nucleus. (B) Similarly, CD40-U2OS cells were infected at MOI 30 PFU/cell in the presence and absence of CD40L and VP16 particles that entered the nucleus were counted at 0.5, 1, 2 and 4 h.p.i and are plotted on graph. Statistical analysis was performed by ordinary one-way ANOVA with GraphPad Prism 6.04. Differences of the means were found to be statistically significant ($P < 0.0001$). Error bars represent the mean. (C) VP16, H3K79Me2 and beta-tubulin expression in nuclear and cytoplasmic fractions of CD40-U2OS cells infected with HSV-1 in the presence of CD40L compared to the control at 1.5 h.p.i. Cells were treated with CD40L (0.5 μg/ml) or control medium for 30 min and were then infected with HSV-1 at a multiplicity of 30 PFU per cell, for 1.5 h on ice. Protein extracts were collected and fractioned 1.5 h.p.i.

LY294002 while it was partly restored when cells were treated with both LY294002 and CD40L (Fig. 7B). The association of LC3 foci and HSV-1 was scored and analyzed by ordinary one-way ANOVA at 1.5 and 3 h.p.i. Differences of the means were found to be statistically significant ($P < 0.0001$) which highlights a strong association between LC3 foci with HSV-1 (Fig. 7C & D).

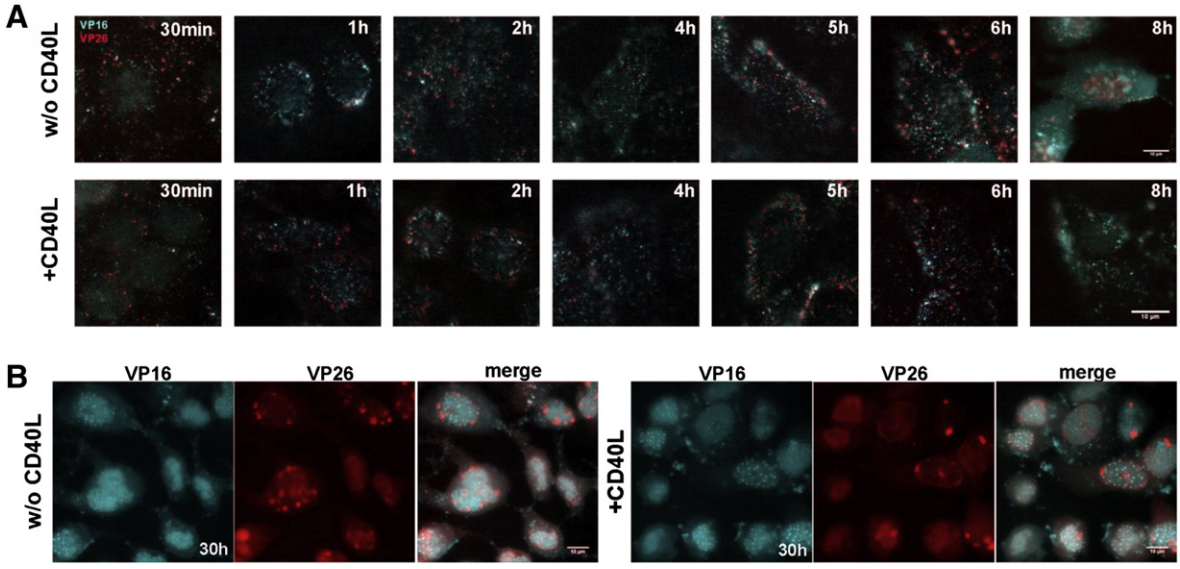

Fig. 4. Kinetics of HSV-1 in the presence of CD40L. (A) Live imaging of rHSV-RYC infected cells in the presence of CD40L. CD40-U2OS cells were plated in a chambered coverglass unit, treated with CD40L (0.5 μg/ml) or control medium for 30 min and were then infected with rHSV-RYC at MOI 20 PFU/cell, for 1.5 h on ice. The cells were then transferred in a humidified chamber on the microscope stage with 5% CO_2 at 37 °C and were observed for at least 8 h. (B) CD40-U2OS cells infected with rHSV-RYC (A) as monitored at 30 h.p.i.

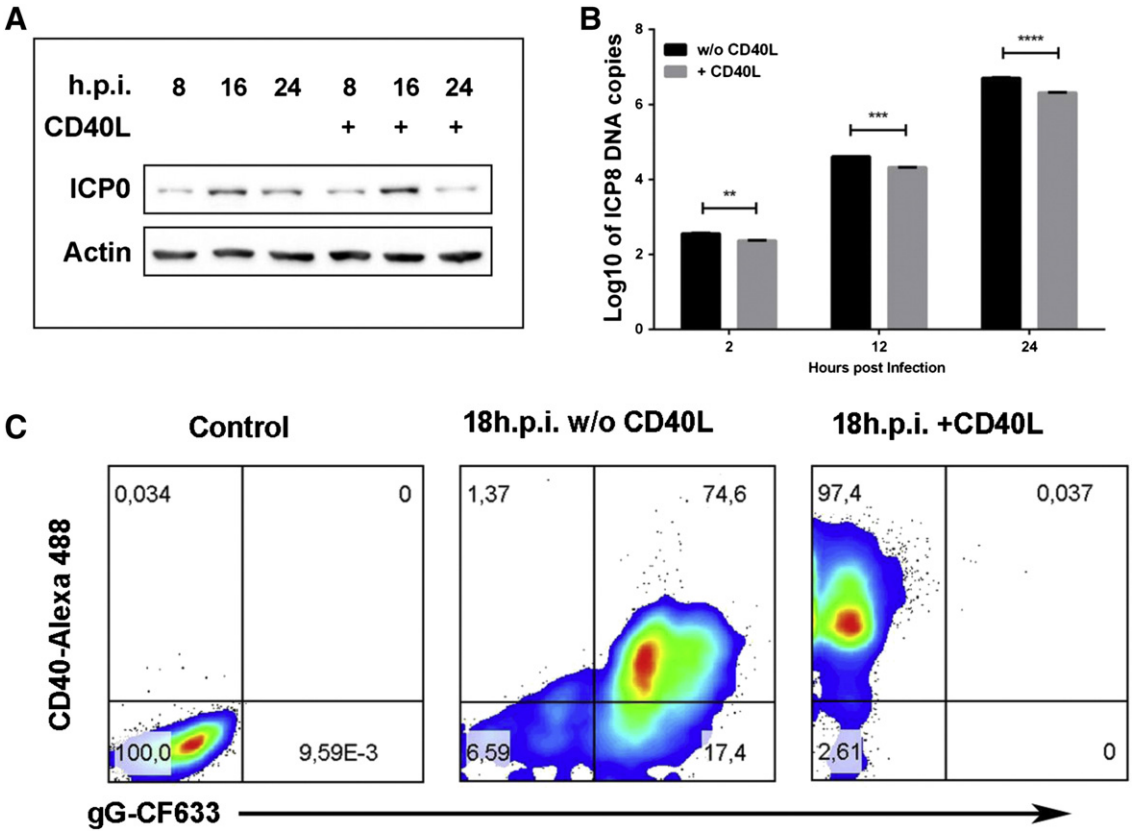

Fig. 5. Analysis of ICP0 expression, viral DNA replication and glycoprotein synthesis during CD40L signaling. (A) ICP0 expression in CD40-U2OS cells infected with HSV-1 at MOI 1 PFU/cell in the presence of CD40L, at various points post-infection. The cells were treated with CD40L (0.5 μg/ml) or control medium for 30 min and were then infected with HSV-1 for 8, 16 and 24 h respectively. Protein extracts were collected and 40 μg of protein was analyzed for each time point. (B) DNA copies of ICP8 in CD40-U2OS cells infected with HSV-1 at MOI 1 PFU/cell in the presence of CD40L at various points post-infection. The cells were treated with CD40L (0.5 μg/ml) or control medium for 30 min and were then infected with HSV-1 for 2, 12 and 24 h, respectively. The cells were lysed, DNA was extracted and ICP8 copies were quantified by qPCR. For the statistical analysis, an unpaired t-test was performed using GraphPad Prism 6.04. The asterisks indicate statistical significance. ** indicate $P = 0.001$ to 0.01, *** indicate $P = 0.0001$ to 0.001 and **** indicate $P < 0.0001$. (C) Glycoprotein G (gG) expression of CD40-U2OS cells infected with HSV-1 at MOI 1 PFU/cell for 18 h. The cells were treated with CD40L (0.5 μg/ml) or control medium for 30 min and were then infected with HSV-1 for 18 h, stained with both CD40 and gG, and analyzed by flow cytometry (the control panel depicts CD40-U2OS cells stained only with the secondary antibodies).

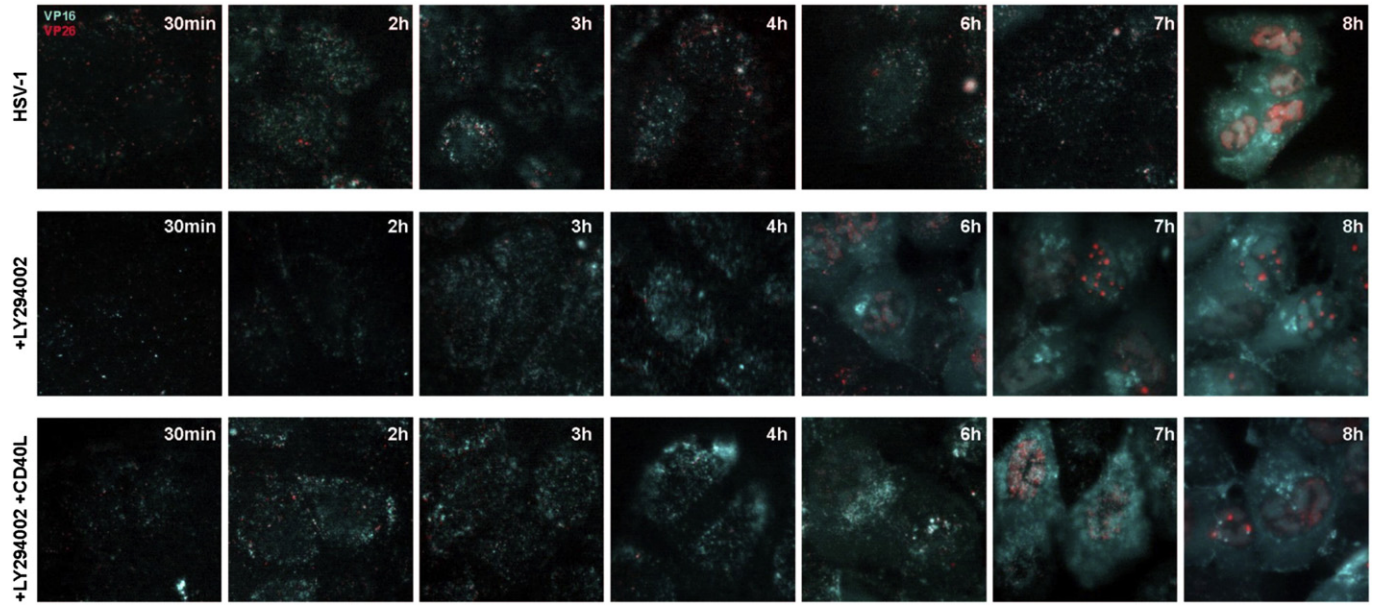

Fig. 6. Dynamics of HSV-1 infection in the presence of CD40L and the PI3K inhibitor LY294002. CD40-U2OS cells were plated in a chambered coverglass unit, treated with the PI3K inhibitor LY294002 (25 μM) for 30 min, CD40L (0.5 μg/ml) or control medium was added for another 30 min and the cells were then infected with rHSV-RYC at MOI 20 PFU/cell, for 1.5 h on ice. Following incubation with the virus at 4 °C, the cells were transferred in a humidified chamber on the microscope stage with 5% CO_2 at 37 °C and were monitored for at least 8 h.

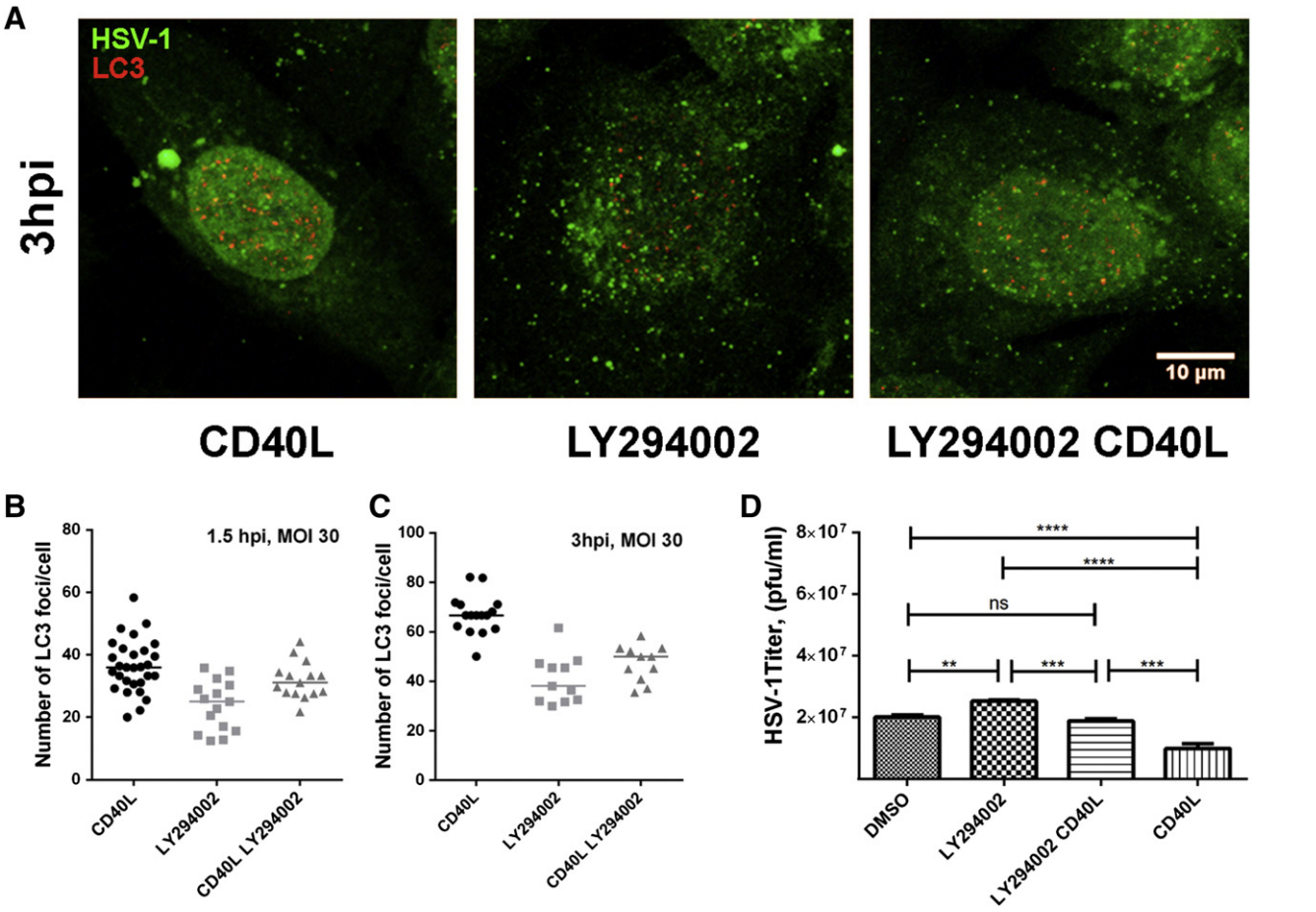

Fig. 7. Effect of the PI3K inhibitor LY294002 and of CD40L on LC3 colocalization with HSV-1 as well as on HSV-1 progeny virus. CD40-U2OS cells were treated with either the PI3K inhibitor LY294002, CD40L or both LY294002 and CD40L. The cells were pretreated with the inhibitor or solvent vehicle for 30 min, followed by addition of CD40L (0.5 μg/ml) for another 30 min. Neither the inhibitor nor the CD40L was removed from the medium for the course of infection. After pretreatments, the cells were infected at MOI 1 PFU/cell and the supernatants were collected at 24 h.p.i. and were titrated on Vero cells. For the immunofluorescence microscopy (panel A), cells were infected at MOI 30 PFU/cell while a binding step was added. (A) CD40-U2OS cells were stained for HSV-1 with a rabbit anti-HSV type-1 antibody and were also stained for LC3 isoforms I and II (red). (B and C) The number of LC3 foci per cell that colocalized with HSV-1 was counted from images obtained after confocal microscopy in cells of the experiment described in (A), using the ImageJ cell counter application. Statistical analysis was performed by ordinary one-way ANOVA with GraphPad Prism 6.04. Differences of the means were found to be statistically significant ($P < 0.0001$). Error bars represent the median. (D) Titration of HSV-1 treated with either DMSO, LY294002 (25 μM), LY294002 and CD40L or CD40L alone. The data are representative of three independent experiments and are shown as means ± SEM. For the statistical analysis, we performed a Repeated Measures one-way ANOVA followed by an uncorrected Fisher's LSD test using GraphPad Prism 6.04. The asterisks indicate statistical significance. ** indicate $P = 0.001$ to 0.01, *** indicate $P = 0.0001$ to 0.001 and **** indicate $P < 0.0001$. ns = not significant.

3.6. Spautin-1 does not reverse the effect of CD40L on HSV-1 replication

Based on the aforementioned findings, we proceeded to investigate whether the autophagy inhibitor spautin-1 has an effect on the production of progeny virions. To address this issue, we treated CD40-U2OS cells with spautin-1 in the presence or absence of CD40L and assessed progeny virion production 24 h.p.i. Interestingly, spautin-1 significantly inhibited the production of progeny virions compared to the control infection and its effect was found to be comparable to the inhibitory effect of CD40L on HSV-1 (Fig. 8A). Treatment of CD40-U2OS cells with CD40L in combination with spautin-1 did not inhibit virion production beyond the effect of each compound alone (Fig. 8B), suggesting that CD40L exerts its effect via a pathway upstream of Beclin-1 or p53, which are both inhibited by spautin-1 [44].

3.7. JNK is not required for CD40-mediated suppression of progeny virion production

CD40 ligation induces the JNK pathway [45] which has been implicated in autophagy induction [46]. We incubated CD40-U2OS cells with the JNK inhibitor SP600125 in combination with CD40L and spautin-1. The cells were subsequently infected with wild-type HSV-1 at MOI 1 PFU/cell for 24 h and the progeny virions produced were determined by plaque assay. We found that the SP600125 inhibitor caused a marked decrease in the production of progeny virus equal to that caused by CD40L and that inhibition of JNK with parallel activation of the CD40 pathway caused an even greater effect (Fig. 8B) suggesting that JNK and CD40L have opposite effects as to the inhibition of HSV-1 progeny production. Interestingly, CD40L in combination with SP600125 leads to a decrease in LC3 II/LC3 I ratio and the same is true for spautin-1 (Fig. 8C and D). Moreover, we confirmed that in the presence of CD40L, there is an induction of LC3 II, independently of HSV-1 infection (Fig. 8C). Intriguingly, CD40 activation favors LC3 I over LC3 II and the LC3 II/LC3 I ratio decreases in the presence of CD40L.

3.8. Bafilomycin A1 blocks HSV-1 propagation irrespective of CD40 signaling

Bafilomycin A1 is an inhibitor of the vacuolar H+ ATPase (V-ATPase) that prevents acidification of the lysosome [47] and is commonly used as an inhibitor of autophagy since it inhibits autophagosome–lysosome fusion [48]. We treated CD40-U2OS cells with Bafilomycin A1 in combination with CD40L and assessed the progeny HSV-1 virus at 24 h.p.i. We found that HSV-1 was significantly blocked regardless of the presence of CD40L (Fig. 8E) suggesting that acidification of the lysosome is crucial to HSV-1 progression of infection.

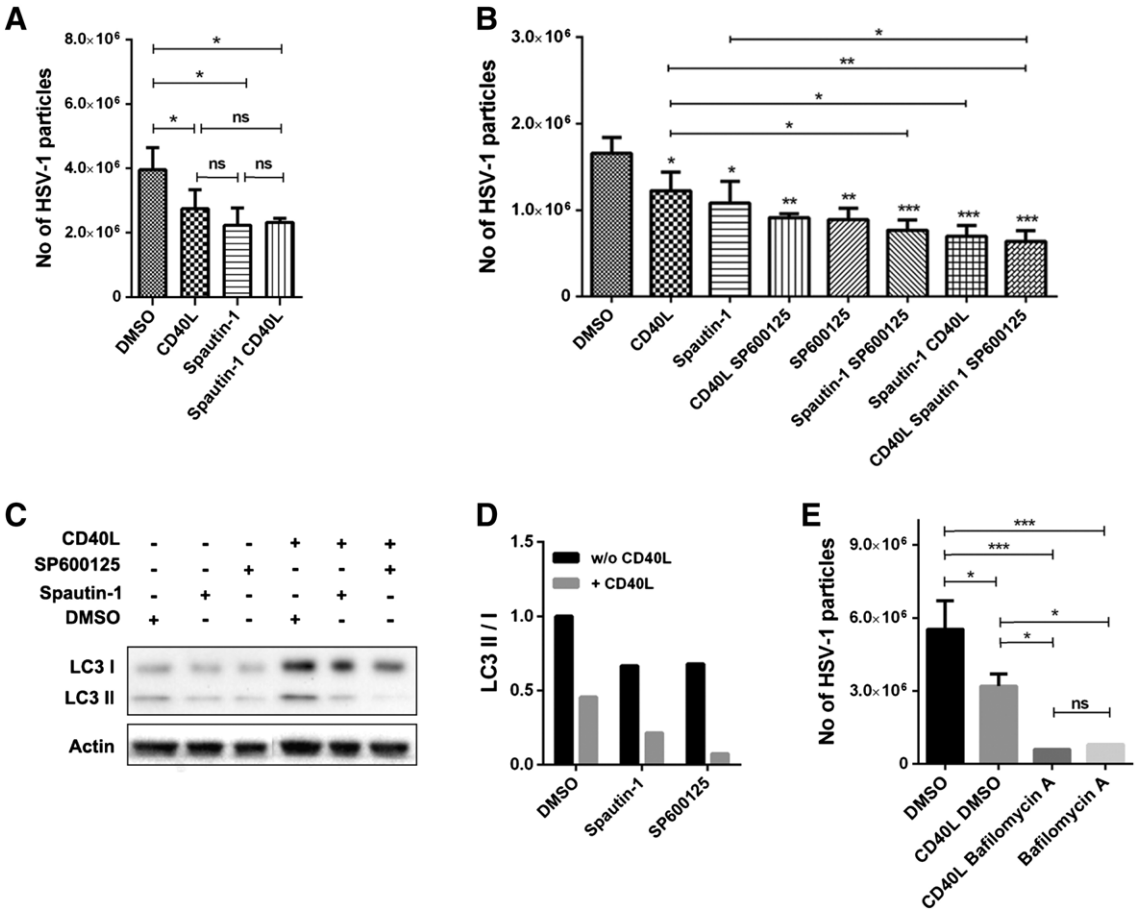

Fig. 8. The effect of various autophagy-related inhibitors and CD40L on HSV-1 progeny virus. CD40-U2OS cells were either treated with the specific autophagy inhibitor spautin-1, the JNK inhibitor SP600125, Bafilomycin A, CD40L, or a combination of the above inhibitors and CD40L. Whenever both an inhibitor(s) and CD40L were used, the cells were pretreated with the inhibitor(s) for 30 min, followed by addition of CD40L (0.5 μg/ml) for another 30 min. Neither the inhibitors nor the CD40L was removed from the medium for the course of infection. After pretreatments, the cells were infected at MOI 1 PFU/cell and the supernatants were collected at 24 h.p.i. and were titrated on Vero cells. (A) Titration of HSV-1 treated with DMSO, CD40L, spautin-1 (10 μM), or with both spautin-1 and CD40L. (B) Titration of HSV-1 treated with DMSO, CD40L, spautin-1, SP600125 (7.5 μM) or a combination of them. (C). LC3 I and II expression in CD40-U2OS cells treated with spautin-1, SP600125 or vehicle solvent as well as in cells treated with both the inhibitors and CD40L (0.5 μg/ml) for 24 h. (E) Quantification of LC3 II/I ratio after being normalized to actin from the Western blot depicted on (D) using the Image Lab 5.0 software. (D) Titration of HSV-1 treated with DMSO, CD40L, Bafilomycin A (100 nM), or with both Bafilomycin A and CD40L. The titration data are representative of three independent experiments and are shown as means ± SEM. For the statistical analysis, we performed a Repeated Measures one-way ANOVA followed by an uncorrected Fisher's LSD test using GraphPad Prism 6.04. The asterisks indicate statistical significance. * indicates P = 0.01 to 0.05, ** indicate P = 0.001 to 0.01, and *** indicate P = 0.0001 to 0.001. ns = not significant.

3.9. Silencing of Atg5 attenuates production of progeny virions

Atg5 constitutes a key component for the formation of the autophagic vesicle. Atg5 associates covalently with Atg12 forming an E3-like enzyme which forms a complex with Atg16. The Atg5–Atg12/Atg16 complex leads to the lipidation of LC3 I, with the lipid phosphatidylethanolamine (PE) to form LC3 II at the site of expansion of the autophagic membrane [49]. In addition, Atg5 is essential to the cytoplasm-to-vacuole-transport (Cvt) pathway in yeast [49,50]. We transfected CD40-U2OS cells with siAtg5 and control siRNA for 48 h and subsequently treated the cells with CD40L (0.5 μg/ml) or vehicle solvent and assessed the production of progeny virus collected 24 h.p.i. We found that silencing of Atg5 led to a significant decrease in the production of progeny virions as compared to the control. Moreover, CD40L further inhibited HSV-1 production in combination with Atg5 silencing (Fig. 9).

4. Discussion

In this study we demonstrate that CD40 signaling confers direct antiviral effects on HSV-1 by negatively regulating the lytic cycle of the virus. This effect is specifically attributed to CD40-mediated signals, as expression of a mutated receptor that lacks the binding sites of TRAFs 1, 2, 3, 6 and 5 failed to protect U2OS cells from HSV-1 infection upon CD40L treatment. We have also shown that CD40 ligation does not affect the binding of HSV-1 to the cell membrane but causes a delay in the translocation of the viral tegument protein VP16 from the cytoplasm to the nucleus. As VP16 is largely responsible for the transactivation of immediate-early viral genes which are required to evade the host cell response to HSV-1 infection, the observed effects of CD40L on VP16 localization extend our understanding of the direct anti-viral properties of the CD40 pathway.

Furthermore, CD40 signaling was found to delay the trafficking of the viral capsid protein VP26 from the cytoplasm to the nucleus. As VP26 is a late protein, the observation that VP26 lingers to the cytoplasm at the initiation of infection suggests that the delivery of the viral capsid is disturbed. The immediate-early protein ICP0 has been found to decrease at 24 h.p.i. The fact that we do not observe decreased expression of ICP0 throughout the entire course of the infection is likely due to the fact that U2OS cells can substitute the functionality of ICP0 [51]. Congruent with these findings, the DNA copies of the virus are significantly decreased as early as 2 h.p.i while glycoprotein G (gG) synthesis in CD40L treated cells is almost completely abolished at late times of the infection.

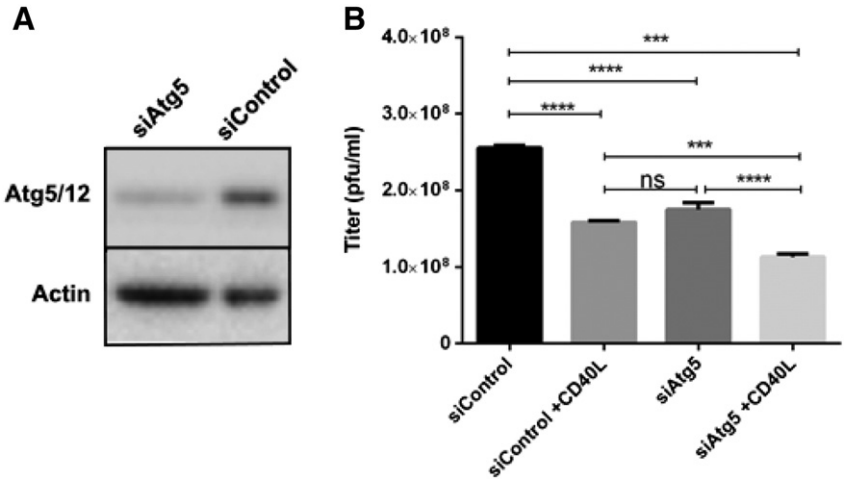

Fig. 9. Knockdown of Atg5 attenuated HSV-1 progeny virus. CD40-U2OS cells were transfected with siAtg5 or siControl RNA and remained in culture for 48 h. They were subsequently treated with CD40L (0.5 μg/ml) for 30 min and were then infected with HSV-1 for 24 h at MOI 1 PFU/cell. (A) Cell extracts were collected and analyzed for Atg5 expression by Western blot. (B) Titration of HSV-1 treated with CD40L in CD40-U2OS cells transfected with siControl or siAtg5. Titration was performed on Vero cells. The data are representative of three independent experiments and are shown as means ± SEM. For the statistical analysis, we performed a Repeated Measures one-way ANOVA followed by an uncorrected Fisher's LSD test using GraphPad Prism 6.04. The asterisks indicate statistical significance. *** indicate P = 0.0001 to 0.001 and **** indicate P < 0.0001. ns = not significant.

The aforementioned observations coupled with the reported effects of CD40L on autophagy [17,19,20] prompted us to investigate whether this process is implicated in CD40-mediated anti-viral responses. To that end, we explored a variety of pharmacological inhibitors to block autophagy including the pan-class I/II/III PI3K inhibitor LY294002 that affects autophagosome formation, spautin-1 that leads to degradation of Beclin-1 and the JNK inhibitor SP600125 which induces the downregulation of Beclin-1. We observed that PI3K inhibition by LY294002 reversed the effect of CD40 ligation on progeny virion production (Fig. 7). Furthermore, LC3, a protein involved in the formation of autophagosomes, exhibited perinuclear colocalization with HSV-1 under CD40 signaling which was abrogated in the presence of LY294002. In contrast, spautin-1 and SP600125 did not reverse the CD40-mediated anti-HSV-1 effect (Fig. 8). Similar results were obtained when a genetic approach was applied to inhibit autophagy by silencing Atg5 (Fig. 9). Intriguingly, suppression of autophagy by spautin-1, SP600125 or Atg5 siRNA inhibited virion production in the absence of CD40 ligation (Figs. 8 & 9).

Collectively, these data suggest that the antiviral properties of CD40L are not mediated through autophagy but depend on the PI3K signaling pathway. When autophagy is upregulated, lysosomes move towards the perinuclear area to fuse with the autophagosomes that are being formed [35]. Interestingly, lysosomes have been shown to localize at the periphery of the cell, when autophagosome synthesis is downregulated and this is associated with increased mTORC1 activity regulated by Akt [35], a downstream target of PI3K. In terms of HSV-1, the virus mobilizes along microtubules to the nucleus, either as a naked capsid [52] or inside vacuoles such as endosomes [53,54], highlighting the importance of vesicular trafficking for HSV-1 infection. Because PI3-kinase regulates membrane trafficking [33], it is likely that the activation of this pathway by CD40L modifies a vesicle trafficking event that is important for the delivery of HSV-1 to the nuclear membrane. The class III PI3K Vsp34, that is also part of the Beclin-1 complex, is critical for the formation of vesicles in the multivesicular bodies (MVPs) and for endocytic recycling [32,55]. However, the operation of other host cell mechanisms that are accountable for the protective properties of CD40L cannot be excluded. It is worth mentioning that in neuronal culture systems PI3K signaling inhibition leads to reactivation of HSV-1 [56,57] and that a recent study strongly associated neonatal encephalitis with active autophagy in the brain of both mice and human specimens [58].

In conclusion, this study demonstrates that CD40 signaling exerts direct anti-viral effects by blocking the progress of HSV-1 lytic cycle. The finding that this phenomenon depends on PI3K signals but not autophagy raises the possibility that the CD40–TRAF–PI3K axis operates by impeding vesicular trafficking within the infected cell resulting in a delay in the trafficking of HSV-1 or its subvirion components to the nuclear membrane of the host.

Conflict of interest

The authors declare no conflict of interest.

Acknowledgments

This work has been co-financed by the European Union (European Social Fund — ESF) and Greek National funds through the Operational Program "Education and Lifelong Learning" of the National Strategic Reference Framework (NSRF) — Research Funding Program: Heracleitous II. Investing in knowledge society through the European Social Fund. A.G.E. and G.S acknowledges the support of the EC FP7 — funded program "Translational Potential" (TransPOT; EC contract number 285948). The authors would like to thank Dr G. Chamilos for providing reagents and helpful discussions, Dr. Bertsias for reagents, as well as Dr E. Tsitoura for productive suggestions and comments.

References

[1] I. Steiner, F. Benninger, Curr. Neurol. Neurosci. Rep. 13 (2013) 414.
[2] C. Smith, R. Khanna, Am. J. Transplant. 13 (Suppl. 3) (2013) 9–23 (quiz 23).
[3] J.O. Wertheim, M.D. Smith, D.M. Smith, K. Scheffler, S.L. Kosakovsky Pond, Mol. Biol. Evol. 31 (2014) 2356–2364.
[4] S.A. Connolly, J.O. Jackson, T.S. Jardetzky, R. Longnecker, Nat. Rev. Microbiol. 9 (2011) 369–381.
[5] J. Wysocka, W. Herr, Trends Biochem. Sci. 28 (2003) 294–304.
[6] A. Arvin, G. Campadelli-Fiume, E. Mocarski, P.S. Moore, B. Roizman, R. Whitley, K. Yamanishi, Human Herpesviruses Biology, Therapy, and Immunoprophylaxis, Cambridge University Press, 2007.
[7] T. Chew, K.E. Taylor, K.L. Mossman, Viruses 1 (2009) 979–1002.
[8] J. Ruby, H. Bluethmann, M. Aguet, I.A. Ramshaw, Nat. Med. 1 (1995) 437–441.
[9] J.L. Beland, H. Adler, N.C. Del-Pan, W. Kozlow, J. Sung, W. Fanslow, I.J. Rimm, Blood 92 (1998) 4472–4478.
[10] K. Inagaki-Ohara, T. Kawabe, Y. Hasegawa, N. Hashimoto, Y. Nishiyama, Arch. Virol. 147 (2002) 187–194.
[11] K.H. Edelmann, C.B. Wilson, J. Virol. 75 (2001) 612–621.
[12] J.A. Winkelstein, M.C. Marino, H. Ochs, R. Fuleihan, P.R. Scholl, R. Geha, E.R. Stiehm, M.E. Conley, Medicine (Baltimore) 82 (2003) 373–384.
[13] M.A. García-Pérez, E. Paz-Artal, A. Corell, A. Moreno, A. López-Goyanes, F. García-Martín, R. Vázquez, A. Pacho, E. Romo, L.M. Allende, Immunobiology 207 (2003) 285–294.
[14] J. Tan, T. Town, T. Mori, D. Obregon, Y. Wu, A. DelleDonne, A. Rojiani, F. Crawford, R.A. Flavell, M. Mullan, EMBO J. 21 (2002) 643–652.
[15] U. Schönbeck, P. Libby, Cell. Mol. Life Sci. 58 (2001) 4–43.

[16] R. Elgueta, M.J. Benson, V.C. de Vries, A. Wasiuk, Y. Guo, R.J. Noelle, Immunol. Rev. 229 (2009) 152–172.
[17] R.M. Andrade, M. Wessendarp, M.J. Gubbels, B. Striepen, C.S. Subauste, J. Clin. Invest. 116 (2006) 2366–2377.
[18] C.S. Subauste, R.M. Andrade, M. Wessendarp, Autophagy 3 (2007) 245–248.
[19] J.A. Portillo, G. Okenka, E. Reed, A. Subauste, J. Van Grol, K. Gentil, M. Komatsu, K. Tanaka, G. Landreth, B. Levine, C.S. Subauste, PLoS One 5 (2010) e14472.
[20] J. Van Grol, L. Muniz-Feliciano, J.A. Portillo, V.L. Bonilha, C.S. Subauste, Infect. Immun. 81 (2013) 2002–2011.
[21] L.E. Leiva, J. Junprasert, D. Hollenbaugh, R.U. Sorensen, J. Clin. Immunol. 18 (1998) 283–290.
[22] A. Orvedahl, B. Levine, Cell. Microbiol. 10 (2008) 1747–1756.
[23] D. Schmid, C. Münz, Immunity 27 (2007) 11–21.
[24] B. Levine, V. Deretic, Nat. Rev. Immunol. 7 (2007) 767–777.
[25] N.C. McKnight, Y. Zhong, M.S. Wold, S. Gong, G.R. Phillips, Z. Dou, Y. Zhao, N. Heintz, W.X. Zong, Z. Yue, PLoS Genet. 10 (2014) e1004626.
[26] A. Orvedahl, D. Alexander, Z. Tallóczy, Q. Sun, Y. Wei, W. Zhang, D. Burns, D.A. Leib, B. Levine, Cell Host Microbe 1 (2007) 23–35.
[27] S. Tang, A.S. Bertke, A. Patel, K. Wang, J.I. Cohen, P.R. Krause, Proc. Natl. Acad. Sci. U. S. A. 105 (2008) 10931–10936.
[28] S. Tang, A. Patel, P.R. Krause, J. Virol. 83 (2009) 1433–1442.
[29] M. Lussignol, C. Queval, M.F. Bernet-Camard, J. Cotte-Laffitte, I. Beau, P. Codogno, A. Esclatine, J. Virol. 87 (2013) 859–871.
[30] A.A. Parkhitko, O.O. Favorova, E.P. Henske, Biochemistry (Mosc) 78 (2013) 355–367.
[31] C.A. Lamb, T. Yoshimori, S.A. Tooze, Nat. Rev. Mol. Cell Biol. 14 (2013) 759–774.
[32] S. Carpentier, F. N'Kuli, G. Grieco, P. Van Der Smissen, V. Janssens, H. Emonard, B. Bilanges, B. Vanhaesebroeck, H.P. Gaide Chevronnay, C.E. Pierreux, D. Tyteca, P.J. Courtoy, Traffic 14 (2013) 933–948.
[33] B. Vanhaesebroeck, J. Guillermet-Guibert, M. Graupera, B. Bilanges, Nat. Rev. Mol. Cell Biol. 11 (2010) 329–341.
[34] Y.M. Kim, C.H. Jung, M. Seo, E.K. Kim, J.M. Park, S.S. Bae, D.H. Kim, Mol. Cell 57 (2015) 207–218.
[35] V.I. Korolchuk, S. Saiki, M. Lichtenberg, F.H. Siddiqi, E.A. Roberts, S. Imarisio, L. Jahreiss, S. Sarkar, M. Futter, F.M. Menzies, C.J. O'Kane, V. Deretic, D.C. Rubinsztein, Nat. Cell Biol. 13 (2011) 453–460.
[36] A. Kondratskyi, M. Yassine, K. Kondratska, R. Skryma, C. Slomianny, N. Prevarskaya, Front. Physiol. 4 (2013) 272.
[37] S.S. Pullen, T.T. Dang, J.J. Crute, M.R. Kehry, J. Biol. Chem. 274 (1999) 14246–14254.
[38] A.P. de Oliveira, D.L. Glauser, A.S. Laimbacher, R. Strasser, E.M. Schraner, P. Wild, U. Ziegler, X.O. Breakefield, M. Ackermann, C. Fraefel, J. Virol. 82 (2008) 4974–4990.
[39] R.D. Everett, G. Sourvinos, C. Leiper, J.B. Clements, A. Orr, J. Virol. 78 (2004) 1903–1917.
[40] H. Polioudaki, M.C. Kastrinaki, H.A. Papadaki, P.A. Theodoropoulos, Cell Prolif. 42 (2009) 434–447.
[41] M.A. Dalrymple, D.J. McGeoch, A.J. Davison, C.M. Preston, Nucleic Acids Res. 13 (1985) 7865–7879.
[42] C.C. Davies, J. Mason, M.J. Wakelam, L.S. Young, A.G. Eliopoulos, J. Biol. Chem. 279 (2004) 1010–1019.
[43] E.F. Blommaart, U. Krause, J.P. Schellens, H. Vreeling-Sindelárová, A.J. Meijer, Eur. J. Biochem. 243 (1997) 240–246.
[44] J. Liu, H. Xia, M. Kim, L. Xu, Y. Li, L. Zhang, Y. Cai, H.V. Norberg, T. Zhang, T. Furuya, M. Jin, Z. Zhu, H. Wang, J. Yu, Y. Hao, A. Choi, H. Ke, D. Ma, J. Yuan, Cell 147 (2011) 223–234.
[45] C.C. Davies, T.W. Mak, L.S. Young, A.G. Eliopoulos, Mol. Cell. Biol. 25 (2005) 9806–9819.
[46] D.D. Li, L.L. Wang, R. Deng, J. Tang, Y. Shen, J.F. Guo, Y. Wang, L.P. Xia, G.K. Feng, Q.Q. Liu, W.L. Huang, Y.X. Zeng, X.F. Zhu, Oncogene 28 (2009) 886–898.
[47] T. Yoshimori, A. Yamamoto, Y. Moriyama, M. Futai, Y. Tashiro, J. Biol. Chem. 266 (1991) 17707–17712.
[48] A. Yamamoto, Y. Tagawa, T. Yoshimori, Y. Moriyama, R. Masaki, Y. Tashiro, Cell Struct. Funct. 23 (1998) 33–42.
[49] T. Hanada, N.N. Noda, Y. Satomi, Y. Ichimura, Y. Fujioka, T. Takao, F. Inagaki, Y. Ohsumi, J. Biol. Chem. 282 (2007) 37298–37302.
[50] J. Romanov, M. Walczak, I. Ibiricu, S. Schüchner, E. Ogris, C. Kraft, S. Martens, EMBO J. 31 (2012) 4304–4317.
[51] F. Yao, P.A. Schaffer, J. Virol. 69 (1995) 6249–6258.
[52] B. Sodeik, M.W. Ebersold, A. Helenius, J. Cell Biol. 136 (1997) 1007–1021.
[53] A.V. Nicola, J. Hou, E.O. Major, S.E. Straus, J. Virol. 79 (2005) 7609–7616.
[54] A.V. Nicola, A.M. McEvoy, S.E. Straus, J. Virol. 77 (2003) 5324–5332.
[55] C.E. Futter, L.M. Collinson, J.M. Backer, C.R. Hopkins, J. Cell Biol. 155 (2001) 1251–1264.
[56] J.Y. Kim, A. Mandarino, M.V. Chao, I. Mohr, A.C. Wilson, PLoS Pathog. 8 (2012) e1002540.
[57] V. Camarena, M. Kobayashi, J.Y. Kim, P. Roehm, R. Perez, J. Gardner, A.C. Wilson, I. Mohr, M.V. Chao, Cell Host Microbe 8 (2010) 320–330.
[58] D.R. Wilcox, N.R. Wadhwani, R. Longnecker, W.J. Muller, PLoS Pathog. 11 (2015) e1004580.